NUREG/CR-2855
BNL-NUREG-51570

Subchannel Analysis of Multiple CHF Events

Prepared by D. G. Reddy, C. F. Fighetti, Columbia University

Department of Chemical Engineering
Columbia University

Brookhaven National Laboratory

Prepared for
U.S. Nuclear Regulatory Commission

Availability of Reference Materials Cited in NRC Publications

Most documents cited in NRC publications will be available from one of the following sources:

1. The NRC Public Document Room, 1717 H Street, N.W.
   Washington, DC 20555
2. The NRC/GPO Sales Program, U.S. Nuclear Regulatory Commission,
   Washington, DC 20555
3. The National Technical Information Service, Springfield, VA 22161

Although the listing that follows represents the majority of documents cited in NRC publications, it is not intended to be exhaustive.

Referenced documents available for inspection and copying for a fee from the NRC Public Document Room include NRC correspondence and internal NRC memoranda; NRC Office of Inspection and Enforcement bulletins, circulars, information notices, inspection and investigation notices; Licensee Event Reports; vendor reports and correspondence; Commission papers; and applicant and licensee documents and correspondence.

The following documents in the NUREG series are available for purchase from the NRC/GPO Sales Program: formal NRC staff and contractor reports, NRC-sponsored conference proceedings, and NRC booklets and brochures. Also available are Regulatory Guides, NRC regulations in the *Code of Federal Regulations*, and *Nuclear Regulatory Commission Issuances*.

Documents available from the National Technical Information Service include NUREG series reports and technical reports prepared by other federal agencies and reports prepared by the Atomic Energy Commission, forerunner agency to the Nuclear Regulatory Commission.

Documents available from public and special technical libraries include all open literature items, such as books, journal and periodical articles, and transactions. *Federal Register* notices, federal and state legislation, and congressional reports can usually be obtained from these libraries.

Documents such as theses, dissertations, foreign reports and translations, and non-NRC conference proceedings are available for purchase from the organization sponsoring the publication cited.

Single copies of NRC draft reports are available free upon written request to the Division of Technical Information and Document Control, U.S. Nuclear Regulatory Commission, Washington, DC 20555.

Copies of industry codes and standards used in a substantive manner in the NRC regulatory process are maintained at the NRC Library, 7920 Norfolk Avenue, Bethesda, Maryland, and are available there for reference use by the public. Codes and standards are usually copyrighted and may be purchased from the originating organization or, if they are American National Standards, from the American National Standards Institute, 1430 Broadway, New York, NY 10018.

GPO Printed copy price: $6.50

NUREG/CR-2855
BNL-NUREG-51570

Subchannel Analysis of Multiple CHF Events

Manuscript Completed: May 1982
Date Published: August 1982

Prepared by
D. G. Reddy, C. F. Fighetti, Columbia University

Department of Chemical Engineering
Columbia University
New York, NY 10027

Under Subcontract to
Brookhaven National Laboratory
Upton, NY 11973

Prepared for
Division of Systems Integration
Office of Nuclear Reactor Regulation
U.S. Nuclear Regulatory Commission
Washington, D.C. 20555
NRC FIN A3353

ABSTRACT

The phenomenon of multiple CHF events in rod bundle heat transfer tests, referring to the occurrence of CHF on more than one rod or at more than one location on one rod is examined. The adequacy of some of the subchannel CHF correlations presently used in the nuclear industry in predicting higher order CHF events is ascertained based on local coolant conditions obtained with the COBRA IIIC subchannel code. The rod bundle CHF data obtained at the Heat Transfer Research Facility of Columbia University are examined for multiple CHF events using a combination of statistical analyses and parametric studies. The above analyses are applied to the study of three data sets of tests simulating both PWR and BWR reactor cores with uniform and non-uniform axial heat flux distributions. The CHF correlations employed in this study include: 1) CE-1 correlation, 2) B&W-2 correlation, 3) W-3 correlation, and 4) Columbia correlation. Examination of the results of this study indicate that: 1) the characteristic behavior of the higher rank CHF are essentially the same as those of the first CHF; and 2) the presently available subchannel CHF correlations are adequate in the prediction of CHF events of higher rank. These correlations predicted the CHF events of higher rank with the same degree of accuracy as the first CHF. The above conclusions are valid for rod bundle CHF tests under normal steady state conditions. Multiple CHF events occurring in steady state conditions designed with rod bundle abnormalities, such as bowed rods and axial heat flux spikes, occasionally encountered in the operation of nuclear reactors, are not addressed in this report. It is recommended that studies be conducted to ascertain predictability of multiple CHF events observed during abnormal rod bundle heat transfer tests, using CHF correlations based on local coolant conditions.

Table of Contents

1. INTRODUCTION 1- 1

2. BACKGROUND 2- 1

3. CHF DATA 3- 1

4. METHOD OF APPROACH 4- 1

  4.1 Single-Phase Friction Factor 4- 4
  4.2 Subcooled Void Correlation 4- 4
  4.3 Bulk Void Correlation 4- 5
  4.4 Two-Phase Friction Multiplier Correlation 4- 5
  4.5 Grid Loss Coefficient 4- 7

5. ANALYSIS OF MULTIPLE CHF DATA 5- 1

  5.1 BWR Uniform Axial Heat Flux Data 5- 3
  5.2 PWR Uniform Axial Heat Flux Data 5-15
  5.3 PWR Non-Uniform Axial Heat Flux Data 5-26

6. SUMMARY, CONCLUSIONS, AND RECOMMENDATIONS 6- 1

7. REFERENCES 7- 1

APPENDIX-A SUMMARY OF TEST SECTION GEOMETRY PARAMETERS A- 1

APPENDIX-B TYPICAL TEST CONDITIONS FOR CHF TESTS FROM THREE DATA SETS B- 1

List of Figures

Figure 3-1:	Radial Geometry	3- 9
Figure 3-2:	Radial Geometry	3-10
Figure 3-3:	Radial Geometry	3-11
Figure 3-4:	Radial Geometry	3-12
Figure 3-5:	Radial Geometry	3-13
Figure 3-6:	Radial Geometry	3-14
Figure 3-7:	Radial Geometry	3-15
Figure 3-8:	Radial Geometry	3-16
Figure 3-9:	Axial Heat Flux Distributions	3-17
Figure 3-10:	Axial Heat Flux Distributions	3-18
Figure 3-11:	Axial Heat Flux Distributions	3-19
Figure 5-1:	Plot of q-calc/q-obs Ratio Versus Quality - Columbia Correlation - First CHF - BWR	5- 9
Figure 5-2:	Plot of q-calc/q-obs Ratio Versus Quality - Columbia Correlation - Higher Order CHF - BWR	5- 9
Figure 5-3:	Plot of q-calc/q-obs Ratio Versus Quality - Columbia Correlation - Second CHF - BWR	5-10
Figure 5-4:	Plot of q-calc/q-obs Ratio Versus Quality - Columbia Correlation - Third CHF - BWR	5-10
Figure 5-5:	Plot of q-calc/q-obs Ratio Versus Mass Flux - Columbia Correlation - First CHF - BWR	5-11
Figure 5-6:	Plot of q-calc/q-obs Ratio Versus Mass Flux - Columbia Correlation - Higher Order CHF - BWR	5-11
Figure 5-7:	Plot of q-calc/q-obs Ratio Versus Pressure - Columbia Correlation - First CHF - BWR	5-12
Figure 5-8:	Plot of q-calc/q-obs Ratio Versus Pressure - Columbia Correlation - Higher Order CHF - BWR	5-12
Figure 5-9:	Plot of q-calc/q-obs Ratio Versus Inlet Quality - Columbia Correlation - First CHF - BWR	5-13
Figure 5-10:	Plot of q-calc/q-obs Ratio Versus Inlet Quality - Columbia Correlation - Higher Order CHF - BWR	5-13
Figure 5-11:	Plot of q-calc/q-obs Ratio Versus Observed CHF - Columbia Correlation - First CHF - BWR	5-14
Figure 5-12:	Plot of q-calc/q-obs Ratio Versus Observed CHF - Columbia Correlation - Higher Order CHF - BWR	5-14
Figure 5-13:	Plot of q-calc/q-obs Ratio Versus Quality - Columbia Correlation - First CHF	5-28
Figure 5-14:	Plot of q-calc/q-obs Ratio Versus Quality - Columbia Correlation - Higher Order CHF	5-28
Figure 5-15:	Plot of q-calc/q-obs Ratio Versus Quality - Columbia Correlation - Second CHF	5-2

Figure 5-16: Plot of q-calc/q-obs Ratio Versus Quality - Columbia Correlation - Third CHF 5-29
Figure 5-17: Plot of q-calc/q-obs Ratio Versus Mass Flux - Columbia Correlation - First CHF 5-30
Figure 5-18: Plot of q-calc/q-obs Ratio Versus Mass Flux - Columbia Correlation - Higher Order CHF 5-30
Figure 5-19: Plot of q-calc/q-obs Ratio Versus Pressure - Columbia Correlation - First CHF 5-31
Figure 5-20: Plot of q-calc/q-obs Ratio Versus Pressure - Columbia Correlation - Higher Order CHF 5-31
Figure 5-21: Plot of q-calc/q-obs Ratio Versus Quality - CE-1 Correlation - First CHF 5-33
Figure 5-22: Plot of q-calc/q-obs Ratio Versus Quality - CE-1 Correlation - Higher Order CHF 5-33
Figure 5-23: Plot of q-calc/q-obs Ratio Versus Quality - CE-1 Correlation - Second CHF 5-34
Figure 5-24: Plot of q-calc/q-obs Ratio Versus Quality - CE-1 Correlation - Third CHF 5-34
Figure 5-25: Plot of q-calc/q-obs Ratio Versus Mass Flux - CE-1 Correlation - First CHF 5-35
Figure 5-26: Plot of q-calc/q-obs Ratio Versus Mass Flux - CE-1 Correlation - Higher Order CHF 5-35
Figure 5-27: Plot of q-calc/q-obs Ratio Versus Pressure - CE-1 Correlation - First CHF 5-36
Figure 5-28: Plot of q-calc/q-obs Ratio Versus Pressure - CE-1 Correlation - Higher Order CHF 5-36
Figure 5-29: Plot of q-calc/q-obs Ratio Versus Quality - B&W-2 Correlation - First CHF 5-38
Figure 5-30: Plot of q-calc/q-obs Ratio Versus Quality - B&W-2 Correlation - Higher Order CHF 5-38
Figure 5-31: Plot of q-calc/q-obs Ratio Versus Quality - B&W-2 Correlation - Second CHF 5-39
Figure 5-32: Plot of q-calc/q-obs Ratio Versus Quality - B&W-2 Correlation - Third CHF 5-39
Figure 5-33: Plot of q-calc/q-obs Ratio Versus Mass Flux - B&W-2 Correlation - First CHF 5-40
Figure 5-34: Plot of q-calc/q-obs Ratio Versus Mass Flux - B&W-2 Correlation - Higher Order CHF 5-40
Figure 5-35: Plot of q-calc/q-obs Ratio Versus Pressure - B&W-2 Correlation - First CHF 5-41
Figure 5-36: Plot of q-calc/q-obs Ratio Versus Pressure - B&W-2 Correlation - Higher Order CHF 5-41
Figure 5-37: Plot of q-calc/q-obs Ratio Versus Quality - W-3 Correlation - First CHF 5-43
Figure 5-38: Plot of q-calc/q-obs Ratio Versus Quality - W-3 Correlation - Higher Order CHF 5-43
Figure 5-39: Plot of q-calc/q-obs Ratio Versus Quality - W-3 Correlation - Second CHF 5-44
Figure 5-40: Plot of q-calc/q-obs Ratio Versus Quality - W-3 Correlation - Third CHF 5-44
Figure 5-41: Plot of q-calc/q-obs Ratio Versus Mass Flux - W-3 Correlation - First CHF 5-45

Figure 5-42: Plot of q-calc/q-obs Ratio Versus Mass Flux - W-3 Correlation - Higher Order CHF 5-45
Figure 5-43: Plot of q-calc/q-obs Ratio Versus Pressure - W-3 Correlation - First CHF 5-46
Figure 5-44: Plot of q-calc/q-obs Ratio Versus Pressure - W-3 Correlation - Higher Order CHF 5-46

List of Tables

Table 3-1:	Compilation of Test Section Geometry Parameters for BWR Type Geometry	3- 3
Table 3-2:	Compilation of Test Section Geometry Parameters for PWR Type Geometry	3- 4
Table 3-3:	Compilation of Test Section Geometry Parameters for PWR Type Geometry	3- 5
Table 3-4:	Compilation of Test Parameters	3- 6
Table 3-5:	Compilation of Test Parameters	3- 7
Table 3-6:	Compilation of Test Parameters	3- 8
Table 4-1:	Input Parameters Used in COBRA IIIC Code	4- 3
Table 5-1:	Summary of Columbia CHF Correlation	5- 5
Table 5-2:	Columbia CHF Correlation - Parameter Ranges and Error Statistics	5- 6
Table 5-3:	Summary of Cold Wall Correction Factors	5- 7
Table 5-4:	Analysis of BWR Data - Columbia Correlation	5- 8
Table 5-5:	Summary of CE-1 Correlation	5-16
Table 5-6:	Summary of B&W-2 Correlation	5-18
Table 5-7:	Summary of W-3 Correlation	5-20
Table 5-8:	Analysis of PWR Data - Comparison of Correlations	5-23
Table 5-9:	Analysis of PWR Data - Columbia Correlation	5-24
Table 5-10:	Parameter Ranges of Existing CHF Correlations	5-25
Table 5-11:	Analysis of PWR Data - Columbia Correlation	5-27
Table 5-12:	Analysis of PWR Data - CE-1 Correlation	5-32
Table 5-13:	Analysis of PWR Data - B&W-2 Correlation	5-37
Table 5-14:	Analysis of PWR Data - W-3 Correlation	5-42
Table 5-15:	Analysis of Non-Uniform Axial Heat Flux PWR Data - Columbia Correlation	5-49
Table 5-16:	Analysis of Non-Uniform Axial Heat Flux PWR Data - CE-1 Correlation	5-50
Table 5-17:	Analysis of Non-Uniform Axial Heat Flux PWR Data - B&W-2 Correlation	5-51

NOMENCLATURE

De	=	Equivalent diameter
f	=	Single phase friction factor
F_A & F_C	=	Cold wall correction factors
g_C	=	Newton constant
G	=	Mass flux ($M \cdot lbs/hr\text{-}ft^2$)
h_{fg}	=	Latent heat of vaporization
K_g	=	Grid loss coefficient
L	=	Length
n	=	Number of spacer grids
N	=	Number of points
Pr	=	Reduced pressure ($P/P_{critical}$)
q"	=	Critical heat flux ($M \cdot Btu/hr\text{-}ft^2$)
R	=	Ratio of predicted to measured CHF
R_{av}	=	Average ratio
Re	=	Reynold's number
RMS	=	Root mean square error
STD	=	Standard deviation
V	=	Specific volume
X	=	Quality

Greek Letters

α	=	Void fraction
ρ	=	Density
$\Phi_{\ell o}$	=	Two-phase friction multiplier

NOMENCLATURE

Subscripts

c	=	Calculated
f	=	Friction
g	=	Vapor
g	=	Grid
in	=	Inlet
ℓ	=	Local
ℓ	=	Liquid
t	=	Total

Chapter 1

INTRODUCTION

Boiling crisis is characterized by a sudden drop in the boiling heat transfer coefficient due to the change of heat transfer mechanism as indicated by a temperature excursion of the heating surface. The maximum heat flux just before the boiling crisis is called the Critical Heat Flux (CHF). The operative definition of CHF is "that condition in which a small increase in heat flux or inlet fluid temperature or a small decrease in inlet mass flow causes an inordinate deterioration of heat transfer in the system".

The CHF problem has been studied particularly during the last 20 years, especially to aid in the development of nuclear reactors, since the design criteria for nuclear reactors specify that they must operate at a certain percentage below the CHF at all times and locations in order to maintain the cladding temperature of the fuel elements at safe values. Therefore, CHF limits the maximum power extractable from nuclear reactors. For this reason and also because of the commercial interest in increasing reactor power (compatible with reactor safety) as much as possible, the CHF problem is a continuous subject of theoretical and experimental studies.

Because of the complexity of the CHF phenomenon in fuel rod array geometry and lack of dependable and fully verified analytical methods for the prediction of CHF, the knowledge of the rod array CHF is almost entirely based on experimental data and the general state-of-the-art of predicting CHF is substantially of an empirical nature. The technological advances of the past few year. now permit experiments to be performed on large test sections, even simulating the fuel elements of nuclear reactor cores on a full scale. For design purposes, representative experiments are performed on large scale electrically heated models of specific types of fuel elements and empirical correlations are developed based on experimental data for those specific types of bundles. These new data allow assessment of old correlations and calculation methods.

The Columbia University Heat Transfer Research Facility has performed much of the CHF testing for reactor vendors such as Westinghouse, Combustion Engineering, General Electric, and others; and obtained over 14,000 CHF data points. An examination of these data reveal that a significant portion of these data involve the occurrence of CHF on more than one rod or at more than one location on one rod. These data have never been systematically studied for the understanding of multiple CHF events on a local conditions basis. A study of multiple CHF events is important for the following reasons (1):

1. The occurrence of multiple CHF events on the same rod and the axial extent of CHF could significantly influence post-CHF behavior such as the ability to quench the fuel rods. Information on multiple CHF events on the same rod is important for the prediction of the fuel rod behavior.

2. Some reactor vendors have accident criteria on clad temperatures. For example, Westinghouse has a 2700°F criteria for the locked-rotor accident. The calculated clad temperature could be somewhat affected by the occurrence of CHF at more than one location on the same fuel rod. As more information on post-CHF fuel behavior becomes available, it is likely that licensees and license applicants will submit applications in support of a change in this criterion to a more realistic fuel damage criterion based on fuel temperature and perhaps fuel internal pressure. If this occurs, a better understanding of multiple CHF events and post-CHF behavior will be needed by the Nuclear Regulatory Commission (NRC) staff in support of the review of those applications.

3. Multiple CHF events on different fuel rods are of potential safety significance since the calculation of CHF on one fuel rod might imply degraded heat transfer and the potential clad failure of a number of fuel rods.

Based on the above statements, it can be concluded that multiple CHF events can be of importance for the prediction of fuel rod behavior and, therefore, of potential safety significance in the future licensing of light water reactors.

The objective of this study is to obtain local conditions for multiple CHF events using the COBRA IIIC subchannel code and assess the adequacy of existing CHF correlations based on local conditions (particularly those being used in reactor licensing) in predicting multiple CHF occurrences.

This study consists of the following subtasks:

1. Determine local conditions in the rod bundles using the COBRA IIIC code when multiple CHF events are observed. Three data sets are analyzed:

    a. BWR Uniform Axial Heat Flux Data

    b. PWR Unifirm Axial Heat Flux Data

    c. PWR Non-Uniform Axial Heat Flux Data

2. Compare the predictability of higher order CHF events with first CHF using existing CHF correlations based on local conditions.

Chapter 2

BACKGROUND

The evaluation of the thermal hydraulic performance of the reactor core is an important factor in the safety analysis of water-cooled nuclear reactors. These nuclear reactors use fuel assemblies composed of bundles of nuclear fuel rods. From a heat transfer point of view the critical heat flux of a rod bundle at its design conditions is its limiting parameter. Therefore, the continued safe growth of nuclear power requires improved knowlege of the CHF limits of the rod bundle fuel assemblies.

For design purposes, representative heat transfer tests to investigate CHF are performed in rod bundle test facilities, in which a large scale array of electrically heated rods, simulating specific types of rod bundle fuel assemblies, are installed in a vertical pressure housing with the loop water flowing through the rod assemblies.

The Columbia University Heat Transfer Research Facility has carried out CHF tests and collected over 14,000 data points from about 260 test sections. This is by far the largest data bank of this type in the world. These data were obtained for Combustion Engineering, Westinghouse Electric, General Electric, Exxon Nuclear, Babcock & Wilcox, Idaho National Engineering Laboratories for the LOFT program, and United Nuclear Corporation. In addition to the tests for these US sponsors, CHF data were also obtained for the British, Canadian, Japanese, and German reactor designers. Thus, the Heat Transfer Research Facility has attained world wide recognition as one of the principal sources of CHF data in the world. Most of these rod bundle CHF data are proprietary information and so far remain unpublished.

The heat transfer tests performed at the Heat Transfer Research Facility covered a wide range of test section geometries with square pitch rod bundles for both Pressurized Water Reactor (PWR) and Boiling Water Reactor (BWR) designs, and triangular pitch rod bundles for the United Kingdom Atomic Energy Authority (UKAEA) and the Atomic Energy of Canada Limited (AECL) Heavy Water Reactors (HWR), with heated lengths form 30 inches to 168 inches, and uniform and non-uniform axial and radial heat flux distributions. Parameter ranges for the CHF data are: pressures from 200 to 2500 psia, mass velocities from 0.04 to 4.5 M.lbs/hr-ft^2, exit qualities from -25% to +75%, and inlet subcooling of up to 640 Btu/lb.

There are two major thermal hydraulic facilities for CHF testing at the Heat Transfer Research Facility. They are known as the Medium Pressure and the High Pressure Heat Transfer Loops. The Medium Pressure Loop is rated to 2400 psia and 640°F with a maximum flow rate of 550 gpm. The High Pressure Loop is rated to 3500 psia and 700°F, except for the present pumps, which are rated at 2500 psia and 650°F, with a maximum flow rate of 450 gpm.

Flow was maintained by a centrifugal pump in the Medium Pressure Loop and by a set of four canned rotor pumps in the High Pressure Loop. A throttle valve located upstream of the test section automatically controlled the flow, and also maintained its stability during the tests. A turbine flow meter, a calibrated platinum resistance thermometer (RTD) and thermocouples located at the inlet of the test section measured flow and temperature, and a large scale Bourdon pressure gauge and transducers monitored the outlet pressure. All of these measurements were recorded continuously during the tests.

Heating of the test sections was provided by six motor generator sets operatad in parallel for a maximum DC output of 50,000 amps at 230 volts (i.e., 11.5 megawatts). Heat rejection in both loops was accomplished by shell-and-tube heat exchangers with constant temperature water as the coolant. A detailed description of the power system is provided in Reference 2.

Each of the test sections had a different configuration, but all the tests were performed in the same fashion. The tests section outlet pressure, inlet temperature and mass flow rate were established and maintained constant. The total power to the test section was then increased in small increments and the loop brought to the corresponding equilibrium conditions each time. This process was continued until a temperature excursion was observed to start in one or more of the rods in the bundle. The temperature increase varied depending on system conditions, from a minimum of 10°F to 100°F or more. When the indication was judged to be sufficient to have established the presence of CHF, the power to the test section was reduced and the test conditions prior to the temperature excursion were recorded both manually and by a computer-controlled data acquisition system.

A comprehensive documentation of the test section geometric characteristics and test conditions together with the location and the order of occurrence of CHF for data points obtained at the Heat transfer Research Facility, and compiled under an EPRI research program, are described in Reference 3.

An examination of these records reveal that many CHF test involve the occurrence of CHF on more than one rod or at more than one location on one rod. The multiple CHF events can be of importance for the prediction of the fuel rod behavior and, therefore, of potential safety significance in the future licensing of nuclear reactors.

Chapter 3

CHF DATA

A total of 2,671 CHF data points from 51 test sections were analyzed. These data were extracted from a data bank containing 11,077 CHF points obtained from 235 different test sections that was compiled under a research program sponsored by the Electric Power Research Institute (EPRI). The test section geometry figures and the test conditions together with the location and order of occurrence of CHF for all the data can be found in Reference 4. From this data base, three sets of data were analysed:

1. BWR type with uniform axial heat flux distribution
2. PWR type with uniform axial heat flux distribution
3. PWR type with non-uniforn axial heat flux distribution

The first group consists of 18 test sections containing 762 CHF data points. These data were obtained for General Electric Company and the geometric characteristics are summarized in Table 3-1. The second group is the data obtained for Combustion Engineering consisting of 15 test sections with 931 CHF data points. The geometric characteristics for these PWR data are shown in Table 3-2. The third group is data obtained from test sections having non-unifrom axial heat flux distribution; it contains 18 test sections with a total of 978 CHF data points obtained for Combustion Engineering and Westinghouse Electric Corporation and the geometric characteristics are shown in Table 3-3. Also, the range of test parameters (i.e., exit pressure, inlet subcooling enthalpy, mass velocity, and average heat flux) for these data sets are given in Tables 3-4, 3-5, and 3-6 respectively.

Figures 3-1 through 3-8 show the lateral geometry of the rod bundles being referenced by Tables 3-1, 3-2, and 3-3. Figures 3-9, 3-10, and 3-11 show the axial heat flux profiles of the non-uniform axial test sections being refereced by Table 3-3. Detailed geometry parameters for all 51 test sections and the test conditions for one test section for each of the three groups are given in the Appendices A and B.

An explanation of the comments in Tables 3-1, 3-2, and 3-3 are given below.

a. The two digit code specifies the test sponsor. The three digit code that follows describes the reactor type.

b. Total number of grids.

c. Grid loss coefficient calculated based on isothermal flow measurements.

d. Grid spacing for spacers of the same type.

e. Axial heat flux profile as described in Figures 3-9 through 3-11.

TABLE 3-1. COMPILATION OF TEST SECTION GEOMETRY PARAMETERS FOR BWR TYPE GEOMETRY

TEST NO.	SPONSOR GEOMETRY TYPE (a)	TOTAL NO. OF PTS.	NO. OF HT'D RODS	ROD PITCH (IN.)	ROD DIAM. (IN.)	UNHT'D ROD DIAM. (IN.)	TEST SECT. LENGTH (IN.)	NO. OF GRIDS (b)	GRID LOSS COEF. (c)	GRID SPAC. (IN.) (d)	RADIAL PEAK FACTOR	RADIAL FIG. NO.	AXIAL CURVE NO. (e)
301.	GE-BWR	54.	16.	.738	.563	.000	72.0	7.	.800	9.50	1.018	3-1	-
302.	GE-BWR	48.	16.	.738	.563	.000	72.0	4.	1.470	9.50	1.015	3-1	-
303.	GE-BWR	26.	16.	.738	.563	.000	72.0	3.	1.470	19.50	1.016	3-1	-
305.	GE-BWR	4.	16.	.738	.563	.000	72.0	3.	1.470	19.50	1.263	3-1	-
306.	GE-BWR	48.	16.	.738	.563	.000	72.0	3.	1.470	19.50	1.000	3-1	-
307.	GE-BWR	17.	16.	.738	.563	.000	48.0	2.	1.470	19.50	1.000	3-1	-
307.1	GE-BWR	5.	16.	.738	.563	.000	48.0	2.	1.470	19.50	1.000	3-1	-
308.	GE-BWR	31.	16.	.738	.563	.000	72.0	3.	1.470	19.50	1.210	3-1	-
309.	GE-BWR	40.	16.	.738	.563	.000	72.0	3.	1.470	19.50	1.210	3-1	-
310.	GE-BWR	30.	16.	.738	.563	.000	72.0	3.	1.470	19.50	1.610	3-1	-
311.	GE-BWR	59.	16.	.738	.563	.000	72.0	3.	1.470	19.50	1.000	3-1	-
312.	GE-BWR	55.	16.	.738	.563	.000	72.0	3.	1.470	19.50	1.271	3-1	-
313.	GE-BWR	60.	16.	.738	.563	.000	72.0	7.	.800	9.50	1.019	3-1	-
314.	GE-BWR	34.	16.	.738	.563	.000	72.0	3.	1.470	19.50	1.285	3-1	-
315.	GE-BWR	70.	16.	.738	.563	.000	72.0	3.	1.470	19.50	1.018	3-1	-
316.	GE-BWR	65.	16.	.738	.563	.000	72.0	3.	1.470	19.50	1.018	3-1	-
316.1	GE-BWR	44.	16.	.738	.563	.000	72.0	3.	1.470	19.50	1.018	3-1	-
318.	GE-BWR	72.	16.	.738	.563	.000	72.0	3.	1.470	19.50	1.232	3-1	-

TABLE 3-2. COMPILATION OF TEST SECTION GEOMETRY PARAMETERS FOR PWR TYPE GEOMETRY

TEST NO.	SPONSOR GEOMETRY TYPE (a)	TOTAL NO. OF PTS.	NO. OF HT'D RODS	ROD PITCH (IN.)	ROD DIAM. (IN.)	UNHT'D ROD DIAM. (IN.)	TEST SECT. LENGTH (IN.)	NO. OF GRIDS (b)	GRID LOSS COEF. (c)	GRID SPAC. (IN.) (d)	RADIAL PEAK FACTOR	RADIAL FIG. NO.	AXIAL CURVE NO. (e)
13.	CE-PWR	111.	25.	.580	.440	.000	84.0	5.	.815	16.00	1.134	3-2	-
14.	CE-PWR	[illegible]	25.	.580	.440	.000	84.0	5.	.815	16.00	1.134	3-2	-
16.	CE-PWR	56.	21.	.580	.440	1.135	84.0	5.	.884	16.00	1.124	3-3	-
17.	CE-PWR	57.	21.	.580	.440	1.135	84.0	4.	.815	19.00	1.133	3-3	-
18.	CE-PWR	72.	21.	.580	.440	1.135	48.0	3.	.815	16.00	1.095	3-3	-
19.	CE-PWR	53.	21.	.580	.440	1.135	84.0	4.	.815	19.00	1.132	3-3	-
20.	CE-PWR	68.	21.	.580	.440	1.135	84.0	5.	.815	16.00	1.132	3-3	-
22.	CE-PWR	61.	21.	.580	.440	1.135	84.0	5.	1.085	16.00	1.012	3-3	-
23.	CE-PWR	53.	21.	.580	.440	1.135	84.0	10.	1.029	8.00	1.012	3-3	-
24.	CE-PWR	62.	21.	.580	.440	1.115	84.0	4.	.815	18.25	1.153	3-4	-
25.	CE-PWR	65.	21.	.580	.440	1.115	84.0	4.	1.086	18.25	1.152	3-4	-
26.	CE-PWR	54.	21.	.580	.440	1.115	84.0	5.	.815	18.25	1.166	3-4	-
27.	CE-PWR	55.	21.	.580	.440	1.115	84.0	4.	1.053	18.25	1.152	3-4	-
28.	CE-PWR	55.	21.	.580	.440	1.115	84.0	4.	.815	18.25	1.023	3-4	-
29.	CE-PWR	59.	21.	.580	.440	1.115	84.0	10.	.815	8.00	1.020	3-4	-

TABLE 3-3. COMPILATION OF TEST SECTION GEOMETRY PARAMETERS FOR PWR TYPE GEOMETRY

TEST NO.	SPONSOR GEOMETRY TYPE (a)	TOTAL NO. OF PTS.	NO. OF HT'D RODS	ROD PITCH (IN.)	ROD DIAM. (IN.)	UNHT'D ROD DIAM. (IN.)	TEST SECT. LENGTH (IN.)	NO. OF GRIDS (b)	GRID LOSS COEF. (c)	GRID SPAC. (IN.) (d)	RADIAL PEAK FACTOR	RADIAL FIG. NO.	AXIAL CURVE NO. (e)
59.	CE-PWR	89.	21.	.506	.382	.980	150.0	11.	1.083	14.20	1.199	3-5	A
60.	CE-PWR	79.	21.	.580	.440	1.115	150.0	9.	1.430	14.40	1.201	3-4	B
66.	CE-PWR	93.	21.	.506	.382	.980	150.0	11.	1.083	14.20	1.073	3-5	B
68.	CE-PWR	95.	21.	.506	.382	.980	150.0	11.	1.430	14.20	1.199	3-5	A
71.	CE-PWR	87.	21.	.506	.382	.980	150.0	11.	1.430	14.20	1.073	3-5	C
108.	WH-PWR	29.	16.	.555	.422	.000	96.0	9.	1.200	20.00	1.145	3-6	D
109.	WH-PWR	33.	9.	.658	.500	.000	168.0	17.	1.200	20.00	1.000	3-7	E
110.	WH-PWR	23.	16.	.555	.422	.000	96.0	9.	.640	20.00	1.146	3-6	D
111.	WH-PWR	18.	16.	.555	.422	.000	96.0	9.	.640	10.00	1.146	3-6	D
131.	WH-PWR	37.	16.	.555	.422	.000	168.0	13.	1.400	26.00	1.122	3-6	F
132.	WH-PWR	36.	16.	.555	.422	.000	168.0	17.	1.400	20.00	1.122	3-6	F
133.	WH-PWR	38.	16.	.555	.422	.000	168.0	13.	1.400	13.00	1.124	3-6	F
134.	WH-PWR	38.	16.	.555	.422	.000	168.0	10.	1.400	32.00	1.123	3-6	F
141.	WH-PWR	36.	16.	.555	.422	.000	96.0	9.	1.820	20.00	1.127	3-6	G
146.	WH-PWR	39.	16.	.555	.422	.000	168.0	13.	1.900	26.00	1.127	3-6	F
147.	WH-PWR	40.	16.	.555	.422	.000	168.0	13.	1.710	26.00	1.123	3-6	F
162.	WH-PWR	70.	24.	.496	.374	.485	168.0	15.	1.250	22.00	1.099	3-8	H
164.	WH-PWR	98.	25.	.496	.374	.000	168.0	15.	1.250	22.00	1.095	3-2	H

TABLE 3-4. COMPILATION OF TEST PARAMETERS

TEST NO.	SPONSOR GEOMF TYPE	NO. OF PTS.	EXIT PRESSURE RANGE (PSIA)	INLET SUBCOOLING RANGE (BTU/LB)	MASS VELOCITY RANGE (M. LB/HR-SQFT)	AVERAGE HEAT FLUX RANGE (M. BTU/HR-SQFT)
301.	GE-BWR	54.	599. - 1250.	21. - 262.	.22 - 1.29	.27 - .78
302.	GE-BWR	48.	600. - 1250.	18. - 262.	.25 - 1.28	.29 - .80
303.	GE-BWR	26.	1000. - 1000.	18. - 262.	.51 - 1.33	.42 - .81
305.	GE-BWR	4.	1000. - 1000.	26. - 163.	.76 - .78	.43 - .56
306.	GE-BWR	48.	1000. - 1400.	26. - 308.	.24 - 1.25	.26 - .76
307.	GE-BWR	17.	1000. - 1000.	19. - 169.	.50 - 1.26	.54 - .95
307.1	GE-BWR	5.	1000. - 1000.	20. - 154.	.98 - 1.01	.73 - .97
308.	GE-BWR	31.	1000. - 1000.	19. - 278.	.09 - 1.26	.13 - .71
309.	GE-BWR	40.	800. - 1000.	21. - 292.	.10 - 1.27	.13 - .80
310.	GE-BWR	30.	1000. - 1000.	12. - 221.	.10 - 1.27	.11 - .59
311.	GE-BWR	59.	990. - 1418.	25. - 256.	.27 - 1.23	.32 - .76
312.	GE-BWR	55.	950. - 1453.	38. - 525.	.25 - 1.23	.24 - .64
313.	GE-BWR	60.	995. - 1440.	21. - 262.	.25 - 1.23	.33 - .83
314.	GE-BWR	34.	1000. - 1040.	28. - 268.	.24 - 1.26	.23 - .69
315.	GE-BWR	70.	1000. - 1417.	26. - 258.	.25 - 1.27	.27 - .72
316.	GE-BWR	65.	700. - 1420.	29. - 305.	.24 - 1.25	.30 - .74
316.1	GE-BWR	44.	999. - 1410.	30. - 282.	.24 - 1.24	.30 - .77
318.	GE-BWR	72.	995. - 2261.	27. - 180.	.96 - 3.17	.40 - .79

TABLE 3-5. COMPILATION OF TEST PARAMETERS

TEST NO.	SPONSOR GEOMETRY TYPE	NO. OF PTS.	EXIT PRESSURE RANGE (PSIA)	INLET SUBCOOLING RANGE (BTU/LB)	MASS VELOCITY RANGE (M. LB/HR-SQFT)	AVERAGE HEAT FLUX RANGE (M. BTU/HR-SQFT)
13.	CE-PWR	111.	200. - 2329.	14. - 391.	.11 - 3.02	.20 - .55
14.	CE-PWR	50.	1795. - 2311.	3. - 272.	.97 - 3.01	.26 - .56
16.	CE-PWR	56.	902. - 2320.	13. - 219.	.98 - 3.12	.24 - .62
17.	CE-PWR	57.	900. - 2315.	19. - 221.	.98 - 3.09	.23 - .65
18.	CE-PWR	72.	890. - 2315.	22. - 274.	.97 - 3.06	.41 - 1.12
19.	CE-PWR	53.	900. - 2325.	18. - 219.	.98 - 3.17	.23 - .68
20.	CE-PWR	68.	900. - 2315.	21. - 247.	.97 - 3.05	.25 - .68
22.	CE-PWR	61.	900. - 2310.	24. - 189.	.99 - 3.03	.26 - .67
23.	CE-PWR	53.	895. - 2315.	19. - 227.	.99 - 3.01	.30 - .67
24.	CE-PWR	62.	900. - 2325.	21. - 242.	1.00 - 3.12	.26 - .67
25.	CE-PWR	65.	895. - 2315.	10. - 226.	.99 - 3.01	.30 - .78
26.	CE-PWR	54.	900. - 2320.	14. - 216.	.98 - 3.02	.26 - .64
27.	CE-PWR	55.	900. - 2317.	19. - 200.	1.00 - 3.01	.27 - .67
28.	CE-PWR	55.	895. - 2320.	17. - 220.	.98 - 3.04	.16 - .68
29.	CE-PWR	59.	900. - 2315.	22. - 261.	.97 - 3.05	.26 - .67

TABLE 3-6. COMPILATION OF TEST PARAMETERS

TEST NO.	SPONSOR GEOMETRY TYPE	NO. OF PTS.	EXIT PRESSURE RANGE (PSIA)	INLET SUBCOOLING RANGE (BTU/LB)	MASS VELOCITY RANGE (M. LB/HR-SQFT)	AVERAGE HEAT FLUX RANGE (M. BTU/HR-SQFT)
59.	CE-PWR	89.	1495. - 2415.	41. - 334.	.99 - 4.01	.20 - .62
60.	CE-PWR	79.	1495. - 2415.	38. - 338.	.98 - 3.98	.23 - .55
66.	CE-PWR	93.	1500. - 2425.	38. - 339.	.98 - 4.06	.20 - .62
68.	CE-PWR	95.	1500. - 2405.	43. - 340.	.99 - 4.05	.27 - .60
71.	CE-PWR	87.	1500. - 2415.	41. - 362.	.97 - 4.00	.21 - .66
108.	WH-PWR	29.	1515. - 2415.	52. - 196.	1.91 - 3.61	.47 - .69
109.	WH-PWR	33.	1515. - 2415.	63. - 211.	2.00 - 3.58	.46 - .63
110.	WH-PWR	23.	1505. - 2157.	48. - 203.	1.52 - 3.63	.39 - .64
111.	WH-PWR	18.	1515. - 2115.	45. - 203.	1.58 - 3.65	.46 - .61
131.	WH-PWR	37.	1490. - 2415.	52. - 242.	1.94 - 3.53	.28 - .55
132.	WH-PWR	36.	1490. - 2405.	49. - 254.	1.92 - 3.49	.33 - .58
133.	WH-PWR	38.	1495. - 2415.	47. - 260.	1.46 - 3.45	.26 - .57
134.	WH-PWR	38.	1485. - 2425.	54. - 260.	1.89 - 3.54	.28 - .57
141.	WH-PWR	36.	1485. - 2410.	20. - 205.	1.51 - 3.51	.51 - .72
146.	WH-PWR	39.	1490. - 2415.	44. - 295.	1.93 - 3.45	.31 - .50
147.	WH-PWR	40.	1495. - 2405.	44. - 266.	1.95 - 3.53	.28 - .52
162.	WH-PWR	70.	1500. - 2425.	31. - 283.	1.00 - 3.55	.27 - .51
164.	WH-PWR	98.	745. - 2425.	11. - 342.	.51 - 3.53	.25 - .53

FIGURE 3-1. RADIAL GEOMETRY

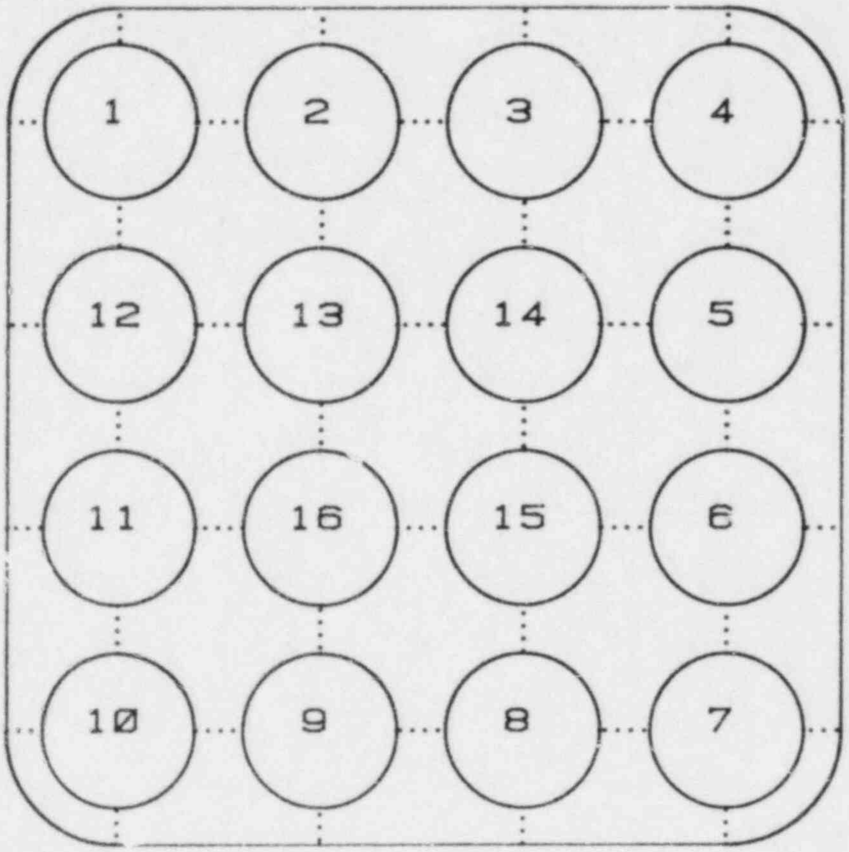

FIGURE 3-2. RADIAL GEOMETRY

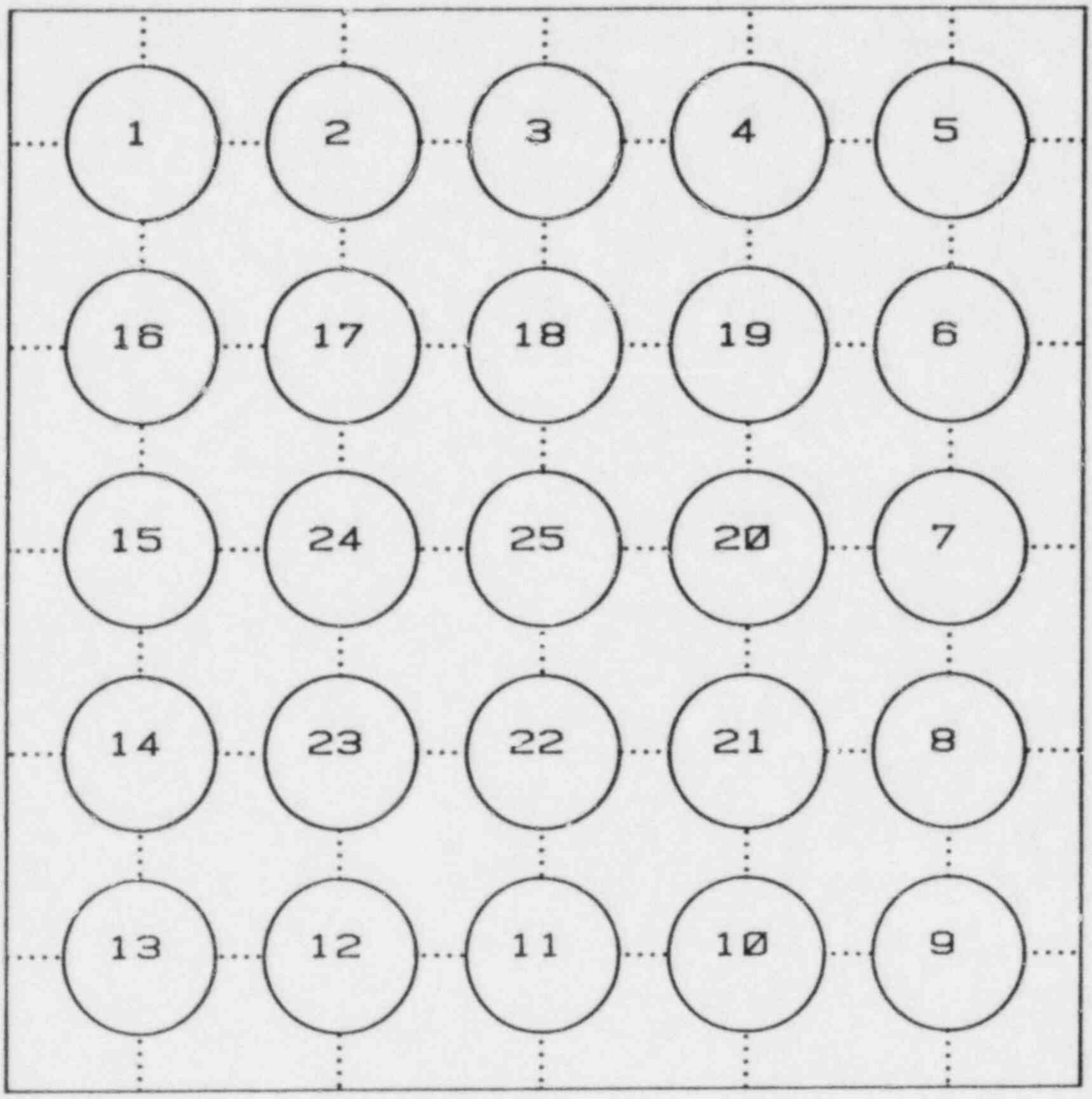

FIGURE 3-3. RADIAL GEOMETRY

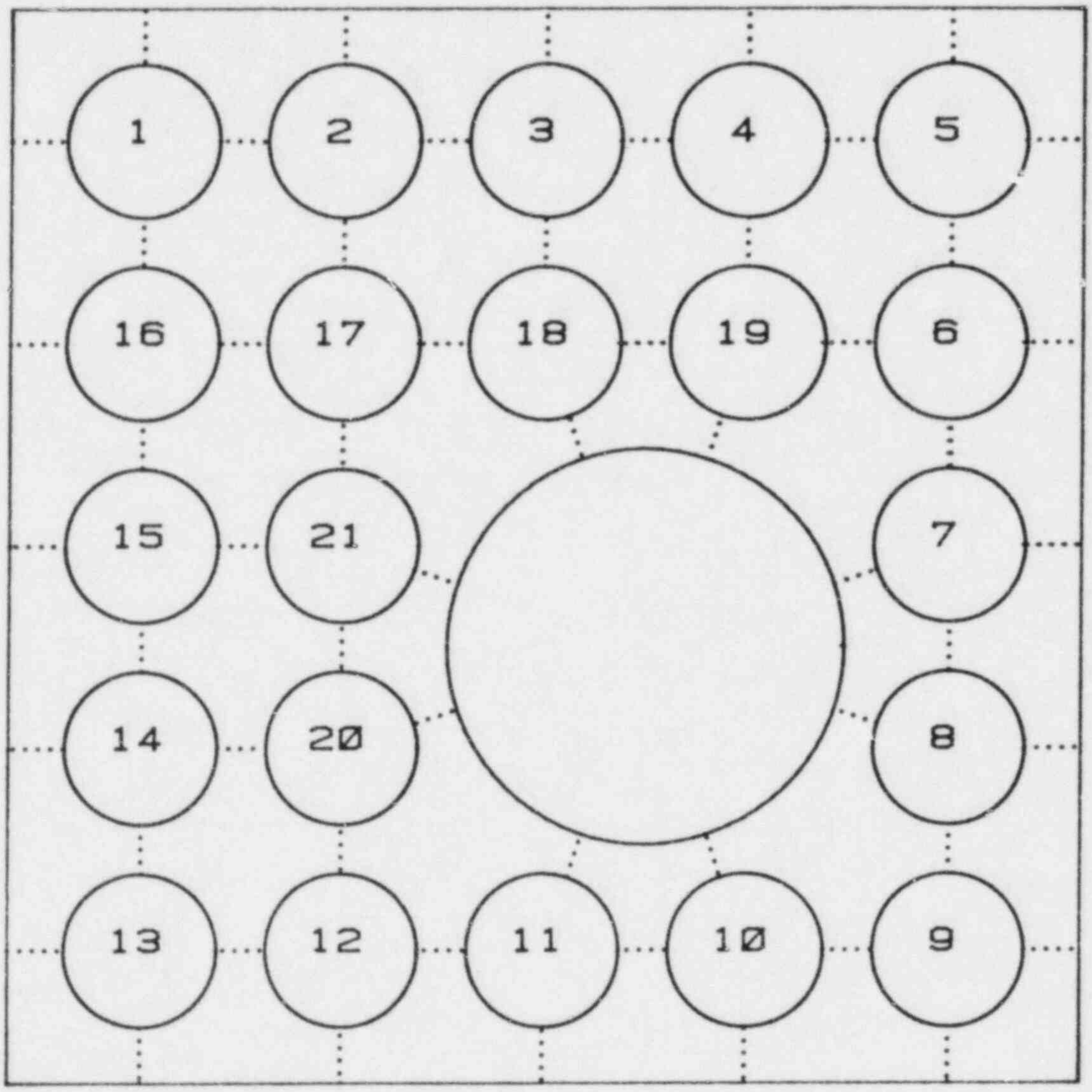

FIGURE 3-4. RADIAL GEOMETRY

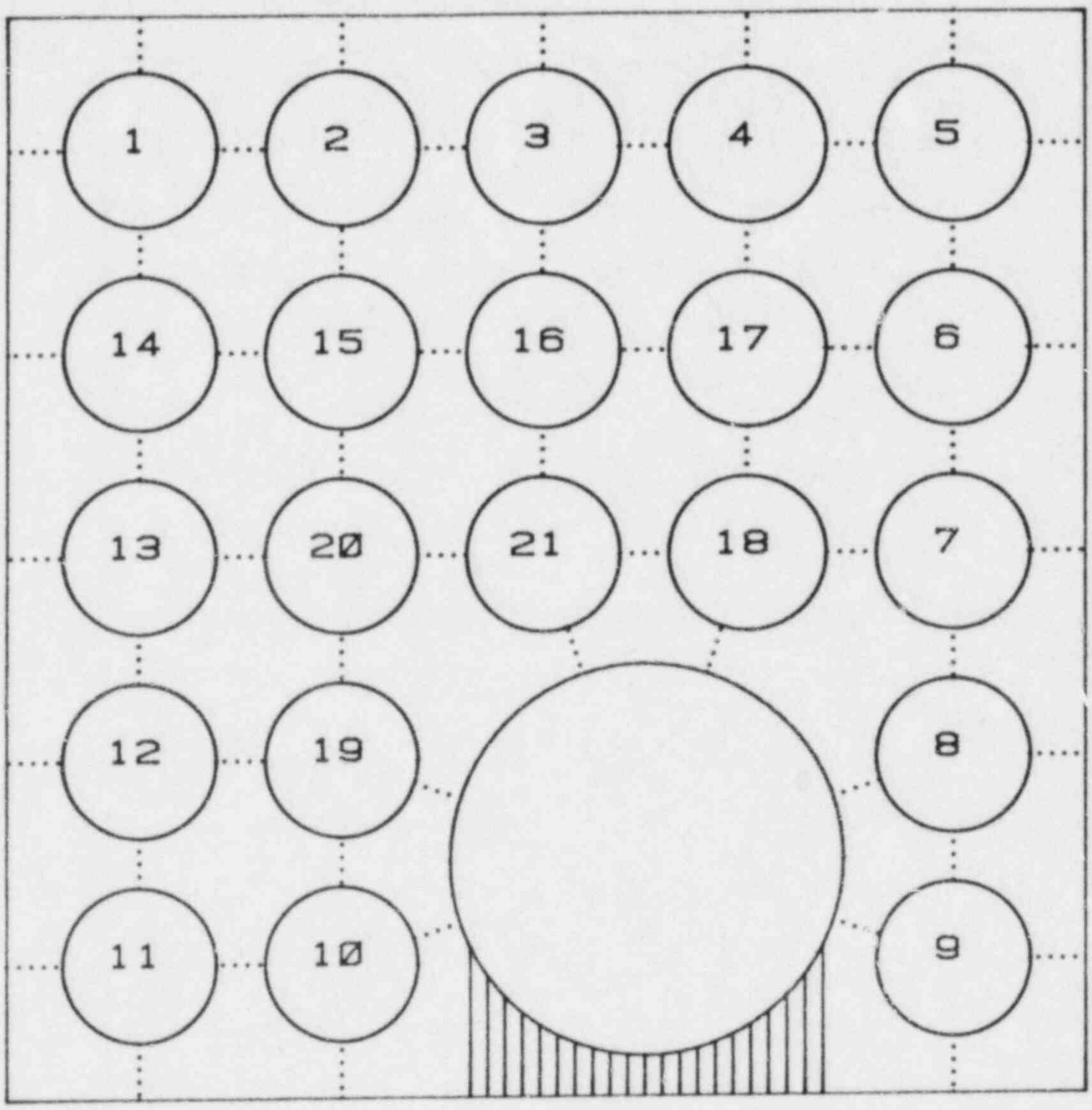

FIGURE 3-5. RADIAL GEOMETRY

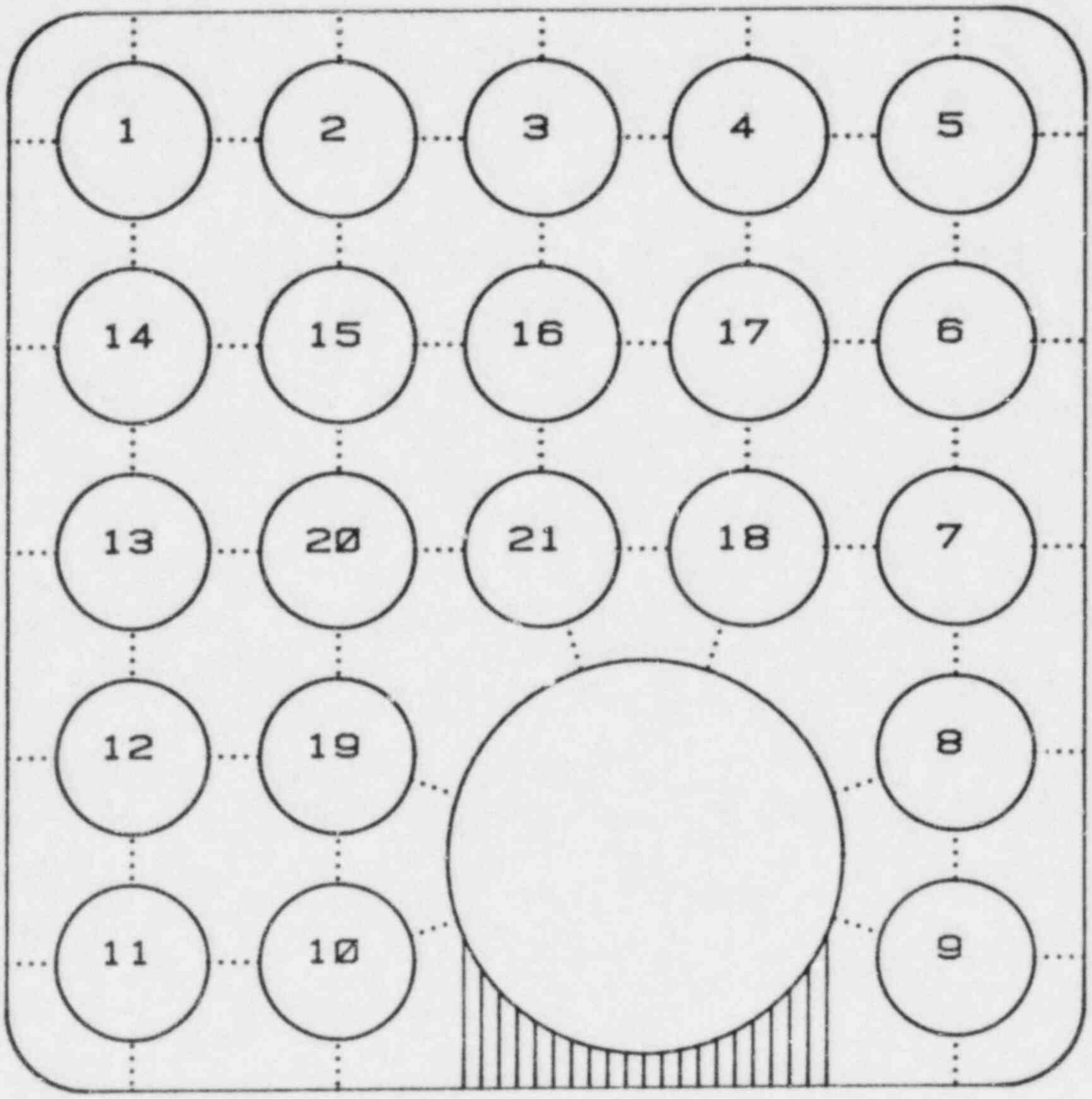

FIGURE 3-6. RADIAL GEOMETRY

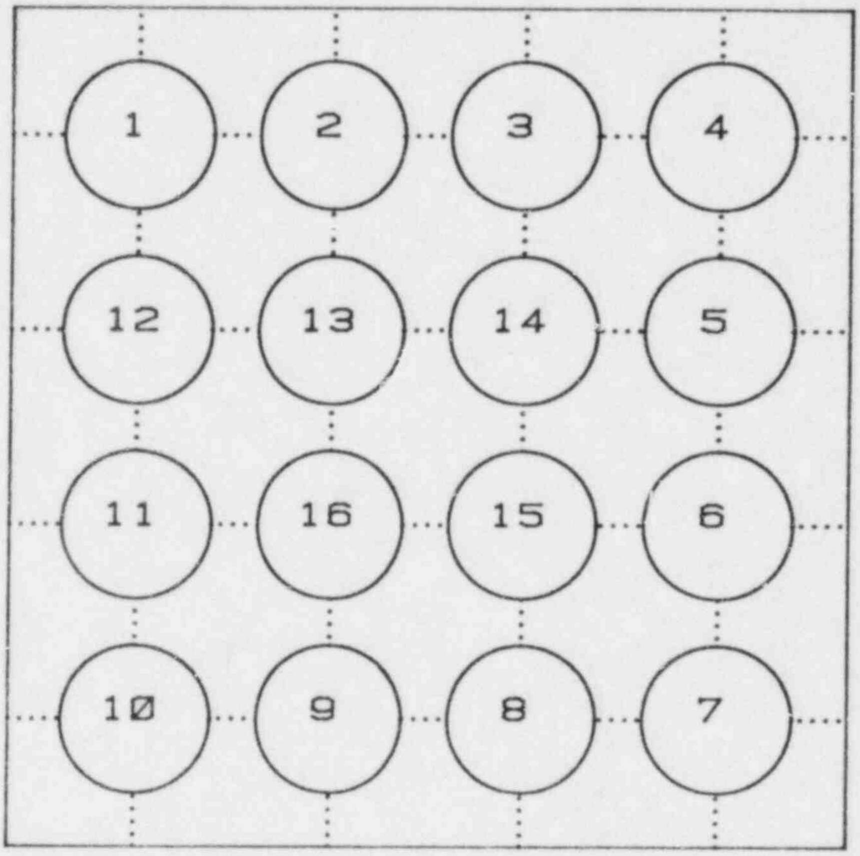

FIGURE 3-7. RADIAL GEOMETRY

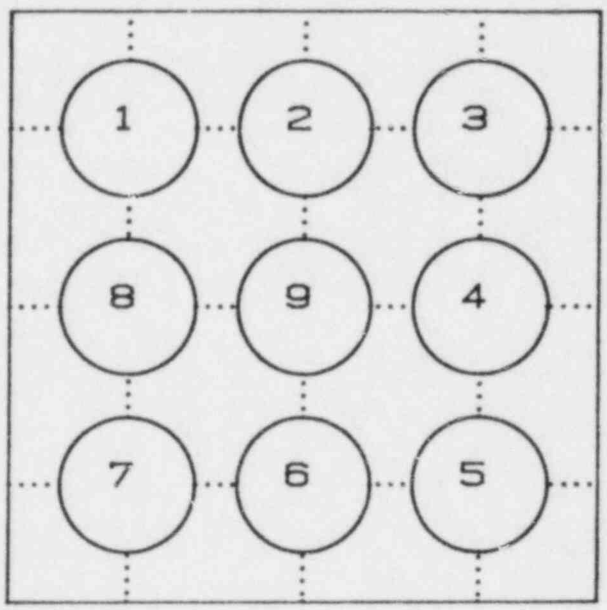

FIGURE 3-8. RADIAL GEOMETRY

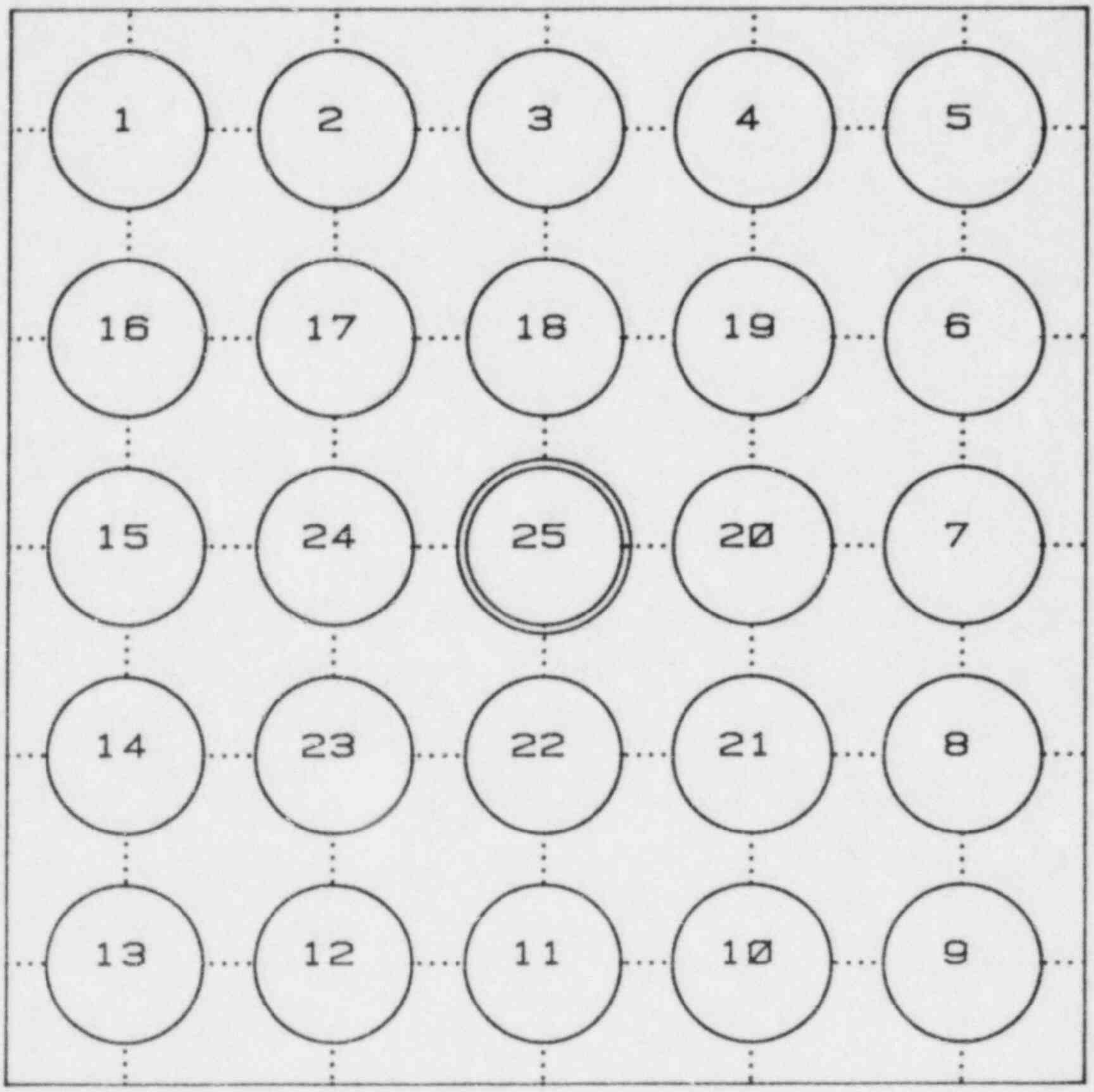

FIGURE 3-9. AXIAL HEAT FLUX DISTRIBUTIONS.

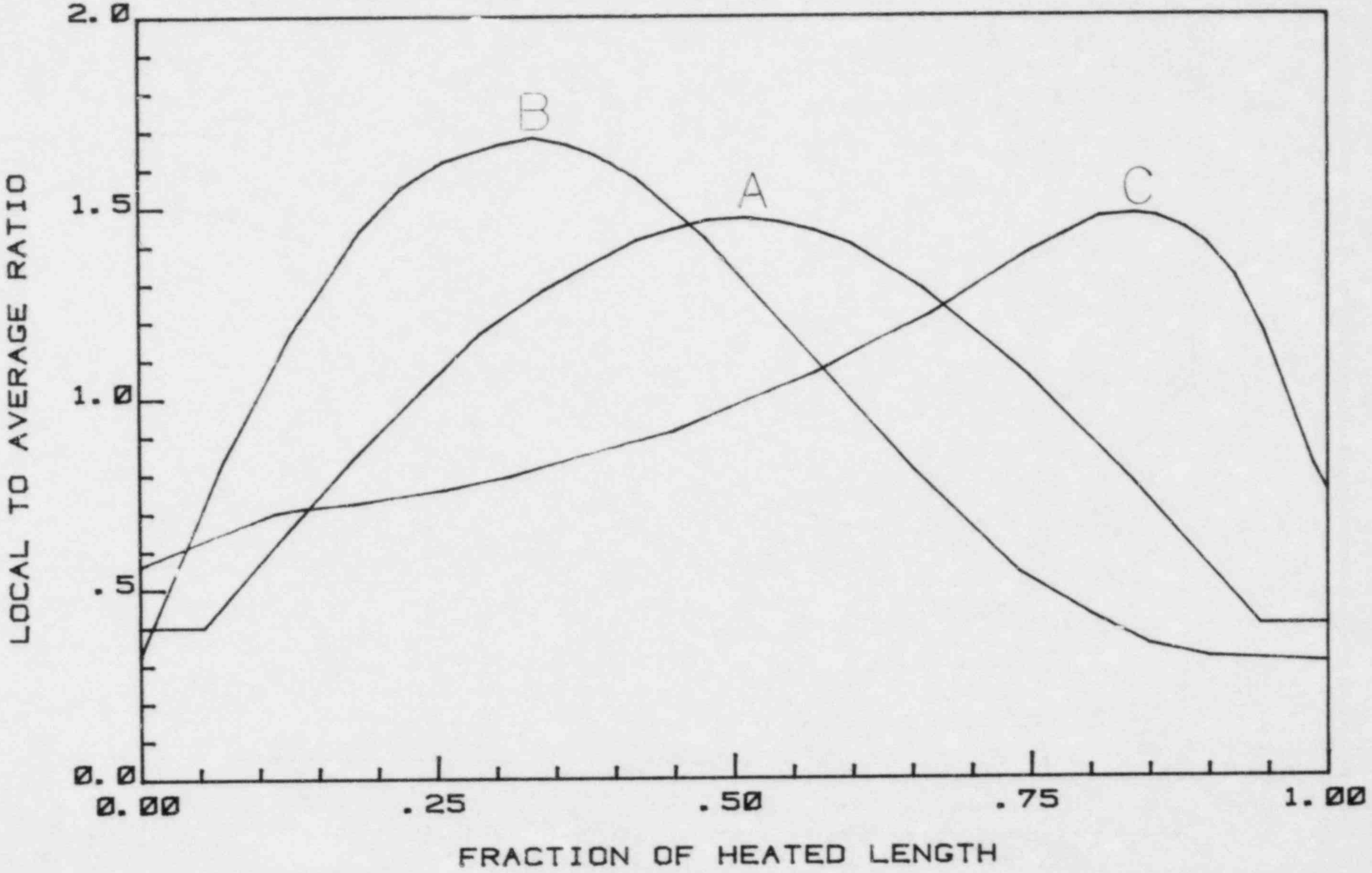

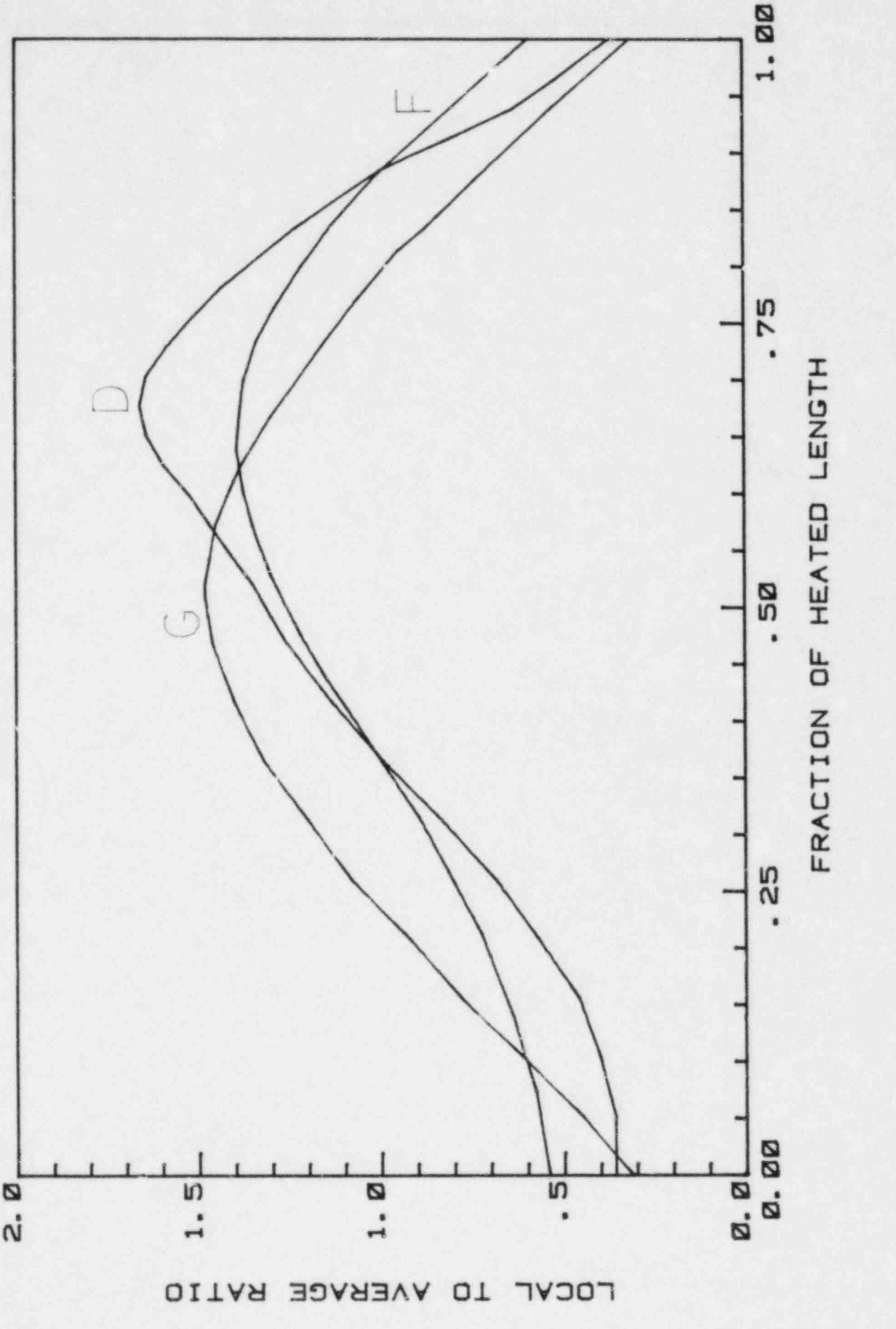

FIGURE 3-10. AXIAL HEAT FLUX DISTRIBUTIONS.

FIGURE 3-11. AXIAL HEAT FLUX DISTRIBUTIONS.

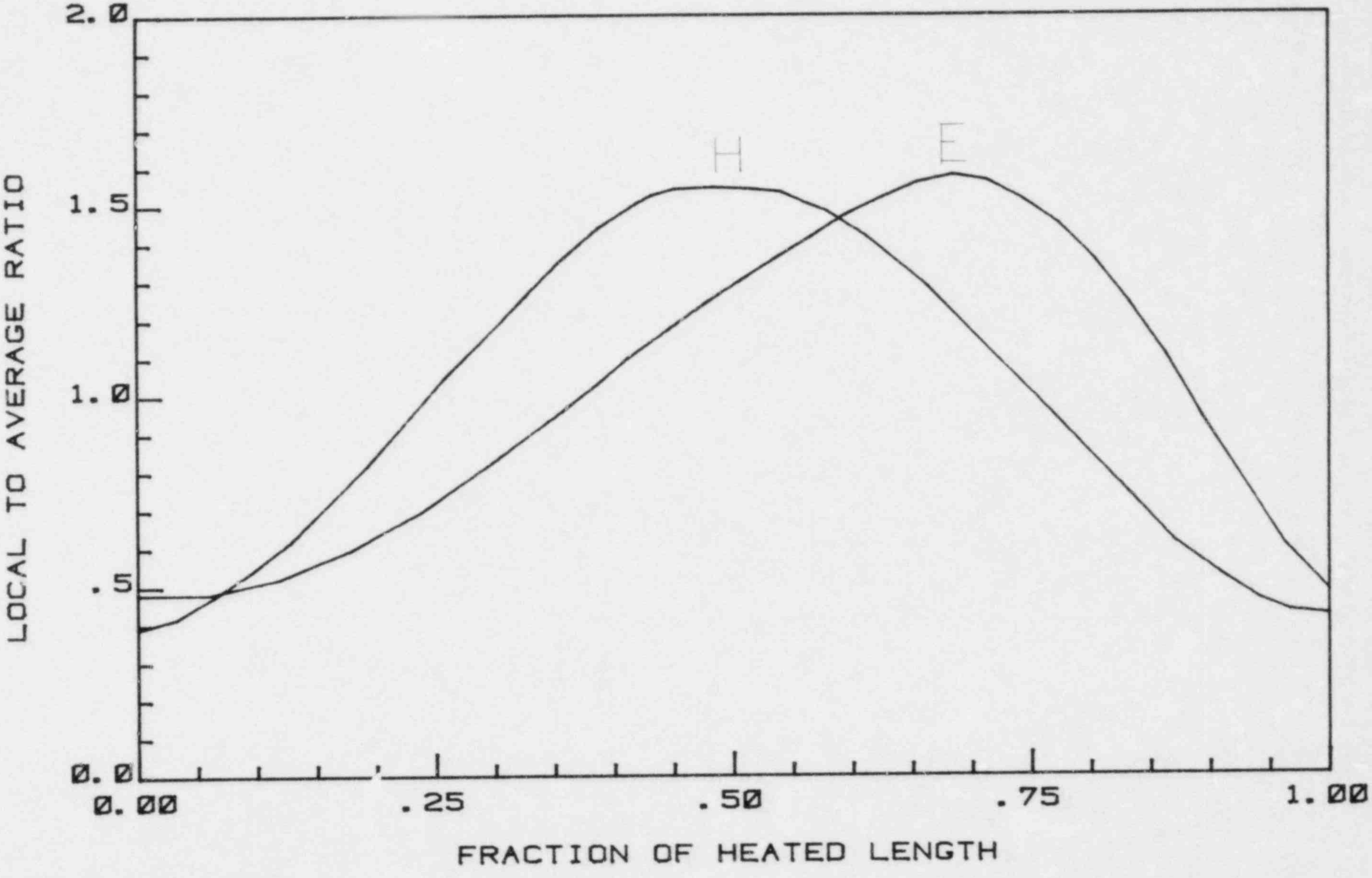

Chapter 4

METHOD OF APPROACH

There are two basic approaches to the prediction of CHF in rod bundles; the first is the mixed flow analysis, and the second is the subchannel analysis. The mixed flow analysis consists of the use of correlations based on the bundle average conditions which relate the CHF to the system nominal pressure, average heat flux, average mass velocity, and bundle inlet temperature, all of which can be easily measured. The subchannel analysis approach uses correlations based on the local conditions which relate the CHF to the pressure, heat flux, coolant velocity, and enthalpy at the CHF location. Since the measurement of the local conditions is practically impossible, the standard procedure is to determine these conditions analytically using various computer models.

A major advantage of correlations based on the bundle average conditions is that they are simple to use and do not require large computer codes to develop a CHF correlation. However, these correlations are valid only for conditions representative of the data on which they are based. They cannot be used with a high degree of confidence to predict CHF in a new rod bundle with a different geometry or with different radial or axial heat flux profiles.

The CHF correlations based on the local conditions at the CHF location require a detailed thermal hydraulic analysis capable of accurately predicting the flow and fluid enthalpy in various regions of the fuel assembly model. Such a need can be met by employing advanced methods of calculation of radial and axial distribution of mass flow rate and enthalpy in the fuel assembly with the help of large digital computers.

These methods are generally referred to as subchannel analyses and have been developed for the thermal hydraulic analysis of nuclear reactors.

The subchannel analysis methods are recognized as a more complete means of analysis and prediction of the steady state thermal and hydraulic behavior of PWR fuel assemblies. Several subchannel codes, COBRA (5), HAMBO (6), THINC (7), TORC (8), MIXER (9), FLICA (10), CORAL (11), and SASS (12) are in use in the nuclear industry. The COBRA codes are the most widely used because they are the best documented of the subchannel analysis procedures. The basic thermal-hydraulic and physical modeling used is based on assumptions common to most suchannel codes.

In subchannel analysis techniques, the cross section of the rod bundles is subdivided into a number of hydraulically interconnected subchannels. The basic principle of subchannel analysis is the application of equations of mass, energy, and momentum conservation to flow along and between these subchannels. The interchange of mass, heat, and momentum between neighboring subchannels is included in these conservation equations. The conservation equations are solved to give radial and axial variations in fluid enthalpy and mass flow rate. Having established local conditions in each subchannel, the CHF is calculated from a CHF correlation developed specifically for use with the subchannel code.

The COBRA codes have undergone considerable improvement in recent years. The COBRA I and the COBRA II were steady state codes. The transient flow calculations were added in the COBRA III code. In the COBRA IIIC code, an improved transverse momentum balance was introduced. The COBRA IIIC subchannel code was employed in the present analysis. In addition to the continuity and conservation equations some physical models or correlations are required for the evaluation of parameters such as subcooled voids, bulk voids, single-phase friction factor, two-phase friction multiplier, turbulent mixing coefficient for single-phase and two-phase conditions, cross flow resistance, etc. The input correlation options and input parameters used in this study are discussed here and summarized in Table 4-1.

Table - 4-1

Input Parameters Used in the COBRA-IIIC Code

Single-phase friction factor	$f = 0.186\ Re^{-0.2}$
Two-phase density	$\rho = \alpha\rho_g + (1-\alpha)\rho_f$
Two-phase specific volume	$v' = 1/\rho$
Cross flow enthalpy (h*)	Donor channel enthalpy
Cross flow axial velocity (U*)	Average velocities of the adjacent channels
Momentum turbulent factor	0
Transverse momentum parameter	0.5
Cross flow resistance	0.5
Number of axial nodes	60
Correlations Investigated	
Subcooled void correlation	No subcooled voids Bowring Jens-Lottes and Griffith-Maurer Levy*
Bulk void Correlation	Homogeneous model* Modified Armand Bankoff Van-Glahn Thom Smith slip ratio
Two-phase friction multiplier	Homogeneous model Armand Tarasova Thom Martinelli-Nelson Columbia*
Turbulent mixing parameter	0.0 0.001 0.005 0.01 0.02* 0.1

*Correlations used in the present study.

4.1 Single-Phase Friction Factor

The flow through the bundle for the range of test conditions covered in the present analysis was turbulent. The following two friction factor correlations, generally used to calculate frictional pressure drop in smooth tubes, were investigated:

- McAdams Correlation ($f = 0.186\ Re^{-0.2}$)
- Blasius Correlation ($f = 0.316\ Re^{-0.25}$)

where Re is the Reynold's number. The McAdams correlation was used in the present analysis, because the local conditions predicted by the COBRA IIIC subchannel code were not very sensitive to the single-phase friction factor.

4.2 Subcooled Void Correlation

The following four subcooled void options were investigated:

1. No subcooled voids
2. Bowring subcooled void model
3. Jens and Lottes and Griffith-Maurer model
4. Levy subcooled model

Levy's subcooled void model was chosen in the present analysis for two reasons. First, unlike other models, it provides a continuous void profile from subcooled to bulk boiling conditions. Second, its agreement with the experimental subcooled void data is good, both at high pressures and low pressures (13,14).

4.3 Bulk Void Correlation

The sensitivity of local conditions predicted by the COBRA IIIC subchannel code to the following void options was investigated:

1. Homogeneous model
2. Modified Armand correlation
3. Bankoff correlation
4. Van Glahn correlation
5. Thom correlation
6. Smith slip ratio

In general, the sensitivity of the local conditions to the bulk void option was found to be not very significant. Given this insensitivity, the homogeneous model was chosen because it is widely used and is generally recognized to show good agreement with the available data, particularly at high pressures.

4.4 Two-Phase Friction Multiplier Correlation

The Columbia two-phase friction multiplier (15,16) described below, was used in the present study. Recently, an accurate two-phase friction multiplier for use with the homogeneous model in nuclear reactor core analysis was developed at the Heat Transfer Research Facility of Columbia University under a research program sponsored by EPRI. Several other correlations investigated were the homogeneous, Armand, Tarasova, Thom, and Martinelli-Nelson. The Columbia friction multiplier was chosen for the following reasons:

- It is compatible with the homogeneous model.
- It is based on data covering a very wide range of parameters.
- The dependency on mass flux is properly accounted for by this correlation.

The basic form of the Columbia friction multiplier is,

$$\Phi^2_{\ell o} = 1 + X\left(\frac{V_g}{V_\ell} - 1\right)C$$

For pressures >600 psia,

$$C = 1.02\ X^{-0.175}\ G^{-0.45}$$

For pressures between 300 and 600 psia,

$$C = 0.357\ (1 + 10\,Pr)\ X^{-0.175}\ G^{-0.45}$$

where,

$\Phi^2_{\ell o}$ is the two-phase friction multiplier,

X is the equilibrium quality,

V_g and V_l are the specific volumes,

G is the mass flux, and

Pr is the reduced pressure ($P/P_{critical}$).

The Columbia friction multiplier predicts the source data (1533 adiabatic two-phase pressure drop data points) with a standard deviation of 9.7%. The applicability of the correlation in diabatic conditions was established by comparing it with 865 diabatic data points. The adequacy of the correlation at the high pressure range was evaluated by comparing the correlation with Sher and Green's friction multiplier table (17), the Thom correlation, and the homogeneous model. Good agreement between these correlations established the applicability of the Columbia two-phase friction multiplier correlation at high pressures encountered in PWRs.

4.5 Grid Loss Coefficient

In the COBRA IIIC subchannel code, the pressure drop accross grid spacers is calculated using user defined coefficients for each spacer and subchannel within the node where a grid spacer is present. The grid loss coefficient is defined as

$$K_g = \frac{\Delta P_G}{nG^2/2g_c\rho}$$

where

ΔP_G is the pressure drop due to the spacers,

G is the mass flux,

g_c is the Newton constant,

n is the number of spacer grids.

The spacer coefficients used in this work were calculated using isothermal pressure drop data. The total pressure drop in the rod bundle due to both friction and spacer was determined at various flow rates under isothermal conditions. The pressure drop due to grid spacers is,

$$\Delta P_G = \Delta P_t - \Delta P_f$$

where,

ΔP_t is the total frictional pressure drop, and

ΔP_f is the pressure drop due to friction.

The pressure drop exclusively due to friction was calculated by determining the equivalent diameter of the bundle and using the following equation:

$$\Delta P_f = \frac{fG^2L}{2g_c \rho De}$$

where,

f is the single phase friction factor,

L is the length of the bundle,

D_e is the equivalent diameter of the bundle, and

ρ is density of the coolant.

A summary of the correlations investigated and input parameters used in the present study are presented in Table 4-1.

Chapter 5

ANALYSIS OF MULTIPLE CHF DATA

As stated earlier, the method of approach adopted in the study of multiple CHF was to assume that the critical heat flux is dependent on local conditions in the subchannels of a reactor core. Thus, the basic philosophy in the present analysis was to apply the procedures used traditionally for the study of the first CHF to the study of the CHF events of higher rank in order to determine similarities, differences, or trends among the multiple CHF events. Therefore, local coolant conditions were predicted at the first CHF indication as well as at the higher rank CHF indications using the COBRA IIIC subchannel code for the test inlet conditions and the measured bundle power for each of the test runs. These local conditions were then substituted into various subchannel CHF correlations (particularly those used in the nuclear industry) to determine the predicted value of CHF at the location where experimental CHF was observed. Comparisons were then made between the experimental and predicted values of the CHF at the first, second, third, and fourth CHF indications to ascertain the applicability of each correlation to the prediction of higher rank CHF events.

Two methods were adopted in the analysis of multiple CHF data; first the statistical approach, and second the parametric study.

The statistical studies involved computation of the following three statistics:

1. Average Ratio $\quad R_{ave} = \frac{1}{N} \sum_{i=1}^{N} R_i$

2. Root Mean Square Error $\quad RMS = \left[\sum_{i=1}^{N} \frac{(R_i - 1)^2}{N} \right]^{1/2}$

3. Standard Deviation $\quad STD = \left[\sum_{i=1}^{N} \frac{(R_i - Rave)^2}{N} \right]^{1/2}$

where N is the number of points and R is the ratio of predicted to local experimental CHF.

These three correlation statistics were calculated at the location of the first, second, third, and fourth CHF indications separately and the combined statistics for all the higher order CHF indications (all except the first) were also computed. This method reveals the accuracy of the CHF correlation in predicting the second, third , fourth, and higher order CHF indications compared to its accuracy in predicting the first CHF. In addition, the trends in these correlation statistics indicate any systematic errors associated with the application of the CHF correlation to the prediction of multiple CHF.

The parametric studies were performed by the examination of the residual plots. In the residual analysis, the ratio of the predicted to the local experimental CHF was plotted against the parameters appearing in the CHF correlations, such as, pressure, local quality, local mass flux, inlet quality, and local experimental CHF. These figures were prepared for the first, second, third, fourth, and the higher order CHF separately. The distribution of the residuals with respect to the above mentioned parameters was examined to determine similarities, differences, and trends among the multiple CHF events.

The following three data sets were used in the analysis of multiple CHF data:

1. BWR uniform axial heat flux data

2. PWR uniform axial heat flux data

3. PWR non-uniform axial heat flux data

Briefly stated, a combination of statistical analyses and parametric studies (based on the local conditions obtained with the COBRA IIIC subchannel code) were employed to compare the characteristics of the CHF events of the higher rank with those of the first CHF for the three data sets mentioned above, separately. The results of the analysis of each data set are discussed separately in the following sections.

5.1 BWR Uniform Axial Heat Flux Data

The state-of-the-art of determining CHF limits in BWR fuel assemblies is based on the mixed flow analysis, in which bundle average coolant conditions are used to calculate the critical power of the fuel assemblies. At present, there are no CHF correlations available in the open literature applicable to BWR type fuel assemblies which predict CHF in subchannels based on the local coolant conditions. One of the accurate bundle average correlations applicable to BWR type bundles, although not used in the licensing of BWRs in US, is the Bowring correlation (18). The results of using this correlation in the analysis of multiple CHF data were discussed in Reference 1.

Recently, a generalized subchannel CHF correlation was developed at the Heat Transfer Research Facility of Columbia University based on the local coolant conditions obtained with the COBRA IIIC subchannel code. The data base used in the development of the Columbia CHF correlation (16,19) included 3,607 data points from 65 test sections, typical of BWR and PWR fuel assemblies and cover both the PWR and BWR normal operating conditions as well as hypothetical LOCA conditions. The Columbia correlation is the only known CHF correlation (with the exception of the WSC-2 correlation (20) which was developed in concert with the HAMBO (6) subchannel code) which covers both the PWR and BWR operating conditions.

The summary of the Columbia CHF correlation is given in Table 5-1, and the range of the data base and error statistics in predicting the source data are given in Table 5-2. The correction factors to account for the cold wall effect when the correlation is applied to corner channels and corresponding data base and error statistics are presented in Table 5-3. Unlike most other subchannel CHF correlations in the literature, this correlation is based on the local coolant conditions at the first CHF indication; the second and higher rank CHF were not utilized in its development. For these reasons, the Columbia CHF correlation was used in the analysis of multiple CHF events in the BWR type fuel assemblies.

The data employed in this study consist of 762 CHF points from 18 General Electric test sections with uniforn axial heat flux distribution. Of these data, a total of 612 CHF points which were within the parameter ranges of the Columbia CHF correlation, were reduced to local condition form using the COBRA IIIC subchannel code. Employing the local coolant conditions of these data, the CHF at the first, second, third, and fourth CHF indications were calculated using the Colunbia CHF correlation. The critical heat flux ratio CHFR, defined as the ratio of the predicted to the local experimental CHF, at the first, second, third, and fourth CHF indications were computed for all the data and a combination of statistical analysis and parametric studies were performed to evaluate the applicability of the Columbia CHF correlation to higher rank CHF.

The results of the statistical analysis consisting of the three statistics, the average ratio, RMS error, and standard deviation from the mean, were computed and compiled in Table 5-4 for four sets of data; the first, second, third, and fourth CHF indications. Also, similar statistics for higher order CHF (the second, third, and fourth CHF indications) and all the CHF data (the first and higher rank CHF indications) are given in Table 5-4.

The parametric studies involved plotting of the ratio of the predicted to observed CHF for the first, second, third, and higher rank CHF events versus the following variables in Figures 5-1 through 5-12:

TABLE 5-1

Columbia CHF Correlation Summary

$$q''_c = \frac{A - X_{in}}{C + \left[\frac{X_\ell - X_{in}}{q''_\ell}\right]}$$

where,

$$A = P_1 P_r^{P_2} G^{(P_5 + P_7 P_r)}$$

and

$$C = P_3 P_r^{P_4} G^{(P_6 + P_8 P_r)}$$

q''_c and q''_L are critical and local heat fluxes $\frac{\text{M.BTU}}{\text{HR-FT}^2}$

X_{in} and X_L are inlet and local qualities,

G is mass flux (M.LBS/HR-FT^2) and

P_r is reduced pressure ($P/P_{Critical}$),

P_1 through P_8 are constants.

P_1 = 0.5328

P_2 = 0.1212

P_3 = 1.6151

P_4 = 1.4066

P_5 = -0.3040

P_6 = 0.4843

P_7 = -0.3285

P_8 = -2.0749

TABLE 5-2

Columbia Correlation - Parameter Ranges and Error Statistics

Local Mass Flux:	0.2 to 4.1 M.LBS/HR-FT^2
Pressure:	200 to 2450 PSIA
Local Quality :	-0.25 to -0.75
Inlet Quality:	-1.1 to 0.0
Hydraulic Diameter:	0.35 to 0.55 Inches
Heated Diameter:	0.25 to 0.55 Inches
Length:	36 to 168 Inches
Rod Diameter:	0.38 to 0.68 Inches
Number of Rods:	3X3 to 5X5
Radial Profile:	Uniform & Non-Uniform (Radial and Corner Peaking)
Axial Profile:	Uniform
Subchannel Type:	Matrix Channels Only
Rod Bundle Type:	PWR and BWR (With and Without Unheated Rods)

Error Statistics

Number of Test Sections:	TSNS = 65
Number of Points:	NPTS = 3607
Average Ratio:	RAVE = 0.995
RMS Error:	RMS = 7.20%
Standard Deviation:	STD = 7.20%
Residual Distribution:	51 % of Points Within ± 5% Error Band
	82 % of Points Within ± 10% Error Band
	97 % of Points Within ± 15% Error Band
	99.9 % of Points Within ± 20% Error Band

TABLE 5-3

Summary of Cold Wall Correction Factors

$$q''_c = \frac{A F_A - X_{in}}{C F_c + \left[\frac{X_\ell - X_{in}}{q''_\ell}\right]}$$

Where F_A and F_C are cold wall correction factors

$$F_A = G^{0.1}$$

and $$F_C = 1.183\ G^{0.1}$$

Parameter Ranges:

Pressure:	600 to 1500 PSIA
Local Mass Flux:	0.15 to 1.2 M.LBS/HR-FT^2
Local Quality:	0.0 to 0.70
S. C. Type:	Corner Channels Only

Error Statistics:

Number of Test Sections:	TSNS	=	22
Number of Points:	NPTS	=	638
Average Ratio:	RAVE	=	0.997
RMS Error:	RMS	=	6.13 %
Standard Deviation:	STD	=	6.13 %

TABLE 5-4

ANALYSIS OF BWR DATA

NUMBER OF TEST SECTIONS	=	18
NUMBER OF DATA POINTS	=	612
PRESSURE RANGE (PSIA)	=	900 TO 1450
MASS FLUX RANGE (M.LBS HR-SQFT)	=	0.15 TO 2.50
LOCAL QUALITY RANGE (%)	=	0.0 TO 70.

COLUMBIA CHF CORRELATION

CHF RANK	NO. OF POINTS	AVE. RATIO	RMS ERROR	STD. DEVIATION
FIRST CHF	612	1.005	0.054	0.054
SECOND CHF	223	0.991	0.052	0.051
THIRD CHF	63	0.981	0.050	0.046
FOURTH CHF	17	0.983	0.048	0.046
HIGHER ORDER CHF (SECOND & HIGHER)	307	0.988	0.051	0.050
ALL CHF	915	1.000	0.053	0.053

FIGURE 5-1 PLOT OF Q-CALC/Q-OBS RATIO VERSUS QUALITY
COLUMBIA CORRELATION - FIRST CHF - BWR

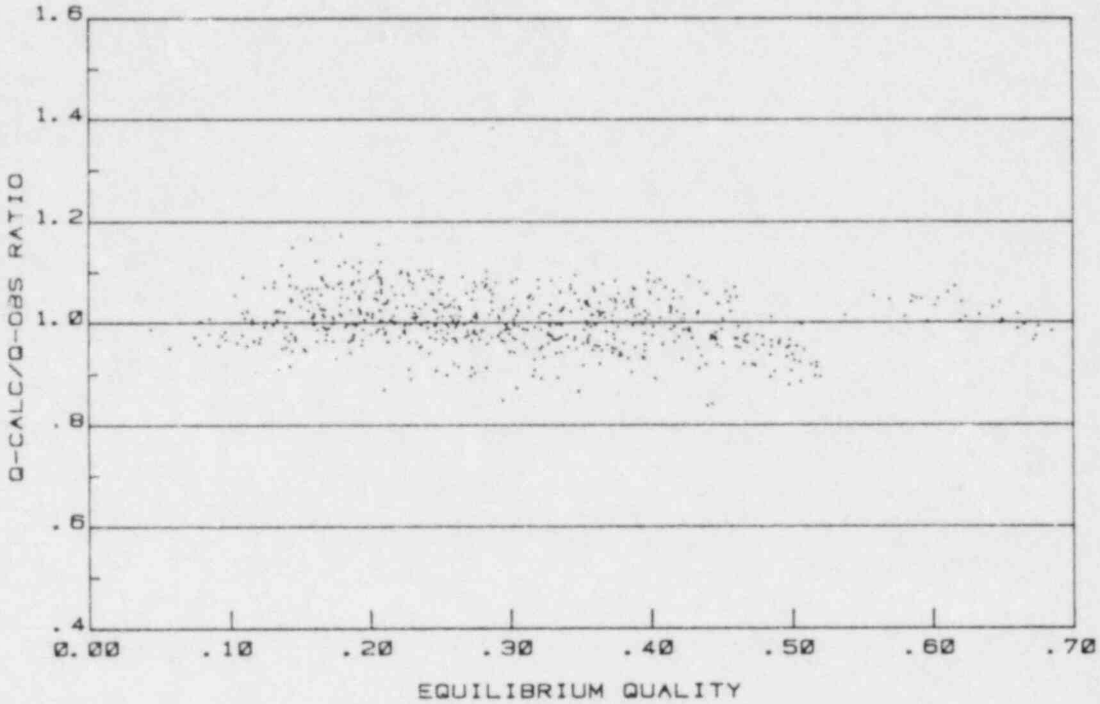

FIGURE 5-2 PLOT OF Q-CALC/Q-OBS RATIO VERSUS QUALITY
COLUMBIA CORRELATION - HIGHER ORDER CHF - BWR

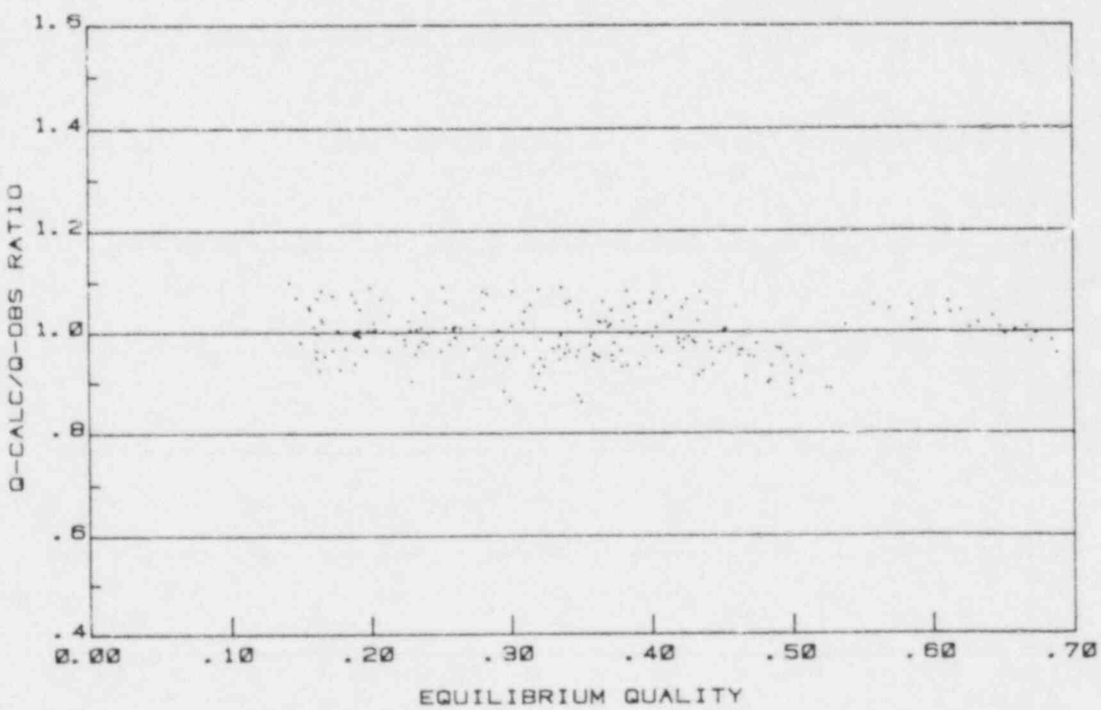

FIGURE 5-3 PLOT OF Q-CALC/Q-OBS RATIO VERSUS QUALITY
COLUMBIA CORRELATION - SECOND CHF - BWR

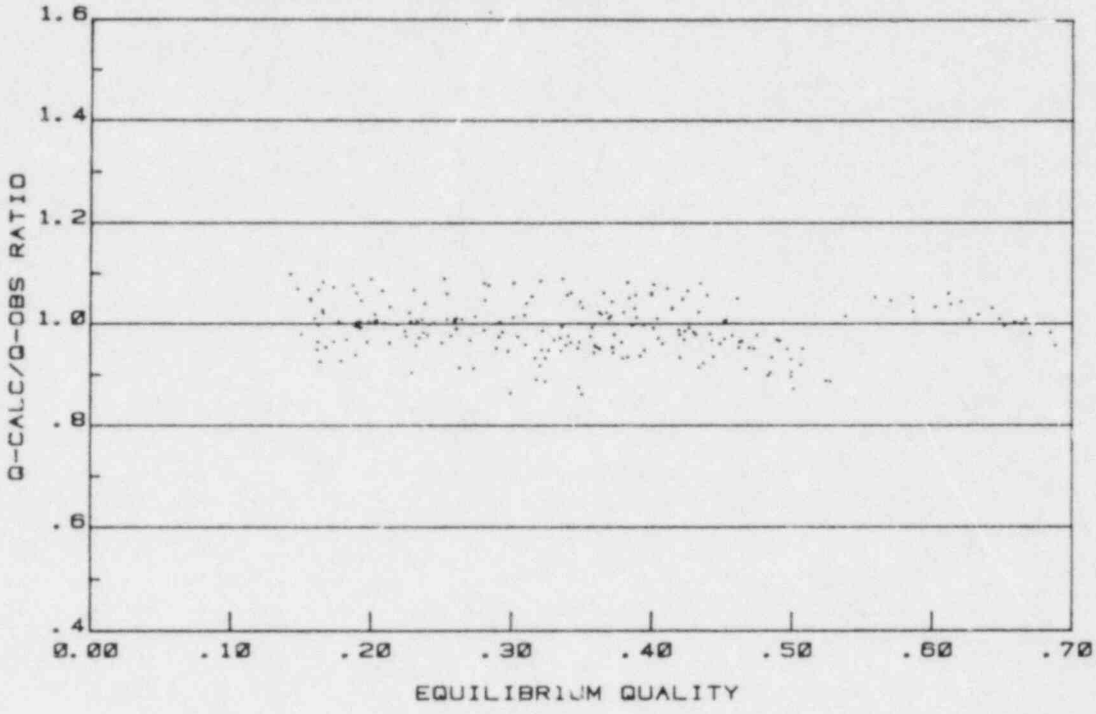

FIGURE 5-4 PLOT OF Q-CALC/Q-OBS RATIO VERSUS QUALITY
COLUMBIA CORRELATION - THIRD CHF - BWR

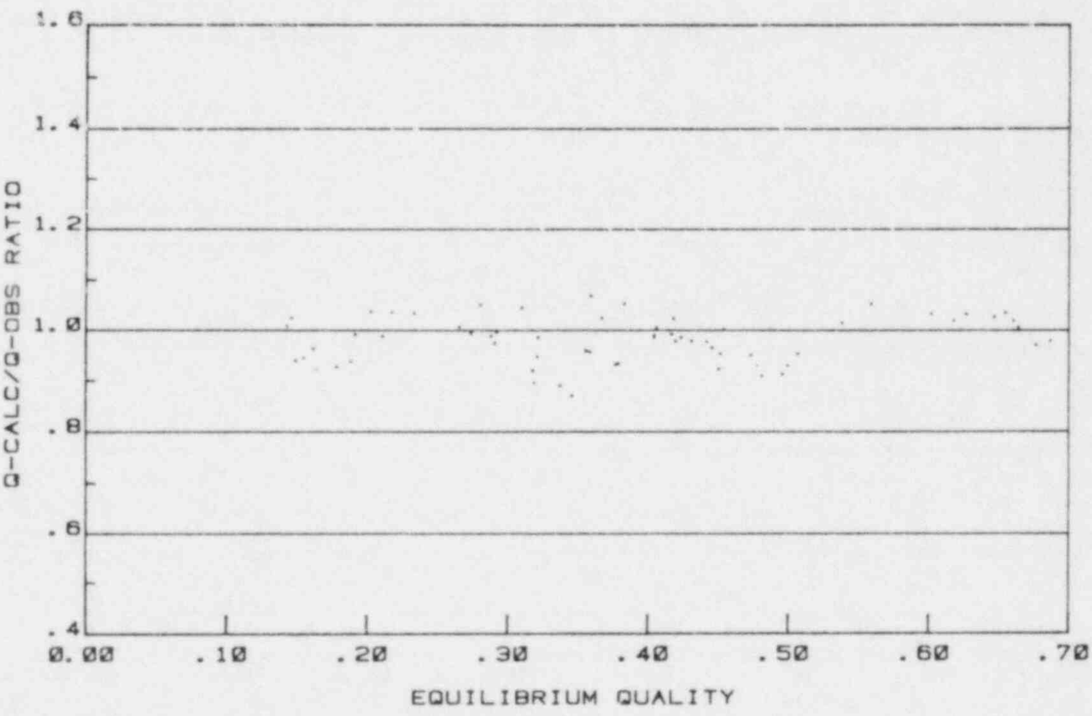

FIGURE 5-5 PLOT OF Q-CALC/Q-OBS RATIO VERSUS MASS FLUX
COLUMBIA CORRELATION - HIGHER ORDER CHF - BWR

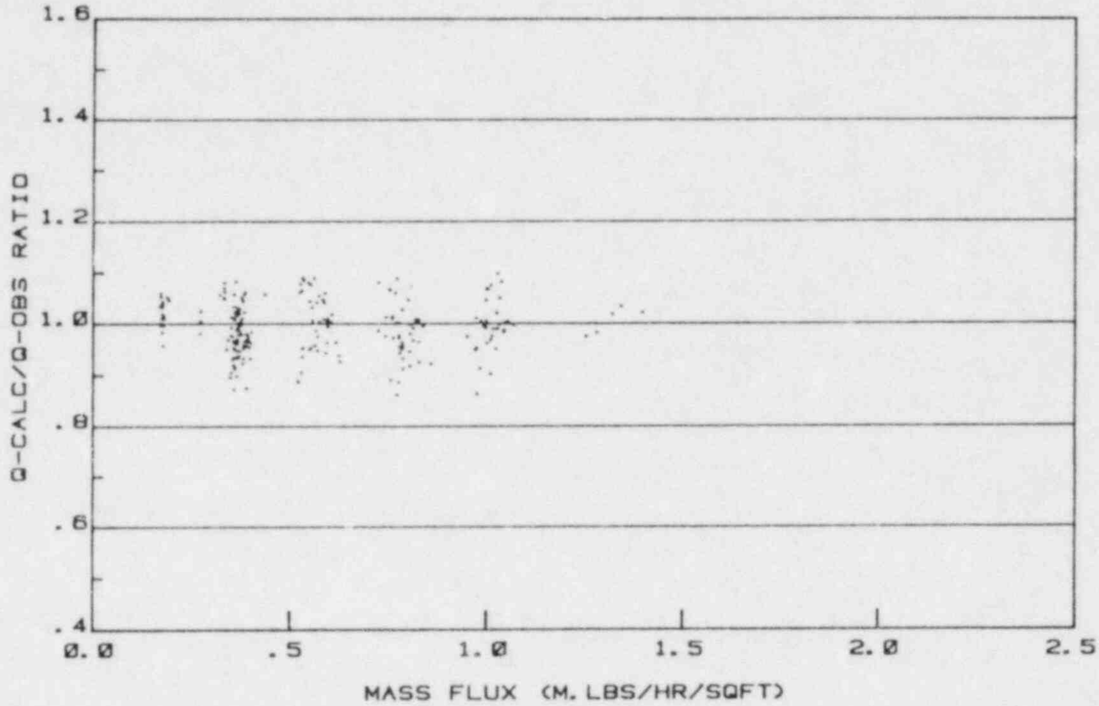

FIGURE 5-6 PLOT OF Q-CALC/Q-OBS RATIO VERSUS MASS FLUX
COLUMBIA CORRELATION - FIRST CHF - BWR

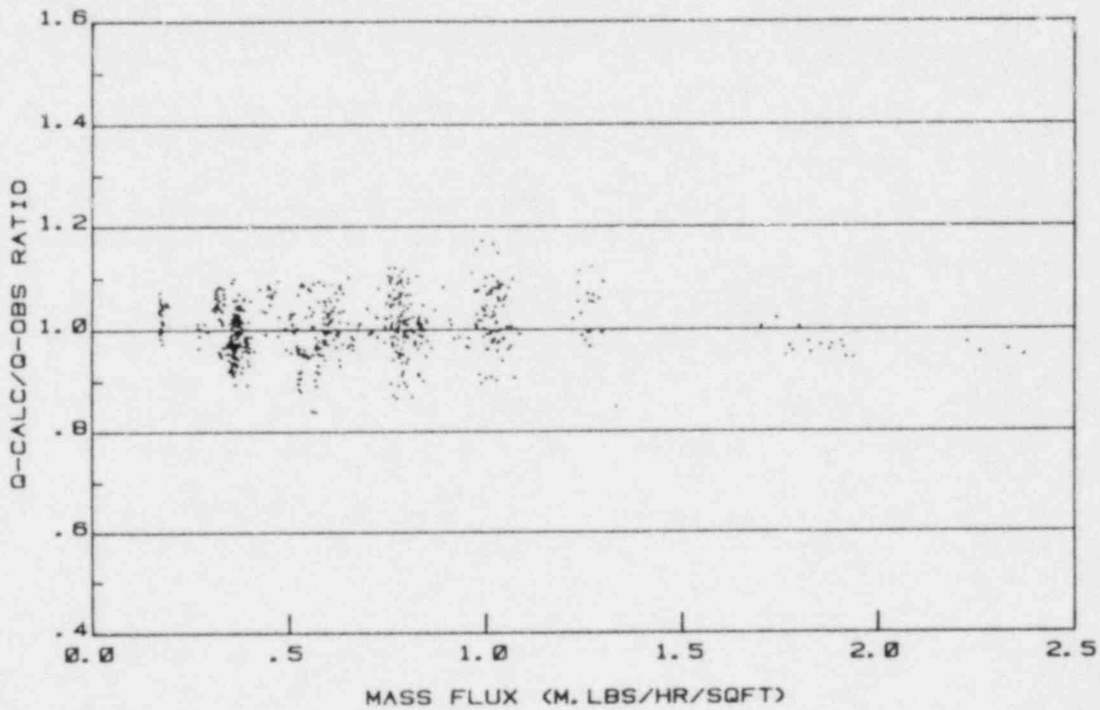

FIGURE 5-7 PLOT OF Q-CALC/Q-OBS RATIO VERSUS PRESSURE
COLUMBIA CORRELATION - FIRST CHF - BWR

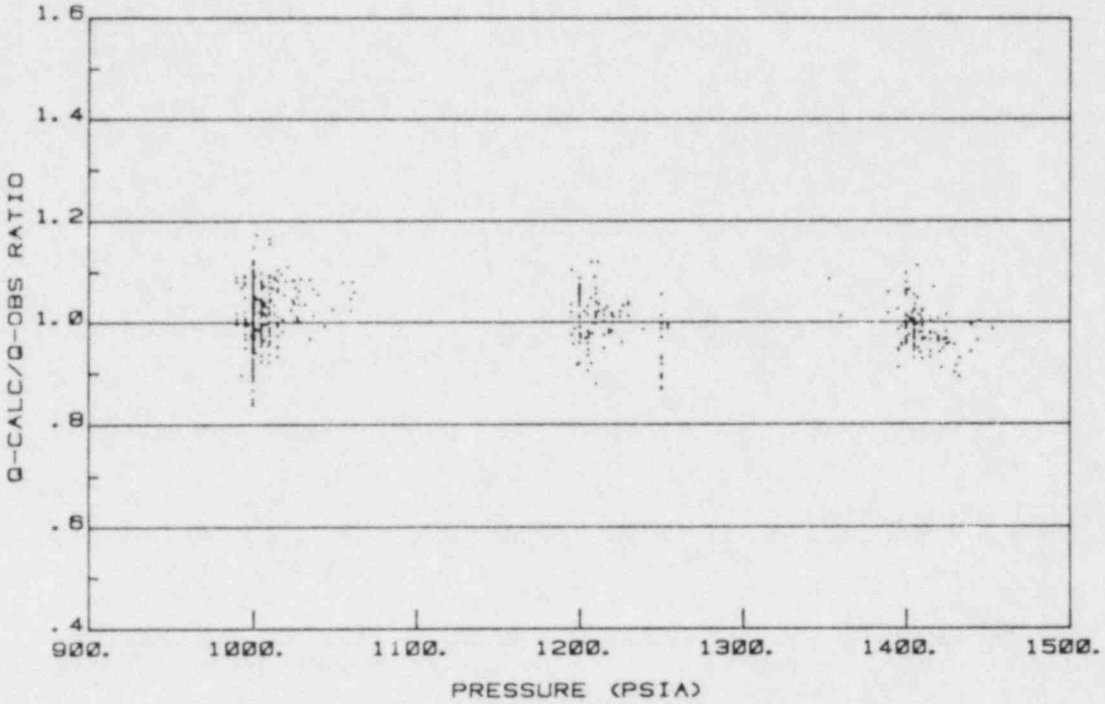

FIGURE 5-8 PLOT OF Q-CALC/Q-OBS RATIO VERSUS PRESSURE
COLUMBIA CORRELATION - HIGHER ORDER CHF - BWR

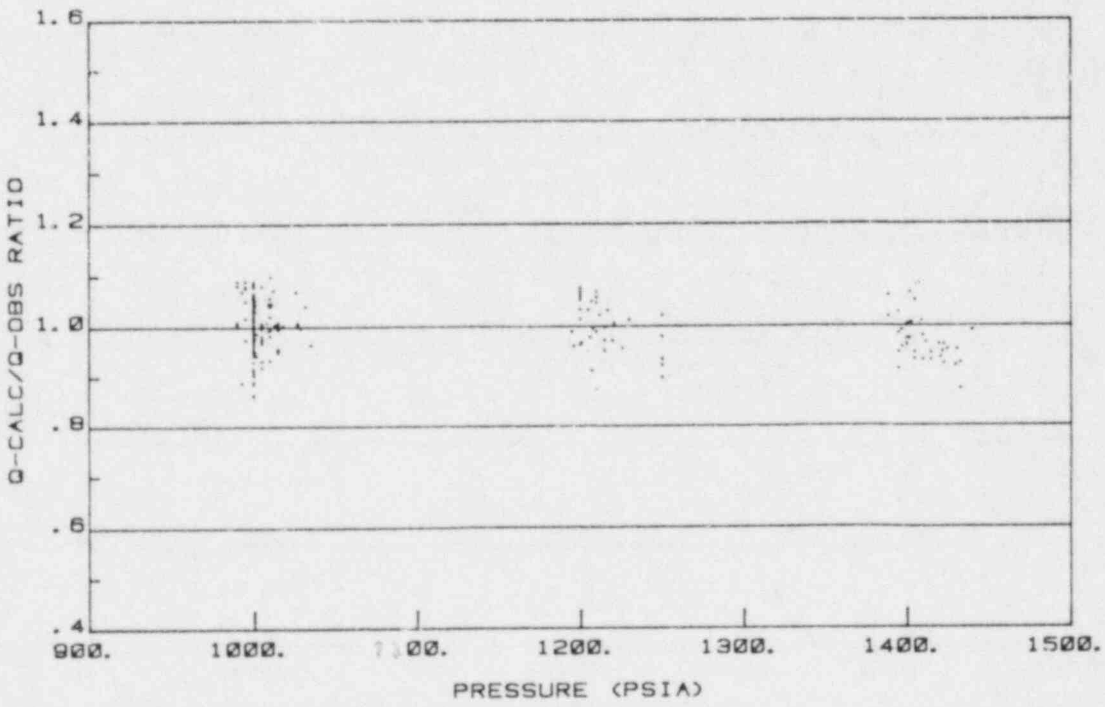

FIG. 5-9 PLOT OF Q-CALC/Q-OBS RATIO VERSUS INLET QUALITY
COLUMBIA CORRELATION - FIRST CHF - BWR

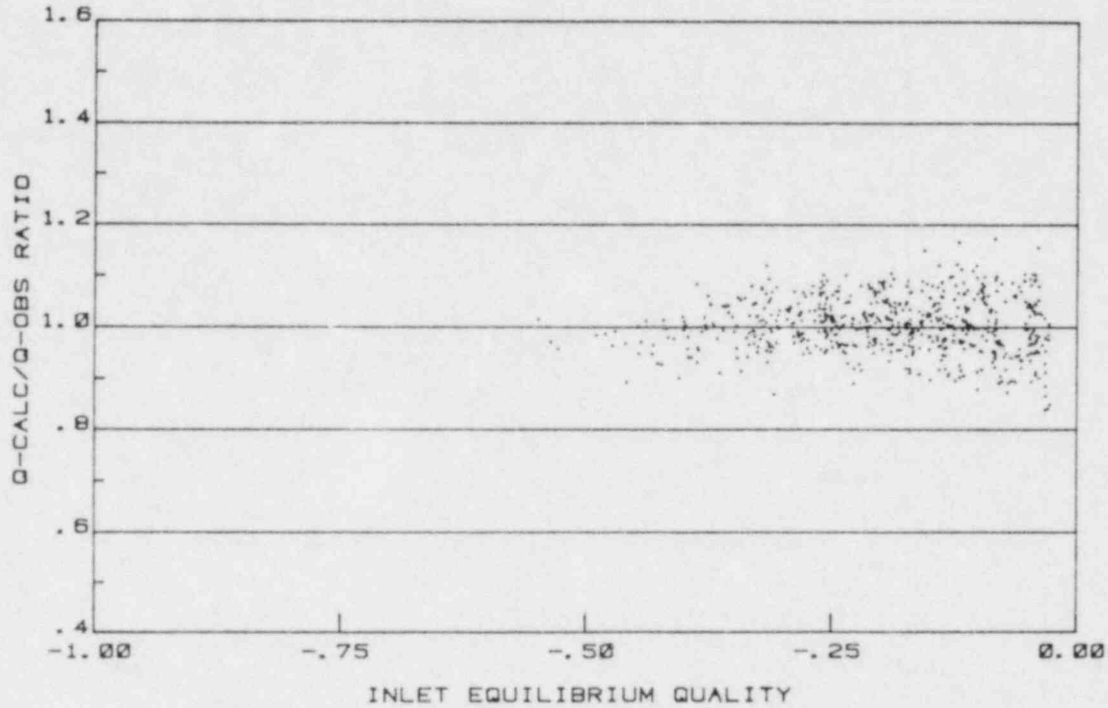

FIG. 5-10 PLOT OF Q-CALC/Q-OBS RATIO VERSUS INLET QUALITY
COLUMBIA CORRELATION - HIGHER ORDER CHF - BWR

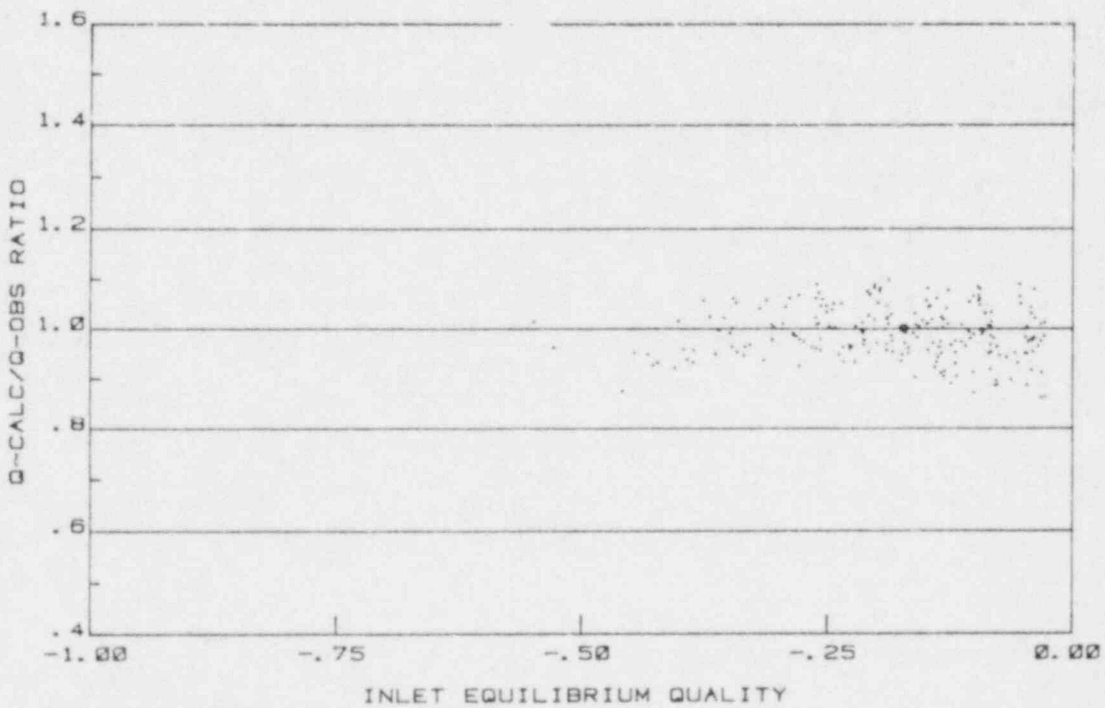

FIG. 5-11 PLOT OF Q-CALC/Q-OBS RATIO VERSUS OBSERVED CHF
COLUMBIA CORRELATION - FIRST CHF - BWR

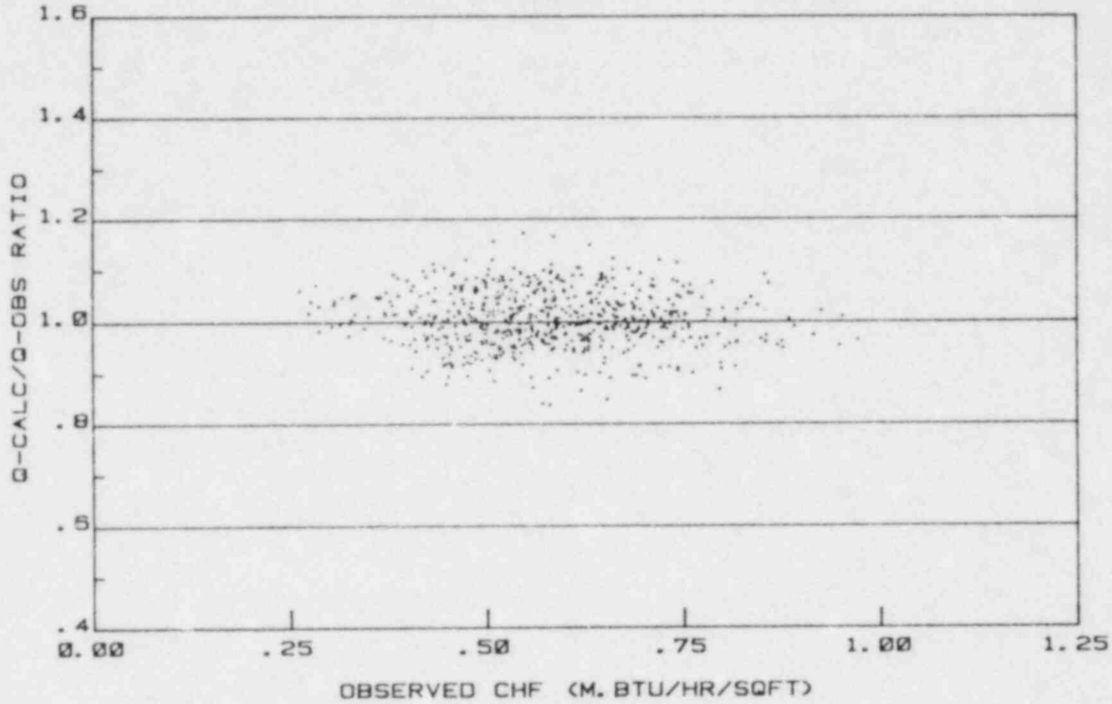

FIG. 5-12 PLOT OF Q-CALC/Q-OBS RATIO VERSUS OBSERVED CHF
COLUMBIA CORRELATION - HIGHER ORDER CHF - BWR

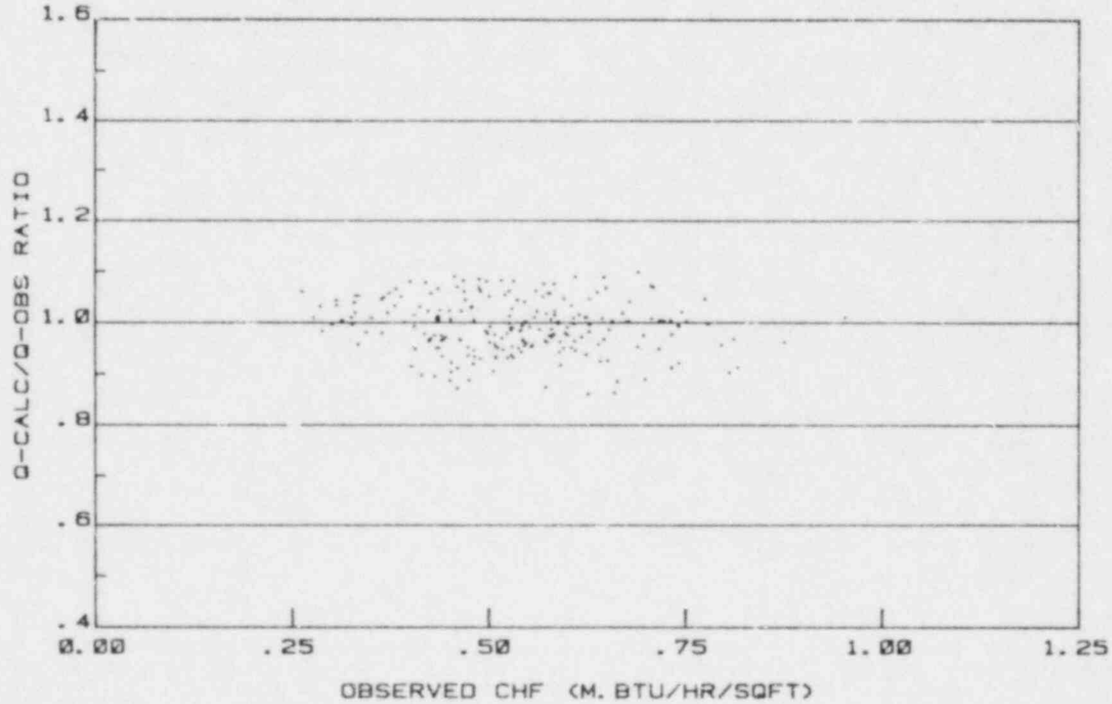

- Local quality
- Local mass flux
- Pressure
- Inlet quality
- Local experimental CHF

In the case of local quality, all the four residual plots (the first, second, third, and higher rank CHF plots) are included in this report. However, for the rest of the parameters, only two plots (the first and higher rank CHF plots) are included; the remaining plots are omitted to avoid unnecessary repetition.

An examination of the results of the statistical analyses (Table 5-4) and parametric studies (Figures 5-1 through 5-12) leads to the following conclusions:

1. The trends in the residual distributions of the first CHF and higher rank CHF events with respect to Local quality, Local mass flux, pressure, inlet quality, and local experimental CHF are almost identical.
2. The Columbia CHF correlation is useful in the prediction of the CHF events of higher rank. This correlation predicts the CHF events of higher rank with the same accuracy as that of the first CHF.

5.2 PWR Uniform Axial Heat Flux Data

The analysis of this set of data was performed with four CHF correlations based on local conditions; the CE-1 correlation (21), the B&W-2 correlation (22), the W-3 correlation (23), and the Columbia CHF correlation (16,19). The summaries of the CE-1, B&W-2, and W-3 correlations are given in Tables 5-5, 5-6, and 5-7 respectively.

The data used in this phase of the study consists of 931 CHF points from 15 Combustion Engineering test sections. The COBRA IIIC code was

Table 5-5

CE-1 CHF Correlation

$$q''_c = \frac{A' (A - BX)}{C}$$

where $A' = b_1 (d/d_m)^{b_2}$,

$A = (b_3 + b_4 P) G^{(b_5 + b_6 P)}$,

$B = G H_{fg}$,

and $C = G^{(b_7 P + b_8 G)}$,

q''_c is critical heat flux (M•Btu/hr-ft^2),

G is mass flux (M•lbs/hr-ft^2),

P is pressure (Psia),

X is quality,

d is subchannel equivalent diameter (inches),

d_m is matrix channel equivalent diameter (inches), and

b_1 through b_8 are constants.

$b_1 = 2.8922 \times 10^{-3}$

$b_2 = -0.50749$

$b_3 = 405.32$

$b_4 = -9.9290 \times 10^{-2}$

$b_5 = -0.67757$

$b_6 = 6.8235 \times 10^{-4}$

$b_7 = 3.1240 \times 10^{-4}$

$b_8 = -8.3245 \times 10^{-2}$

Parameter Ranges:

Pressure:	1785	to	2415	Psia
Local quality:	-0.16	to	0.20	
Local mass flux:	0.87	to	3.21	M·lbs/hr-ft^2
Inlet temperature:	382	to	644	°F
Hydraulic diameter:	0.36	to	0.55	Inches
Heated length:	84,		150	Inches

Table 5-6

B&W-2 CHF Correlation

$$q''_c = \frac{A' (A - BX)}{C}$$

where $A' = b_1 - b_2 d,$

$$A = b_3 (b_4 G)^{(b_5 + b_6 (P-2000))},$$

$$B = b_7 G H_{fg}$$

and $C = b_8 (b_9 G)^{(b_{10} + b_{11} (P-2000))},$

q''_c is critical heat flux (M•Btu/hr-ft^2),

G is mass flux (M•lbs/hr-ft^2),

P is pressure (Psia),

X is quality,

d is subchannel equivalent diameter (inches),

b_1 through b_{11} are constants.

$b_1 = 1.1551$

$b_2 = 0.4070$

$b_3 = 0.3702 \times 10^8$

$b_4 = 0.5914$

$b_5 = 0.8304$

$b_6 = 0.6848 \times 10^{-3}$

$b_7 = 0.1521$

$b_8 = 12.7100$

$b_9 = 3.0545$

$b_{10} = 0.7119$

$b_{11} = 0.2073 \times 10^{-3}$

Parameter Ranges:

Pressure:	2000	to	2400	Psia
Local quality:	-0.03	to	0.20	
Local mass flux:	0.75	to	4.00	$M \cdot lbs/hr\text{-}ft^2$
Hydraulic diameter:	0.20	to	0.50	Inches
Heated length:	72			Inches

Table 5-7

W-3 CHF Correlation

$q_c'' = A \cdot B \cdot C \cdot D \cdot E$

where $A = b_1 + b_2 P + (b_3 + b_4 P) e^{(b_5 + b_6 P) X}$,

$B = b_7 + b_8 X$,

$C = (b_9 + b_{10} X + b_{11} X |X|) G + b_{12}$,

$D = b_{13} + b_{14} e^{b_{15} d}$,

and $E = b_{16} + b_{17} (h_f - h_{in})$,

q_c'' is critical heat flux (M·Btu/hr-ft^2),

G is mass flux (M·lbs/hr-ft^2),

P is pressure (Psia),

X is quality,

d is subchannel equivalent diameter (inches),

h_f is saturated enthalpy (Btu/lb),

h_{in} is inlet enthalpy (Btu/lb),

and b_1 through b_{17} are constants.

b_1 = 2.022

b_2 = -0.0004302

b_3 = 0.1722

b_4 = -0.0000984

b_5 = 18.177

b_6 = -0.004129

b_7 = 1.157

b_8 = -0.869

b_9 = 0.1484

b_{10} = -1.596

b_{11} = 0.1729

b_{12} = 1.037

b_{13} = 0.2664

b_{14} = 0.8357

b_{15} = -3.151

b_{16} = 0.8258

b_{17} = 0.000794

Parameter Ranges:

Pressure:	1000	to	2300	Psia
Local quality"	-0.15	to	0.15	
Local mass flux:	1.0	to	5.0	$M \cdot lbs/hr\text{-}ft^2$
Inlet enthalpy:		$\geq$	400	Btu/lb_m
Hydraulic diameter:	0.2	to	0.70	Inches
Heated length:	10	to	144	Inches

employed to reduce these data to Local conditions form. In this data set, there were some CHF indications which occurred on peripheral rods, probably due to the occurrence of CHF in the corner or side subchannels. Since the prediction of CHF in peripheral subchannels is not of high interest in the PWR thermal-hydraulic analysis, these data were not included in the analysis, thus reducing the number of data points to 819. The pressure, mass flux, and local quality covered by these data are 600 to 2,300 psia, 0.45 to 3.00 M.lbs/hr-ft^2, and -20 to +55% respectively. None of the CHF correlations mentioned above except the Columbia correlation cover the complete range of these data.

In order to assess the performance of these correlations beyond the ranges of their applicability, the CE-1 correlation, the B&W-2 correlation, and the Columbia correlation were employed to predict the first CHF for all the data. The statistics for this comparative study are compiled in Table 5-8. The results show that the CE-1 and the B&W-2 correlations are not useful beyond the ranges of the parameters for which they were developed and also, that the Columbia correlation predicts the data accurately over the complete parameter ranges.

Since the Columbia correlation is applicable to the complete data ranges, the statistical analysis of multiple CHF events was performed with this correlation and the results are shown in Table 5-9.

In order to evaluate the applicability of the other correlations in the prediction of the CHF events of higher rank than first, a common parameter range was established within which all the correlations are applicable. The parameter ranges over which each CHF correlation is applicable as well as the common parameter range are given in Table 5-10. Further study of the multiple CHF analyses of this data set was, therefore, limited to 358 CHF points which cover the pressure, mass flux, and local quality ranges of 1900 to 2300 psia, 0.75 to 3.00 M.lbs/hr-ft^2, and -5 to +20% respectively. The results of the statistical analyses and parametric studies performed on these data by the four correlations are presented in the Tables and Figures as shown below:

TABLE 5-8

ANALYSIS OF PWR DATA

NUMBER OF TEST SECTIONS	=	15
NUMBER OF DATA POINTS	=	819
PRESSURE RANGE (PSIA)	=	600 TO 2300
MASS FLUX RANGE (M.LBS HR-SQFT)	=	0.45 TO 3.00
LOCAL QUALITY RANGE (%)	=	-20. TO 55.

COMPARISON OF CORRELATIONS

CHF CORRELATION	NO. OF POINTS	AVE. RATIO	RMS ERROR	STD. DEVIATION
COLUMBIA	819	1.029	0.075	0.069
C-E	819	0.983	0.122	0.121
B&W-2	819	1.028	0.136	0.133

TABLE 5-9

ANALYSIS OF PWR DATA

NUMBER OF TEST SECTIONS	=	15
NUMBER OF DATA POINTS	=	819
PRESSURE RANGE (PSIA)	=	600 TO 2300
MASS FLUX RANGE (M.LBS HR-SQFT)	=	0.45 TO 3.00
LOCAL QUALITY RANGE (%)	=	-20. TO 55.

COLUMBIA CHF CORRELATION

CHF RANK	NO. OF POINTS	AVE. RATIO	RMS ERROR	STD. DEVIATION
FIRST CHF	819	1.029	0.075	0.069
SECOND CHF	255	1.024	0.065	0.060
THIRD CHF	71	1.010	0.052	0.051
FOURTH CHF	18	0.998	0.044	0.044
HIGHER ORDER CHF (SECOND & HIGHER)	348	1.019	0.061	0.058
ALL CHF	1163	1.026	0.071	0.066

TABLE 5-10

PARAMETER RANGES OF EXISTING CHF CORRELATIONS

CHF CORRELATION	PR. RANGE PSIA	G. RANGE M.LB/HR-FT2	X RANGE
W-3	1000 - 2400	1.00 - 5.00	-0.25 - 0.15
B&W-2	2000 - 2400	0.75 - 4.00	-0.03 - 0.20
CE	1785 - 2415	0.87 - 3.21	-0.16 - 0.20
COLUMBIA	200 - 2450	0.20 - 4.10	-0.25 - 0.75
PARAMETER RANGES FOR COMPARISON	1900 - 2325	0.75 - 3.00	-0.05 - 0.20

Correlation	Statistical Analyses (Tables)	Parametric studies (Figures)
Columbia	5-11	5-13 to 5-20
CE-1	5-12	5-21 to 5-28
B&W-2	5-13	5-29 to 5-36
W-3	5-14	5-37 to 5-44

An examination of these results confirm the conclusions drawn based on the study of the BWR data that the trends in the CHF events of higher rank generally follow those of the the first CHF and the CHF correlations based on local conditions predict the CHF events of higher rank with the same degree of accuracy as the first CHF.

5.3 PWR Non-Uniform Axial Heat Flux Data

There are several methods of evaluating the applicability of a CHF correlation to CHF data in fuel assemblies with non-uniform axial heat flux distribution. Some of the approaches adopted by different researchers for comparing a CHF correlation and the experimetal CHF data from rod bundles with non-uniform axial heat flux distribution are described below.

Bowring (20) used critical power ratio as the figure of merit. In this procedure, the minimum critical heat flux ratio (experimental local heat flux over predicted CHF) is determined for the test section inlet conditions and measured bundle power. The bundle power at which minimum CHFR becomes unity is calculated. The critical power ratio is defined as the ratio of the calculated power at which the minimum CHFR is unity to the experimental power.

TABLE 5-11

ANALYSIS OF PWR DATA

NUMBER OF TEST SECTIONS	=	15
NUMBER OF DATA POINTS	=	358
PRESSURE RANGE (PSIA)	=	1900 TO 2300
MASS FLUX RANGE (M.LBS HR-SQFT)	=	0.75 TO 3.00
LOCAL QUALITY RANGE (%)	=	-5. TO 2C.

COLUMBIA CHF CORRELATION

CHF RANK	NO. OF POINTS	AVE. RATIO	RMS ERROR	STD. DEVIATION
FIRST CHF	358	1.030	0.069	0.062
SECOND CHF	125	1.028	0.062	0.055
THIRD CHF	39	1.012	0.053	0.052
FOURTH CHF	10	1.014	0.039	0.036
HIGHER ORDER CHF (SECOND & HIGHER)	176	1.023	0.059	0.054
ALL CHF	532	1.028	0.066	0.060

FIG. 5-13 PLOT OF Q-CALC/Q-OBS RATIO VERSUS QUALITY
COLUMBIA CORRELATION - FIRST CHF

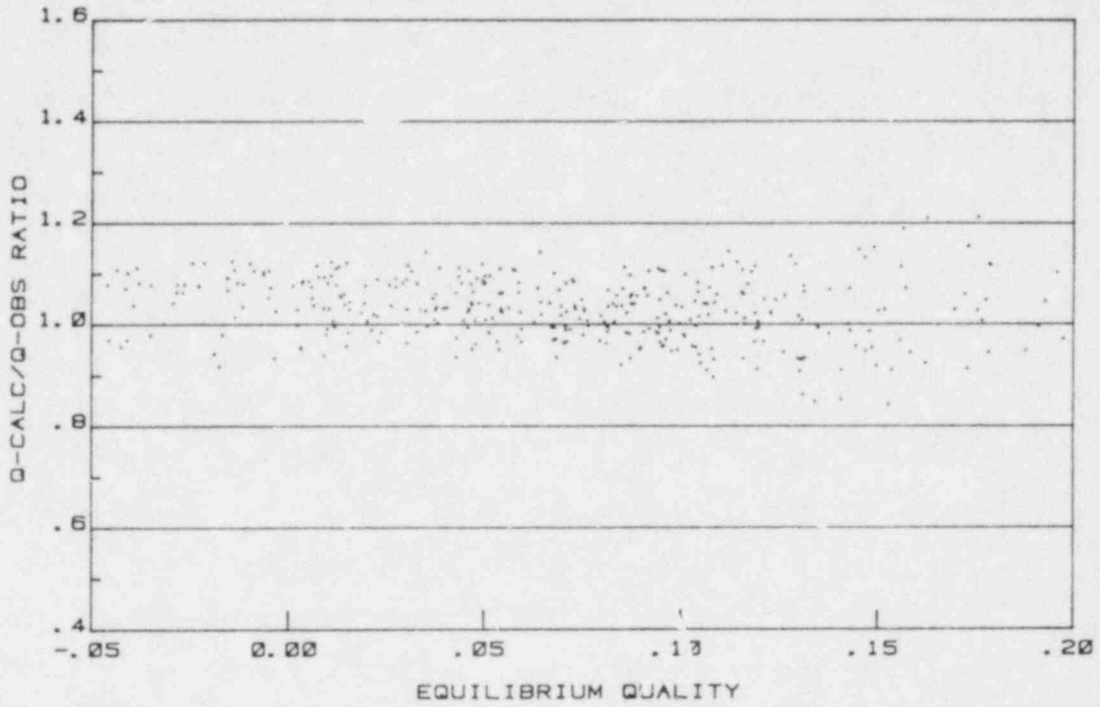

FIG. 5-14 PLOT OF Q-CALC/Q-OBS RATIO VERSUS QUALITY
COLUMBIA CORRELATION - HIGHER ORDER CHF

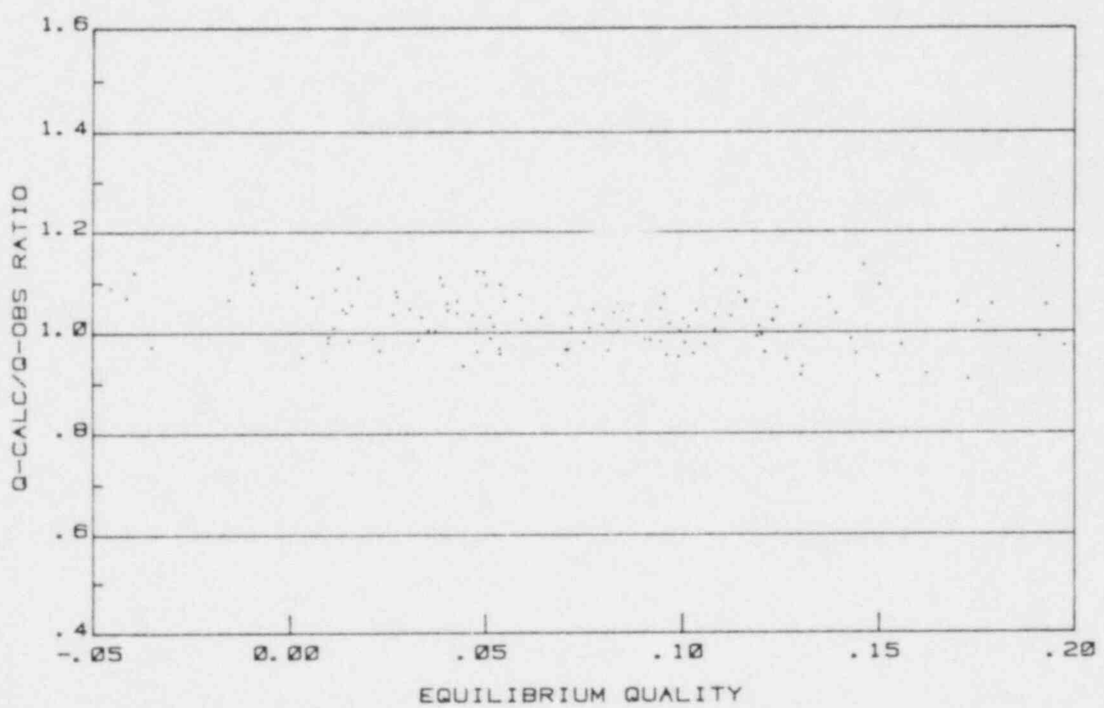

FIG. 5-15 PLOT OF Q-CALC/Q-OBS RATIO VERSUS QUALITY
COLUMBIA CORRELATION - SECOND CHF

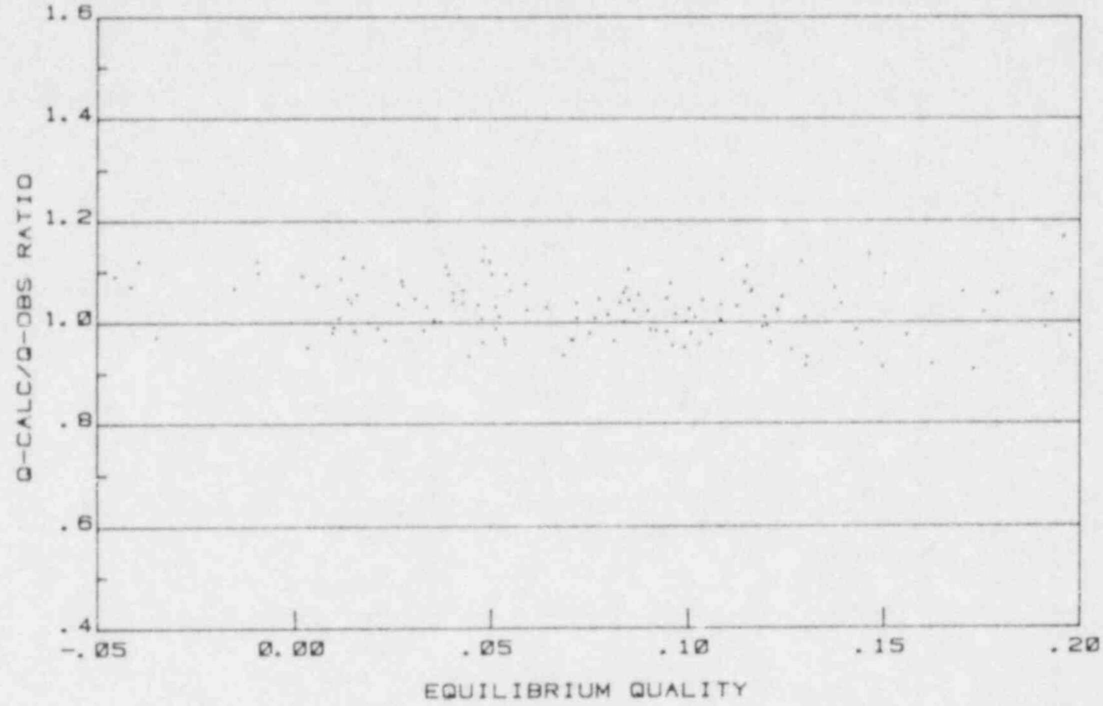

FIG. 5-16 PLOT OF Q-CALC/Q-OBS RATIO VERSUS QUALITY
COLUMBIA CORRELATION - THIRD CHF

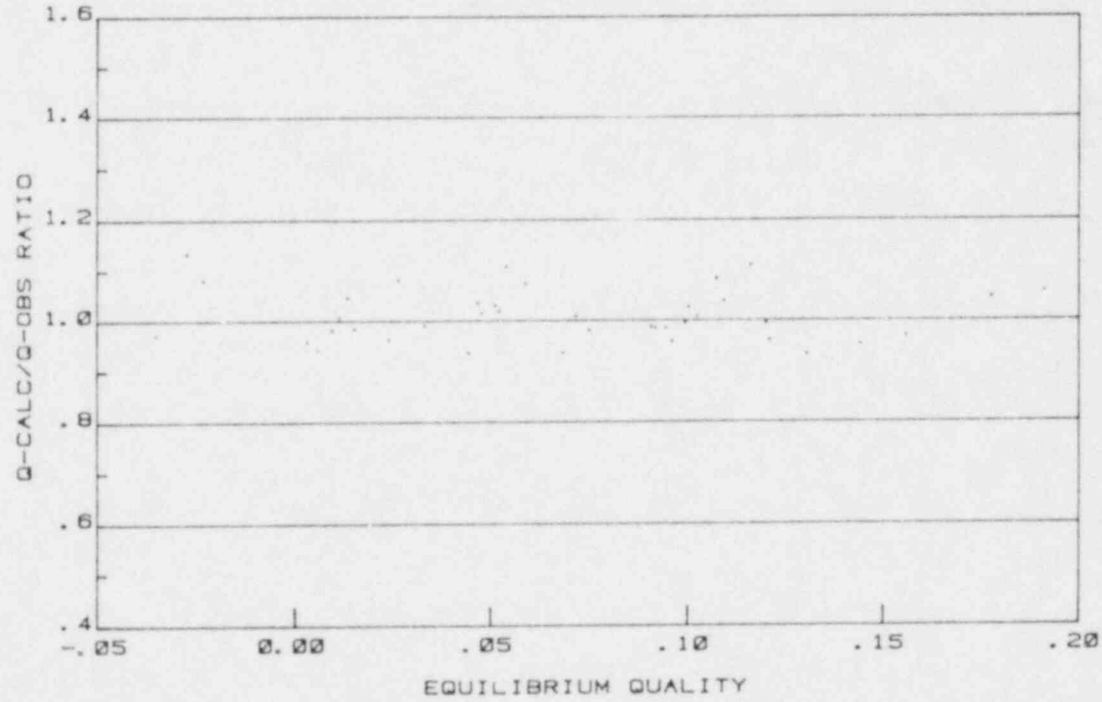

FIG. 5-17 PLOT OF Q-CALC/Q-OBS RATIO VERSUS MASS FLUX
COLUMBIA CORRELATION - FIRST CHF

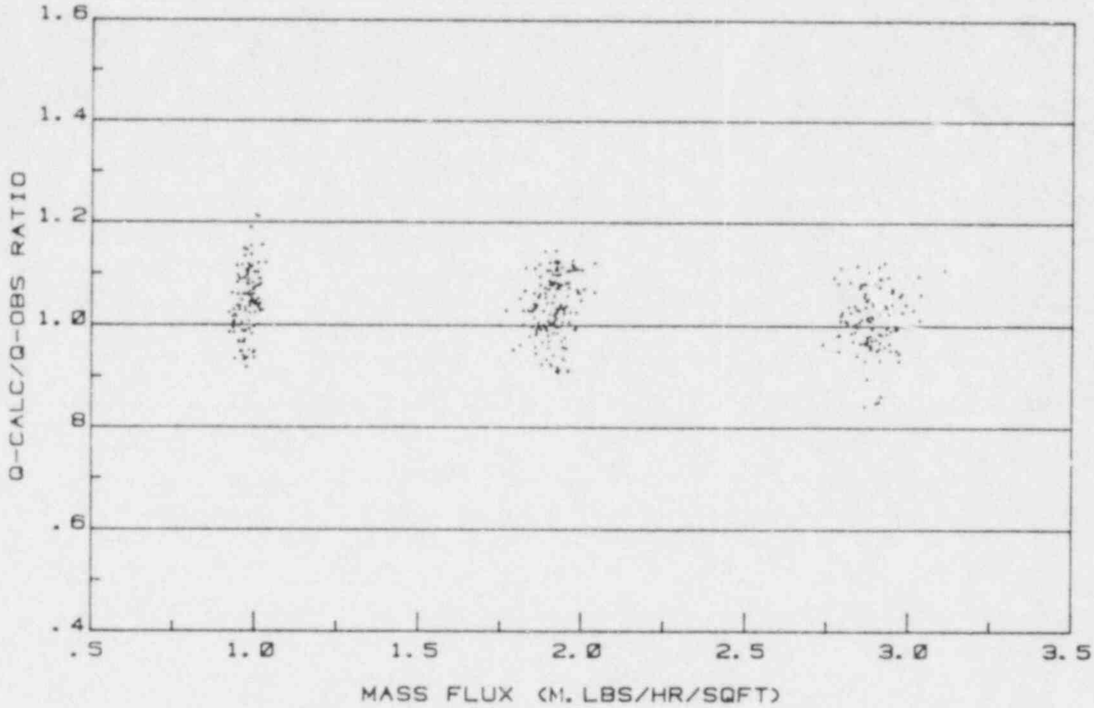

FIG. 5-18 PLOT OF Q-CALC/Q-OBS RATIO VERSUS MASS FLUX
COLUMBIA CORRELATION - HIGHER ORDER CHF

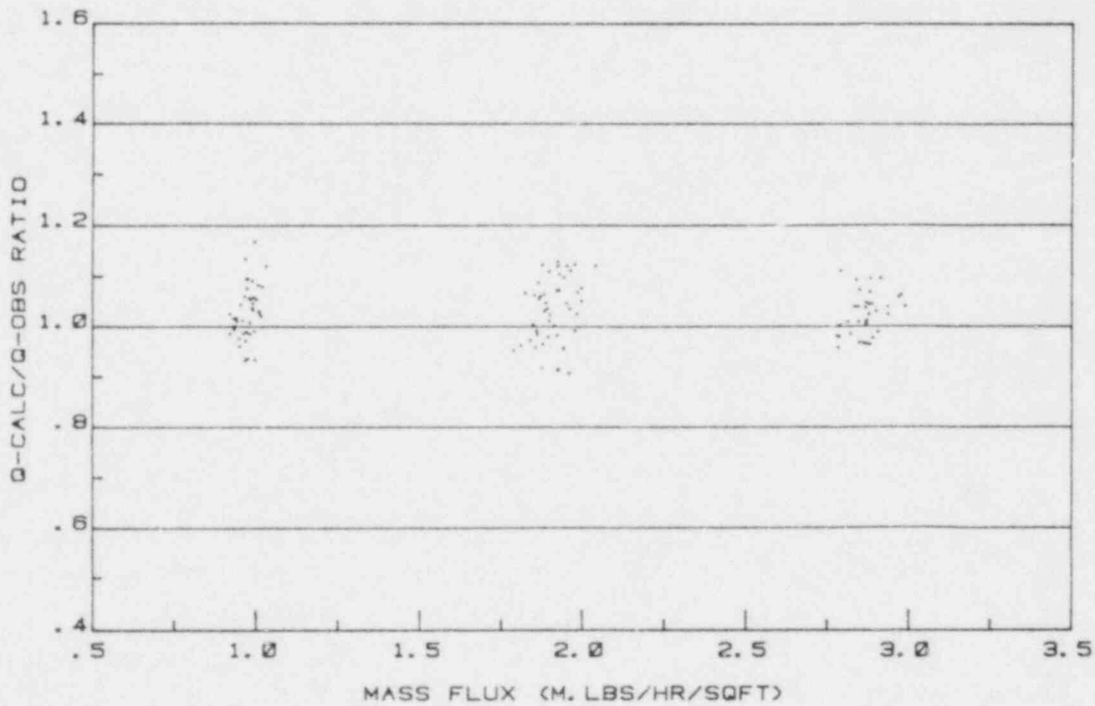

FIG. 5-19 PLOT OF Q-CALC/Q-OBS RATIO VERSUS PRESSURE
COLUMBIA CORRELATION - FIRST CHF

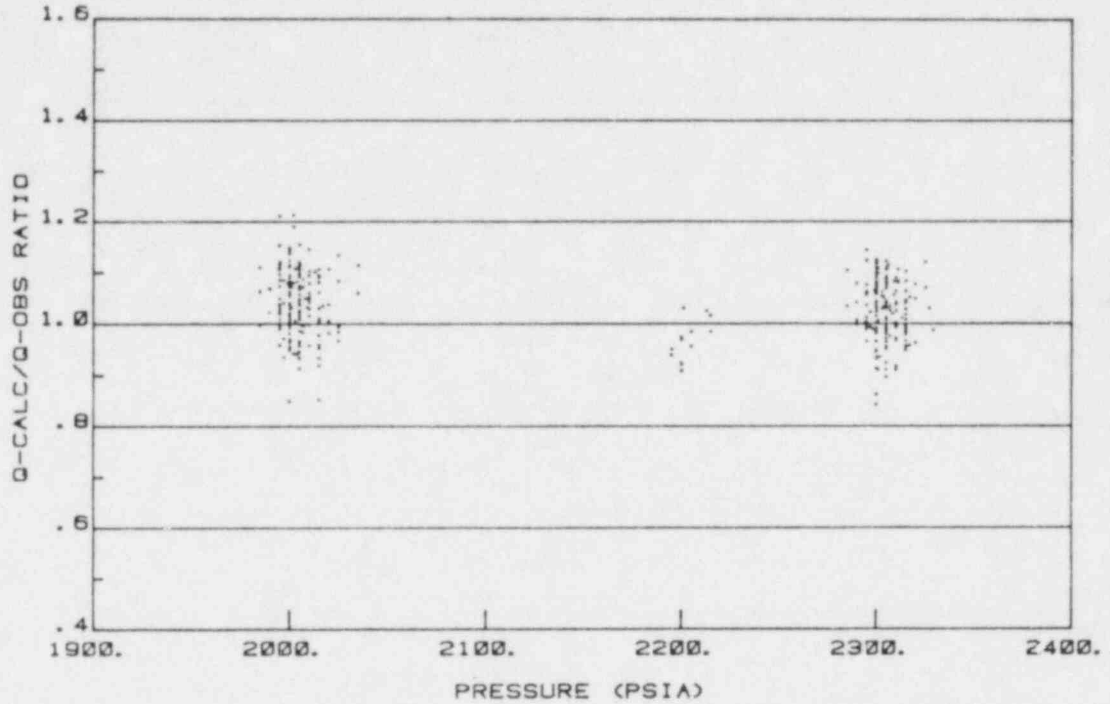

FIG. 5-20 PLOT OF Q-CALC/Q-OBS RATIO VERSUS PRESSURE
COLUMBIA CORRELATION - HIGHER ORDER CHF

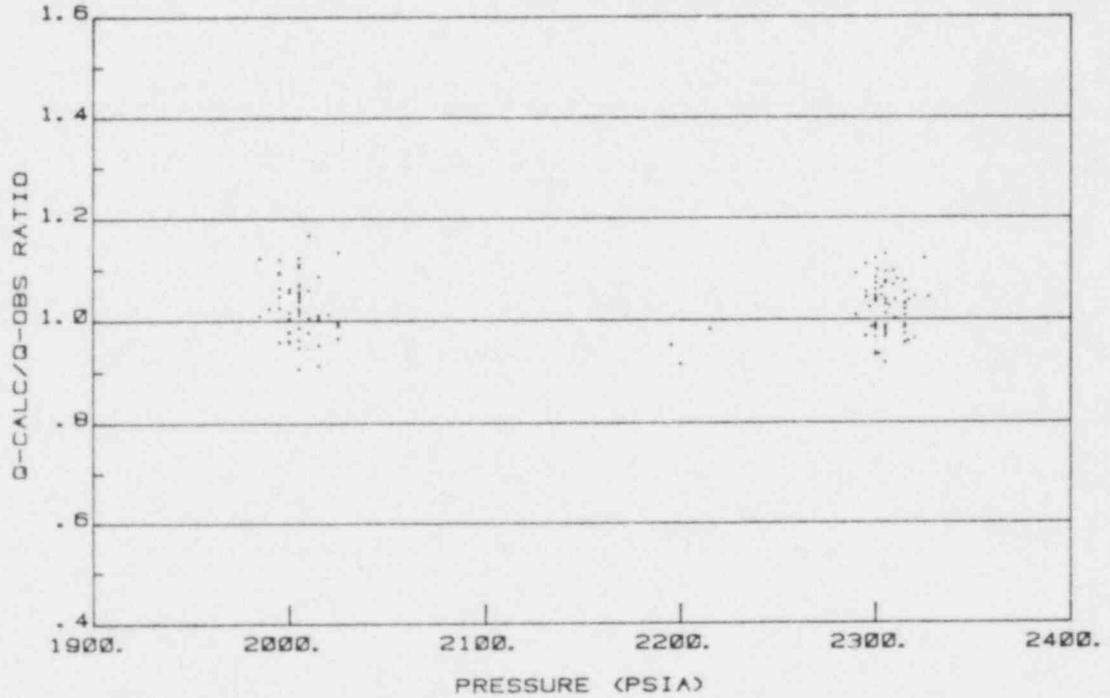

TABLE 5-12

ANALYSIS OF PWR DATA

NUMBER OF TEST SECTIONS	=	15
NUMBER OF DATA POINTS	=	358
PRESSURE RANGE (PSIA)	=	1900 TO 2300
MASS FLUX RANGE (M.LBS HR-SQFT)	=	0.75 TO 3.00
LOCAL QUALITY RANGE (%)	=	-5. TO 20.

CE-1 CHF CORRELATION

CHF RANK	NO. OF POINTS	AVE. RATIO	RMS ERROR	STD. DEVIATION
FIRST CHF	358	1.033	0.075	0.067
SECOND CHF	125	1.028	0.071	0.066
THIRD CHF	39	1.001	0.060	0.060
FOURTH CHF	10	0.997	0.042	0.042
HIGHER ORDER CHF (SECOND & HIGHER)	176	1.019	0.067	0.064
ALL CHF	532	1.029	0.072	0.066

FIG. 5-21 PLOT OF Q-CALC/Q-OBS RATIO VERSUS QUALITY
CE CORRELATION - FIRST CHF

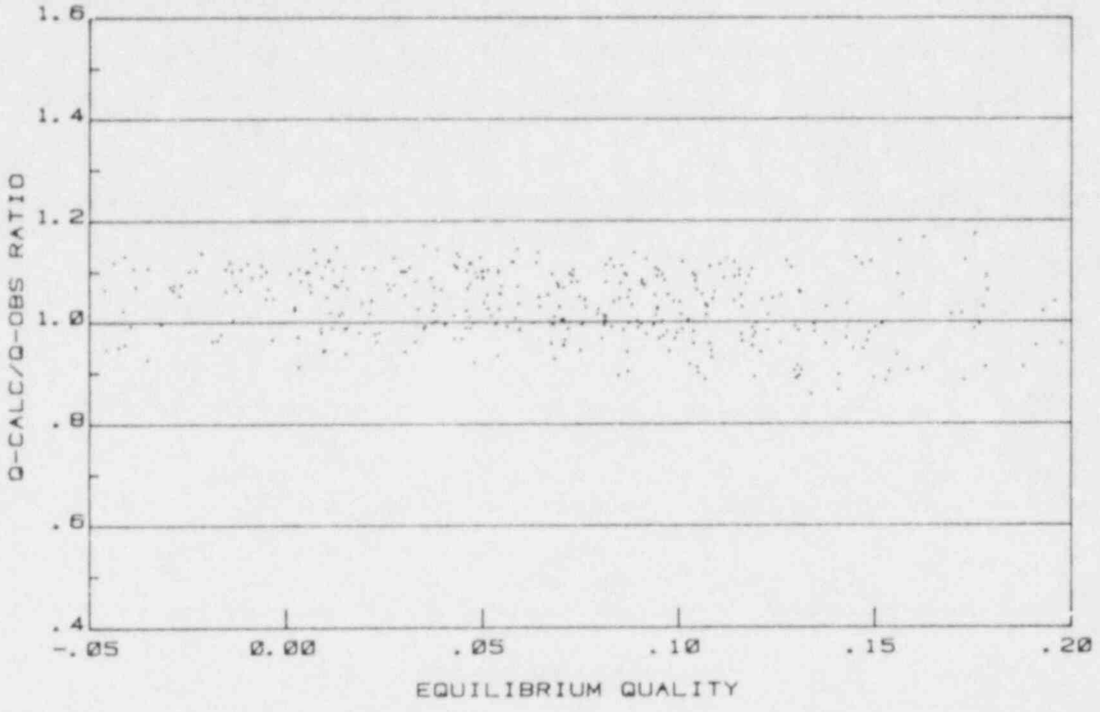

FIG. 5-22 PLOT OF Q-CALC/Q-OBS RATIO VERSUS QUALITY
CE CORRELATION - HIGHER ORDER CHF

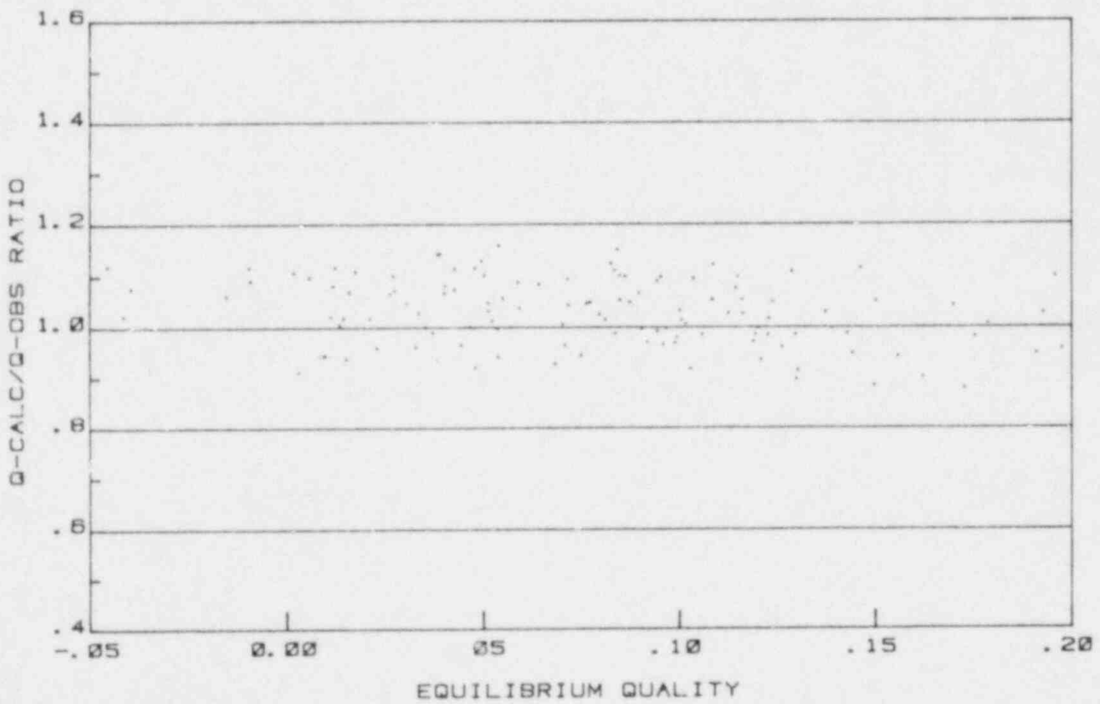

FIG. 5-23 PLOT OF Q-CALC/Q-OBS RATIO VERSUS QUALITY
CE CORRELATION - SECOND CHF

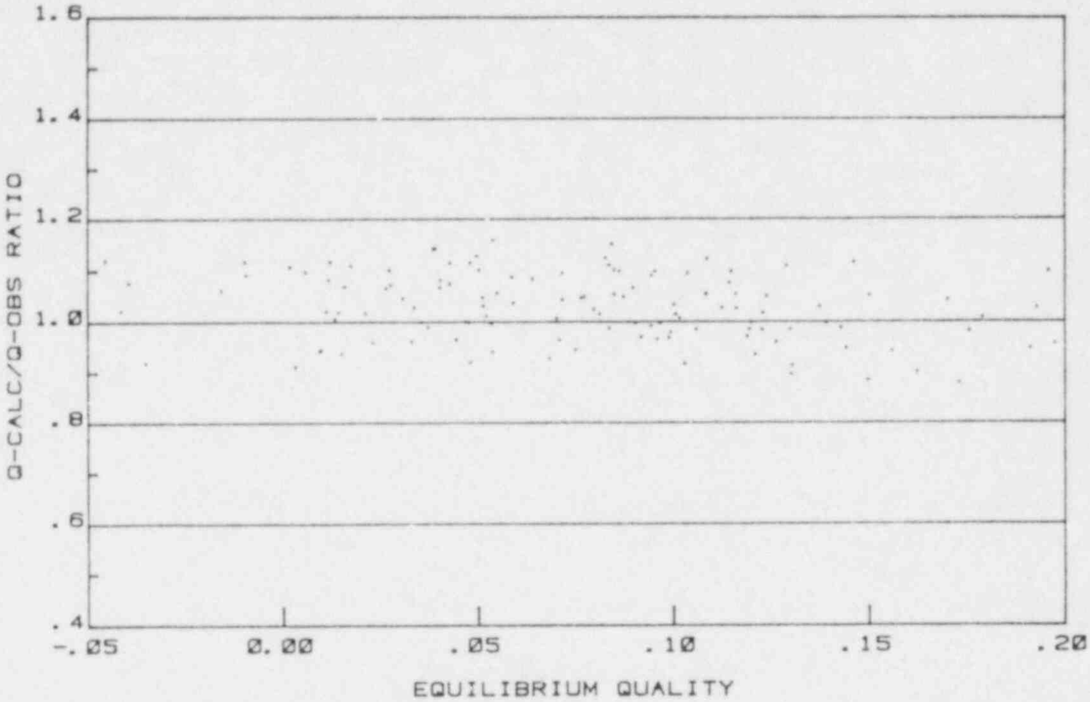

FIG. 5-24 PLOT OF Q-CALC/Q-OBS RATIO VERSUS QUALITY
CE CORRELATION - THIRD CHF

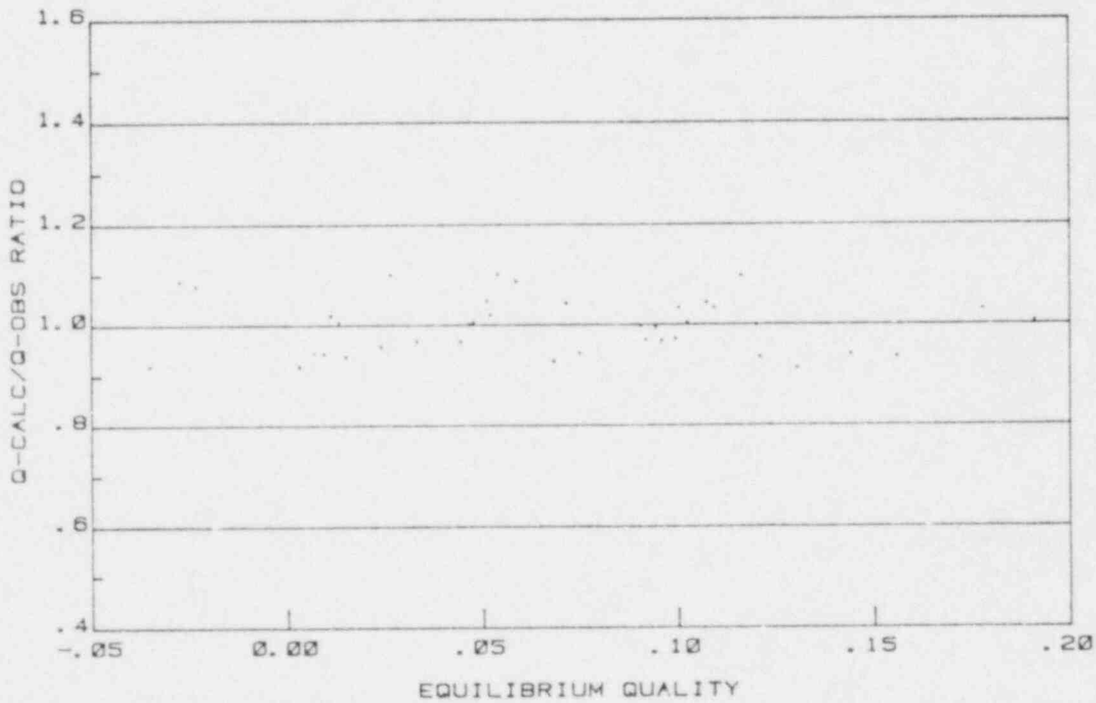

FIG. 5-25 PLOT OF Q-CALC/Q-OBS RATIO VERSUS MASS FLUX
CE CORRELATION - FIRST CHF

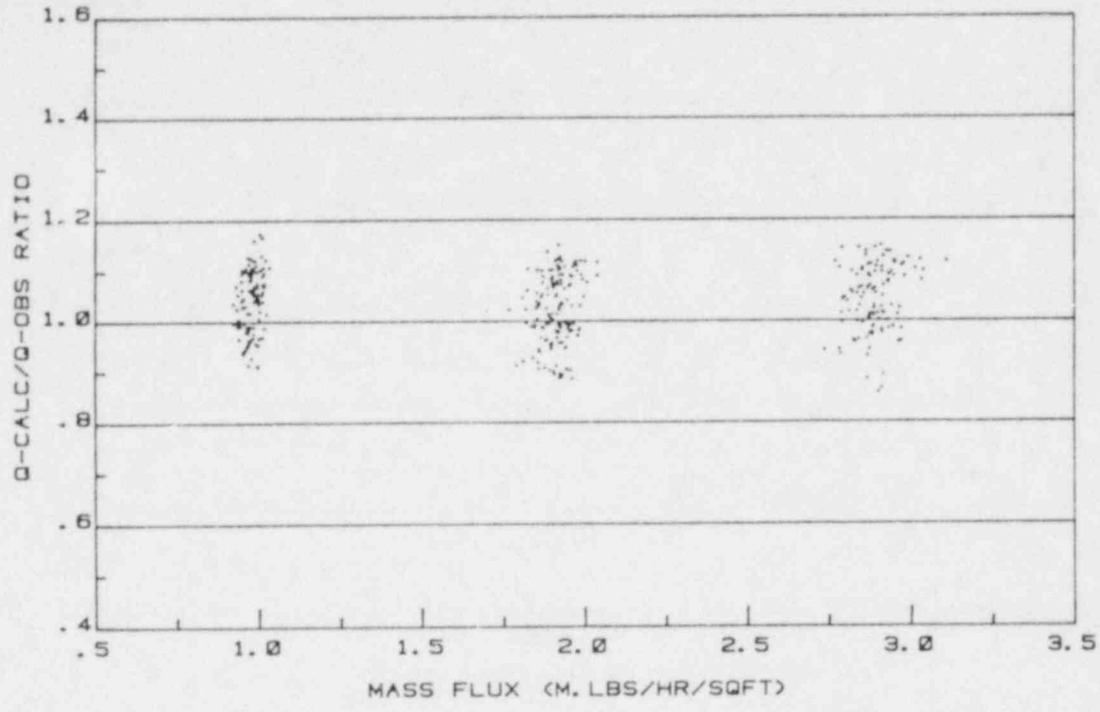

FIG. 5-26 PLOT OF Q-CALC/Q-OBS RATIO VERSUS MASS FLUX
CE CORRELATION - HIGHER ORDER CHF

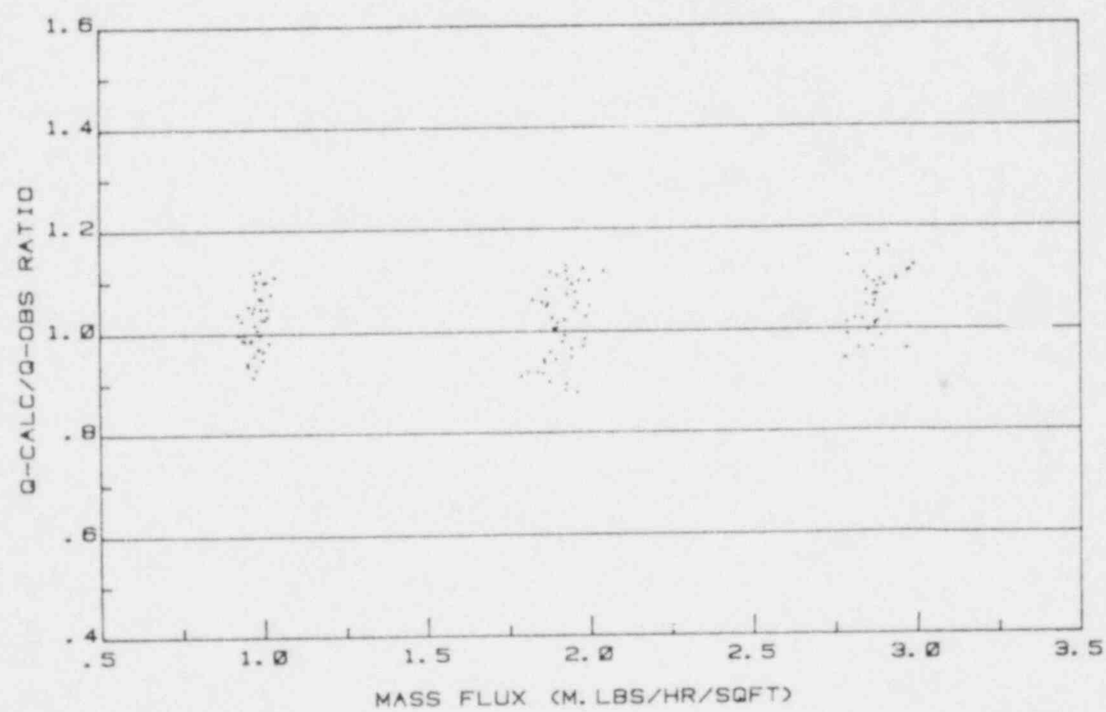

FIG. 5-27 PLOT OF Q-CALC/Q-OBS RATIO VERSUS PRESSURE
CE CORRELATION - FIRST CHF

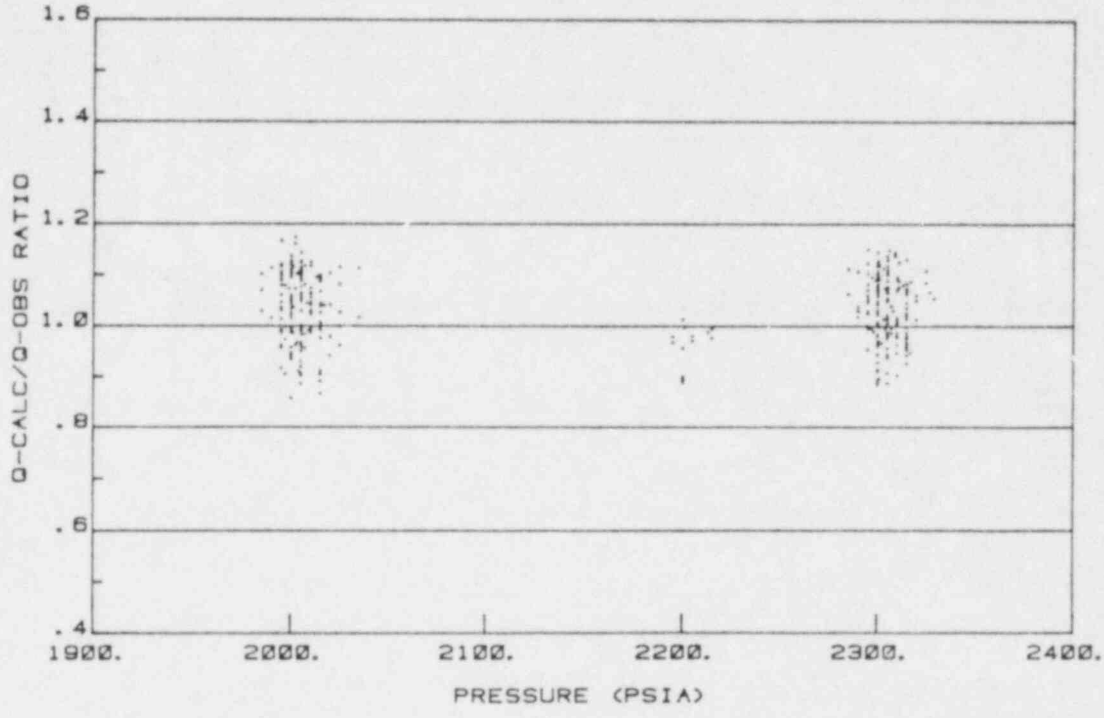

FIG. 5-28 PLOT OF Q-CALC/Q-OBS RATIO VERSUS PRESSURE
CE CORRELATION - HIGHER ORDER CHF

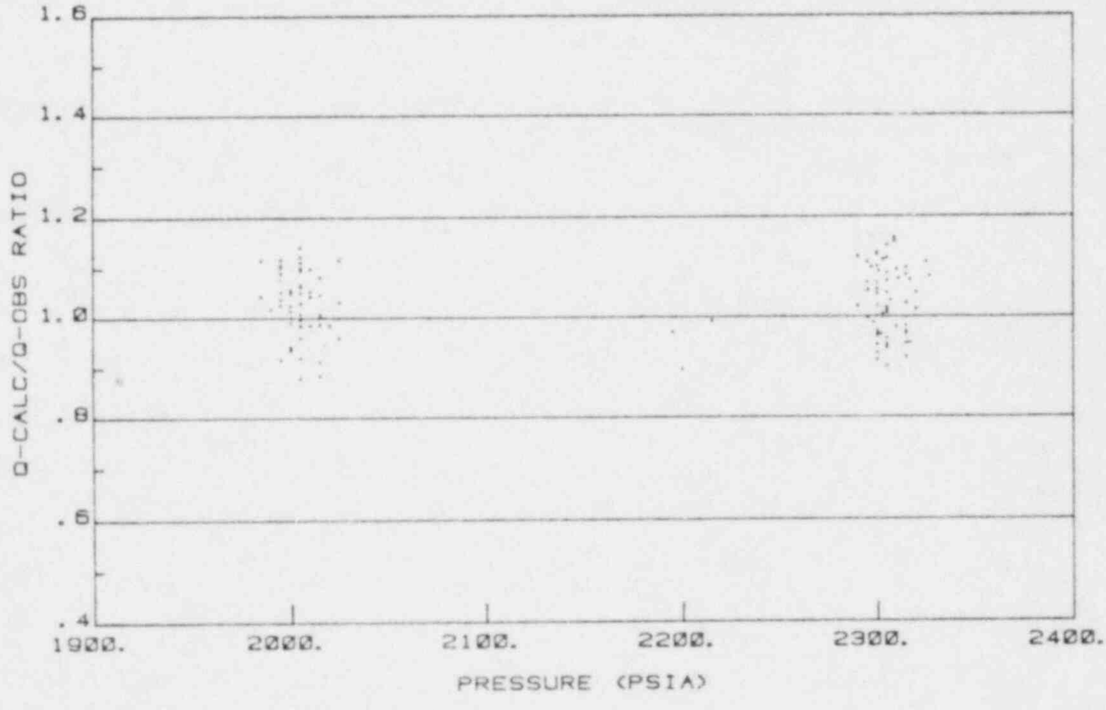

TABLE 5-13

ANALYSIS OF PWR DATA

NUMBER OF TEST SECTIONS	=	15
NUMBER OF DATA POINTS	=	358
PRESSURE RANGE (PSIA)	=	1900 TO 2300
MASS FLUX RANGE (M.LBS HR-SQFT)	=	0.75 TO 3.00
LOCAL QUALITY RANGE (%)	=	-5. TO 20.

B&W-2 CHF CORRELATION

CHF RANK	NO. OF POINTS	AVE. RATIO	RMS ERROR	STD. DEVIATION
FIRST CHF	358	1.093	0.117	0.071
SECOND CHF	125	1.086	0.110	0.068
THIRD CHF	39	1.073	0.092	0.056
FOURTH CHF	10	1.077	0.088	0.044
HIGHER ORDER CHF (SECOND & HIGHER)	176	1.082	0.104	0.064
ALL CHF	532	1.090	0.113	0.069

FIG. 5-29 PLOT OF Q-CALC/Q-OBS RATIO VERSUS QUALITY
B&W-2 CORRELATION - FIRST CHF

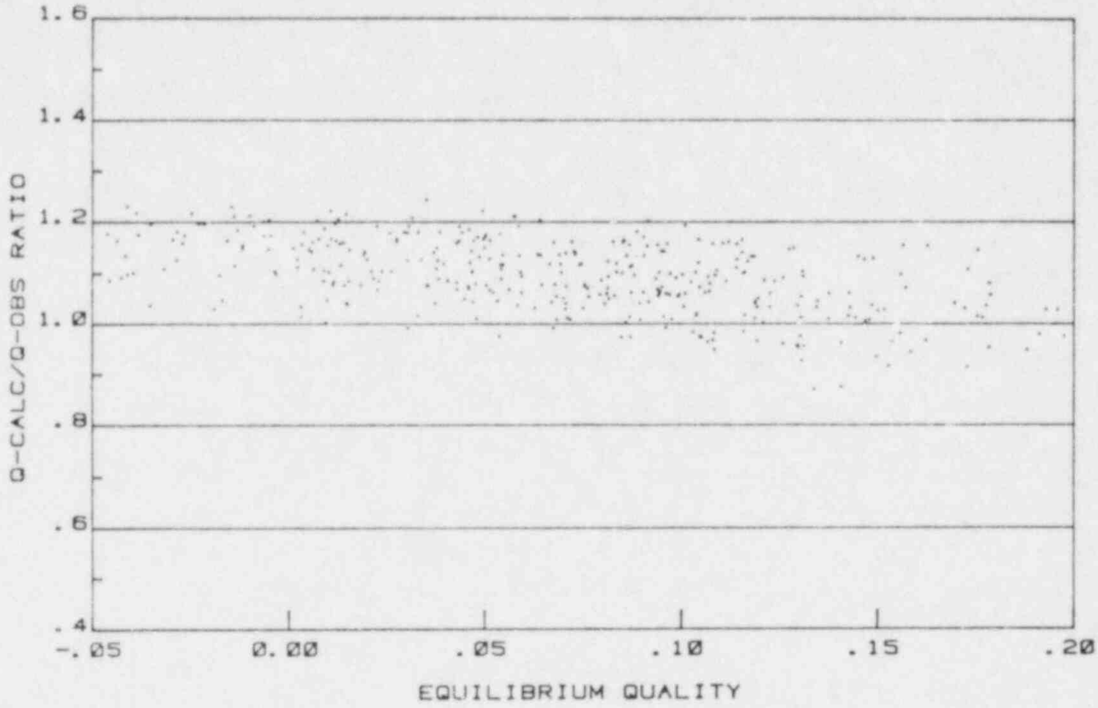

FIG. 5-30 PLOT OF Q-CALC/Q-OBS RATIO VERSUS QUALITY
B&W-2 CORRELATION - HIGHER ORDER CHF

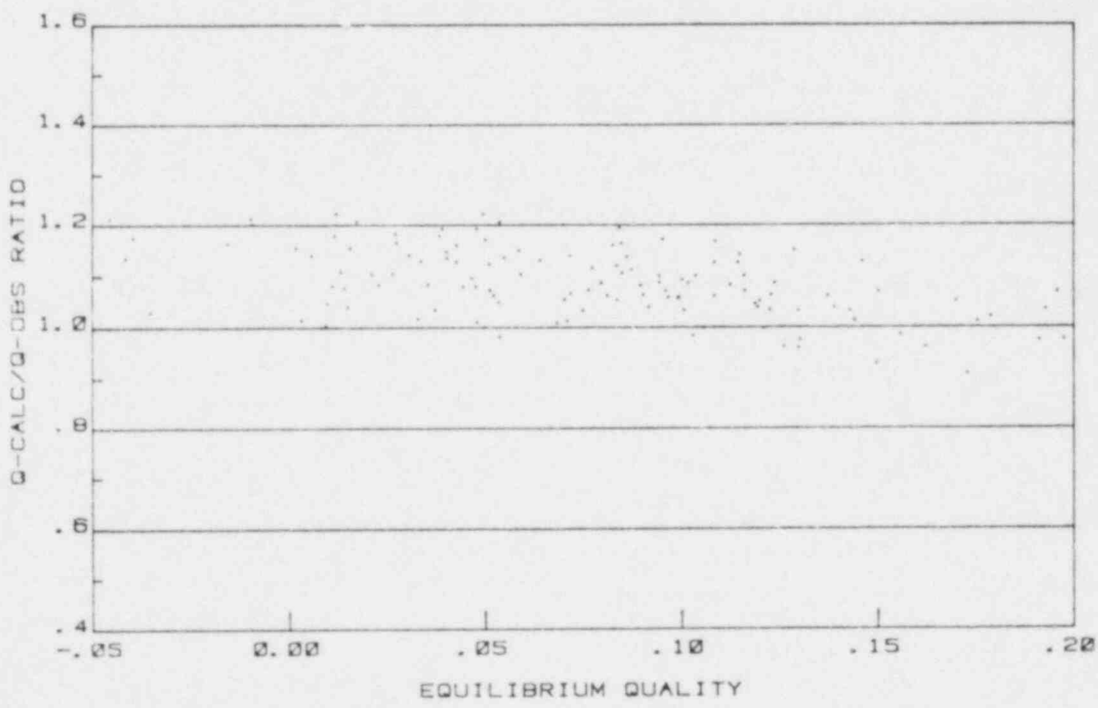

FIG. 5-31 PLOT OF Q-CALC/Q-OBS RATIO VERSUS QUALITY
B&W-2 CORRELATION - SECOND CHF

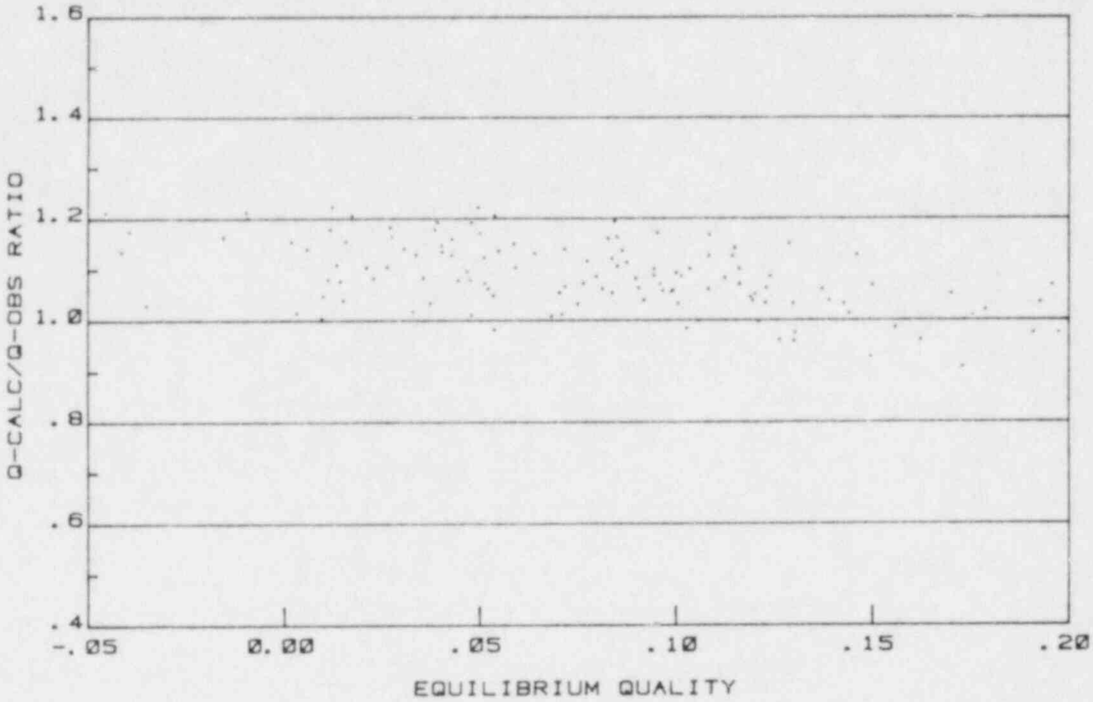

FIG. 5-32 PLOT OF Q-CALC/Q-OBS RATIO VERSUS QUALITY
B&W-2 CORRELATION - THIRD CHF

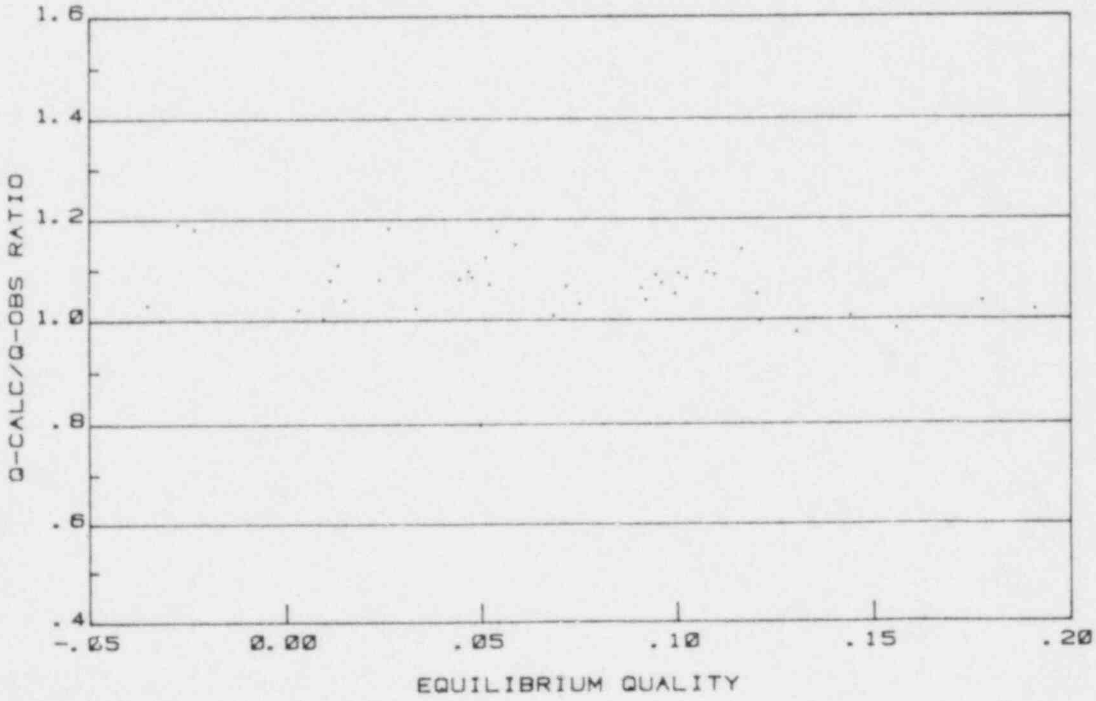

FIG. 5-33 PLOT OF Q-CALC/Q-OBS RATIO VERSUS MASS FLUX
B&W-2 CORRELATION - FIRST CHF

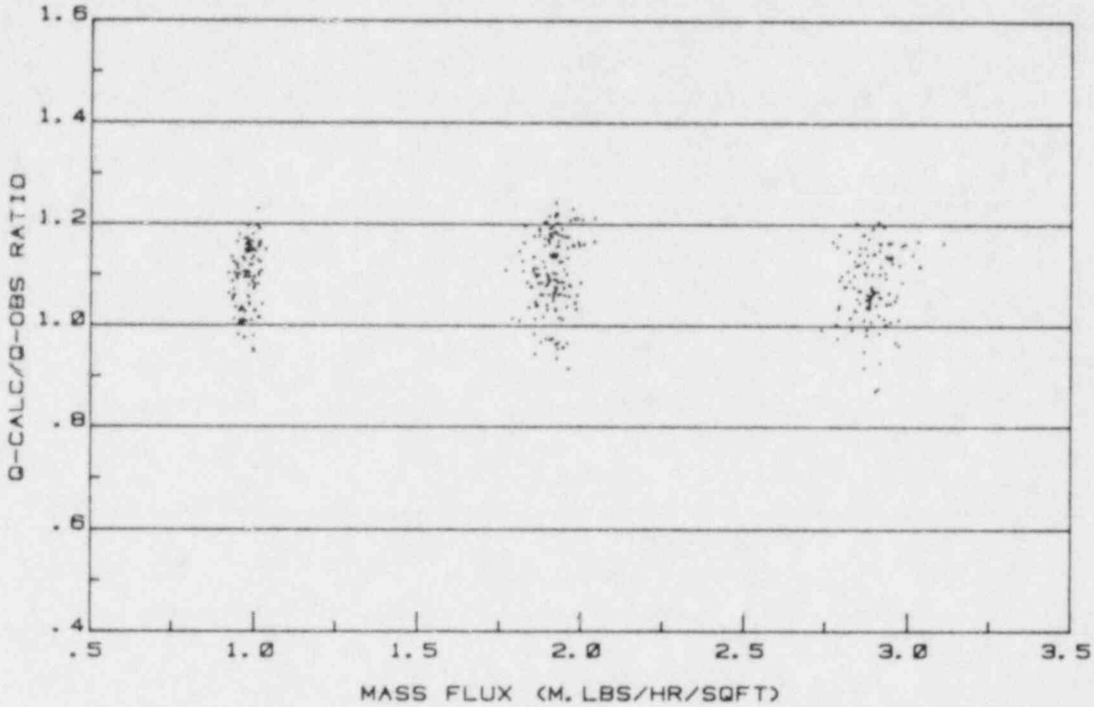

FIG. 5-34 PLOT OF Q-CALC/Q-OBS RATIO VERSUS MASS FLUX
B&W-2 CORRELATION - HIGHER ORDER CHF

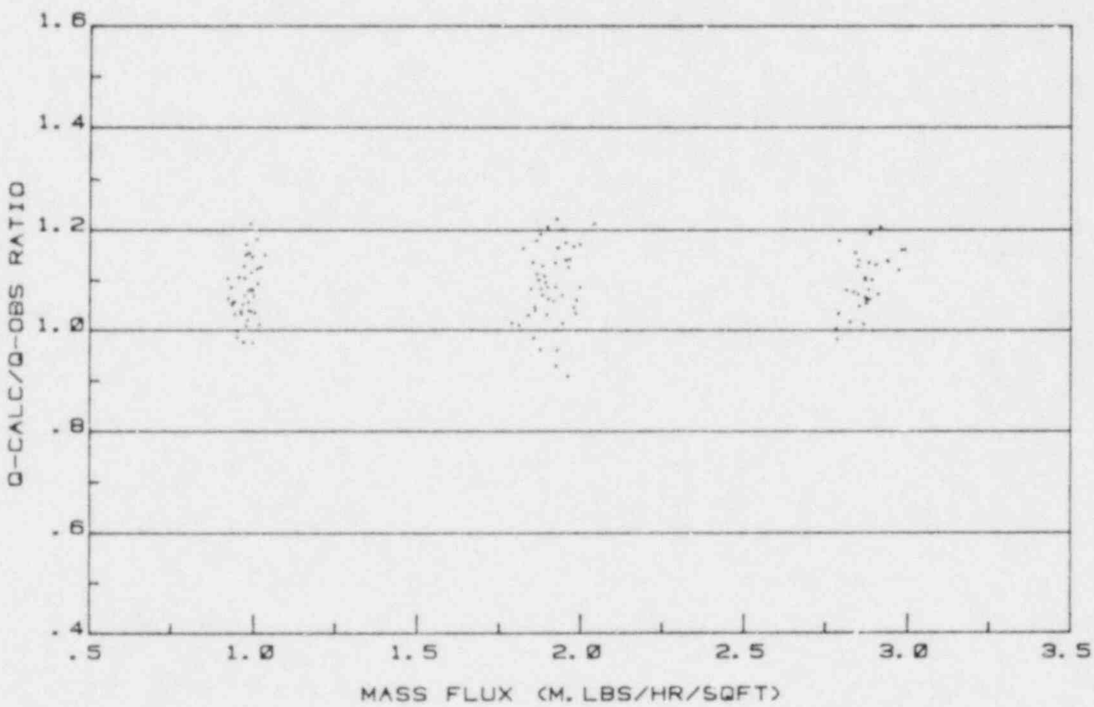

FIG. 5-35 PLOT OF Q-CALC/Q-OBS RATIO VERSUS PRESSURE
B&W-2 CORRELATION - FIRST CHF

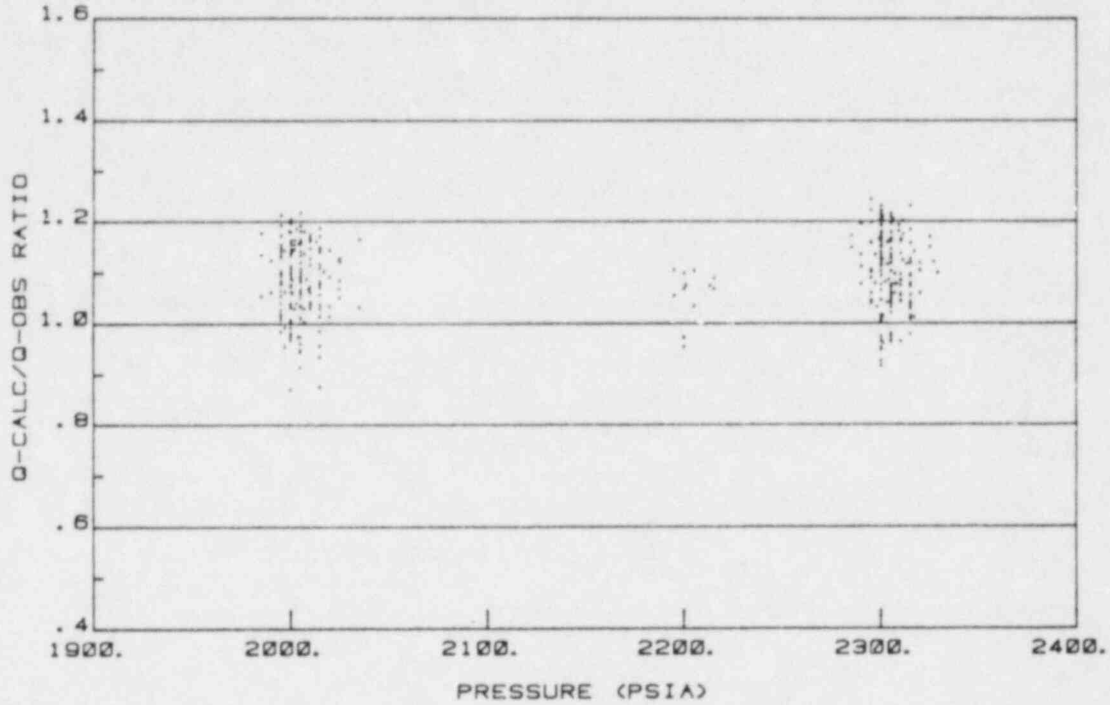

FIG. 5-36 PLOT OF Q-CALC/Q-OBS RATIO VERSUS PRESSURE
B&W-2 CORRELATION - HIGHER ORDER CHF

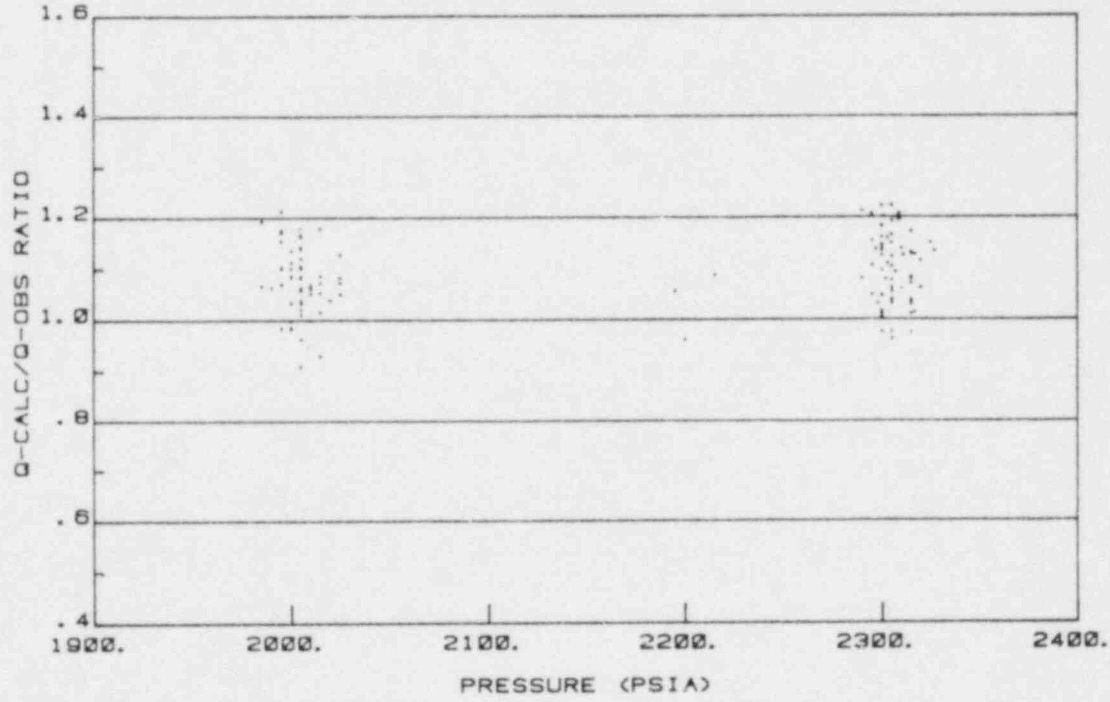

TABLE 5-14

ANALYSIS OF PWR DATA

NUMBER OF TEST SECTIONS	=	15
NUMBER OF DATA POINTS	=	358
PRESSURE RANGE (PSIA)	=	1900 TO 2300
MASS FLUX RANGE (M.LBS HR-SQFT)	=	0.75 TO 3.00
LOCAL QUALITY RANGE (%)	=	-5. TO 20.

W-3 CHF CORRELATION

CHF RANK	NO. OF POINTS	AVE. RATIO	RMS ERROR	STD. DEVIATION
FIRST CHF	358	0.958	0.161	0.156
SECOND CHF	125	0.949	0.149	0.140
THIRD CHF	39	0.945	0.139	0.128
FOURTH CHF	10	0.906	0.160	0.129
HIGHER ORDER CHF (SECOND & HIGHER)	176	0.944	0.148	0.137
ALL CHF	532	0.954	0.157	0.150

FIG. 5-37 PLOT OF Q-CALC/Q-OBS RATIO VERSUS QUALITY W-3 CORRELATION - FIRST CHF

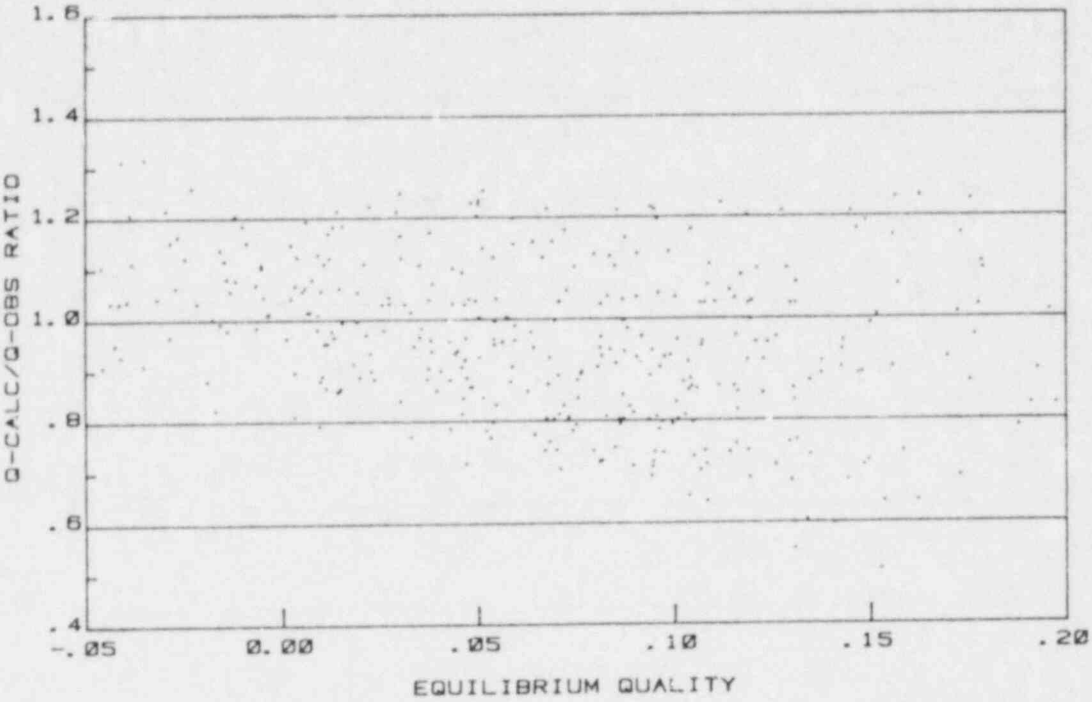

FIG. 5-38 PLOT OF Q-CALC/Q-OBS RATIO VERSUS QUALITY W-3 CORRELATION - HIGHER ORDER CHF

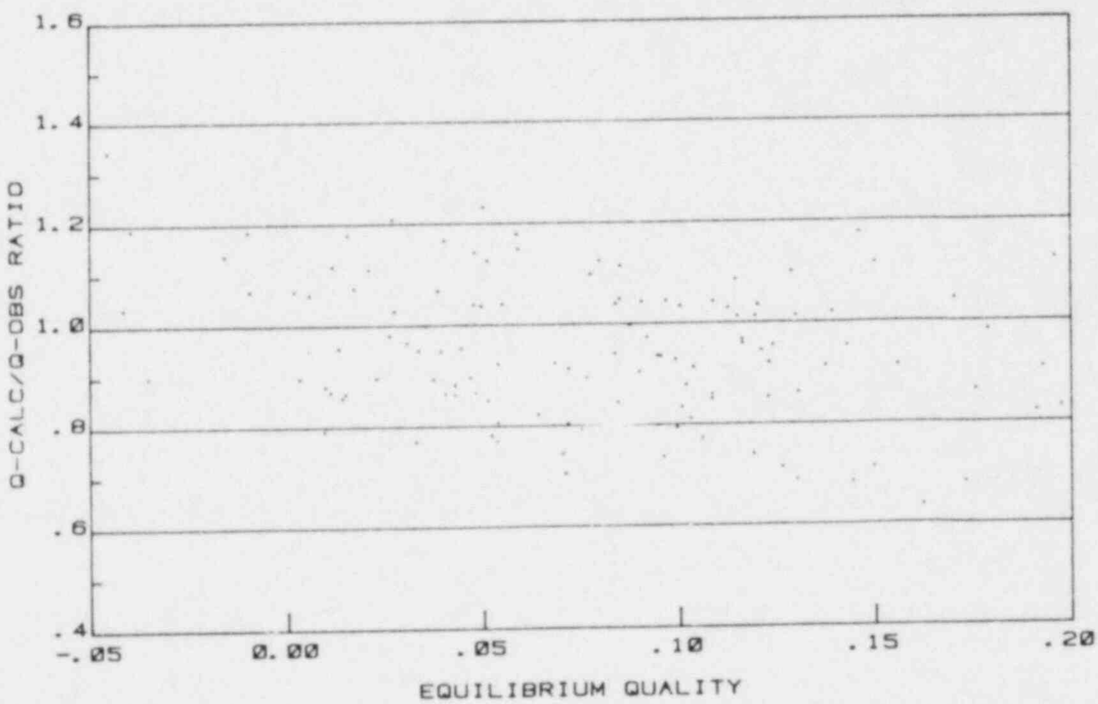

FIG. 5-39 PLOT OF Q-CALC/Q-OBS RATIO VERSUS QUALITY
W-3 CORRELATION - SECOND CHF

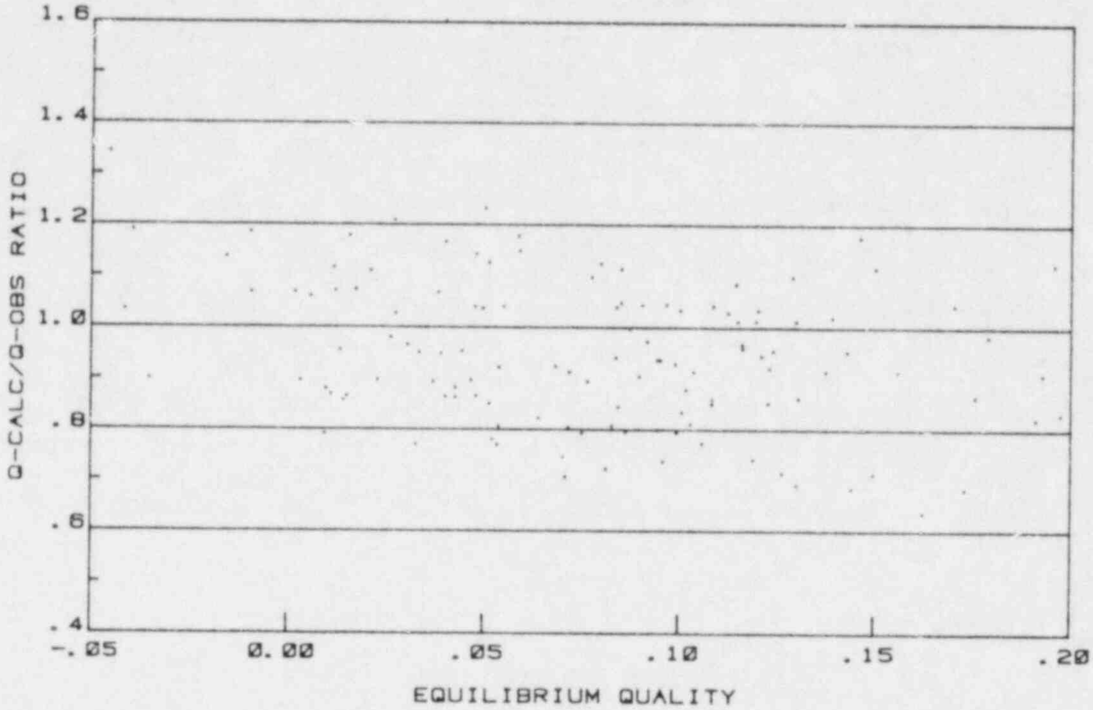

FIG. 5-40 PLOT OF Q-CALC/Q-OBS RATIO VERSUS QUALITY
W-3 CORRELATION - THIRD CHF

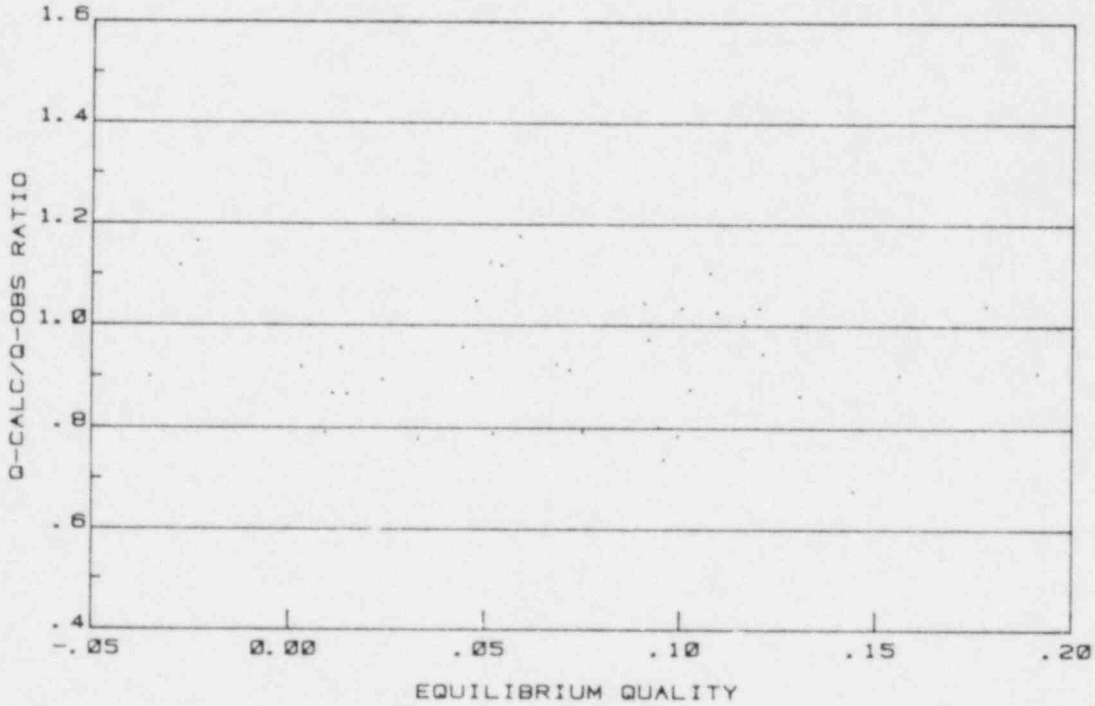

FIG. 5-41 PLOT OF Q-CALC/Q-OBS RATIO VERSUS MASS FLUX
W-3 CORRELATION - FIRST CHF

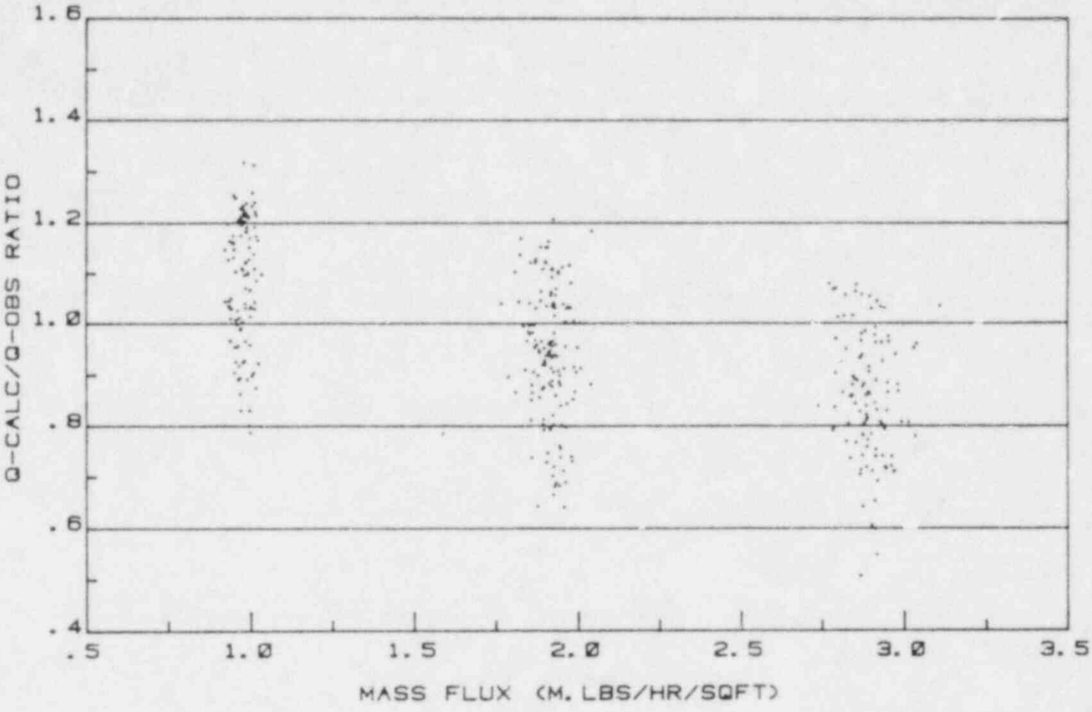

FIG. 5-42 PLOT OF Q-CALC/Q-OBS RATIO VERSUS MASS FLUX
W-3 CORRELATION - HIGHER ORDER CHF

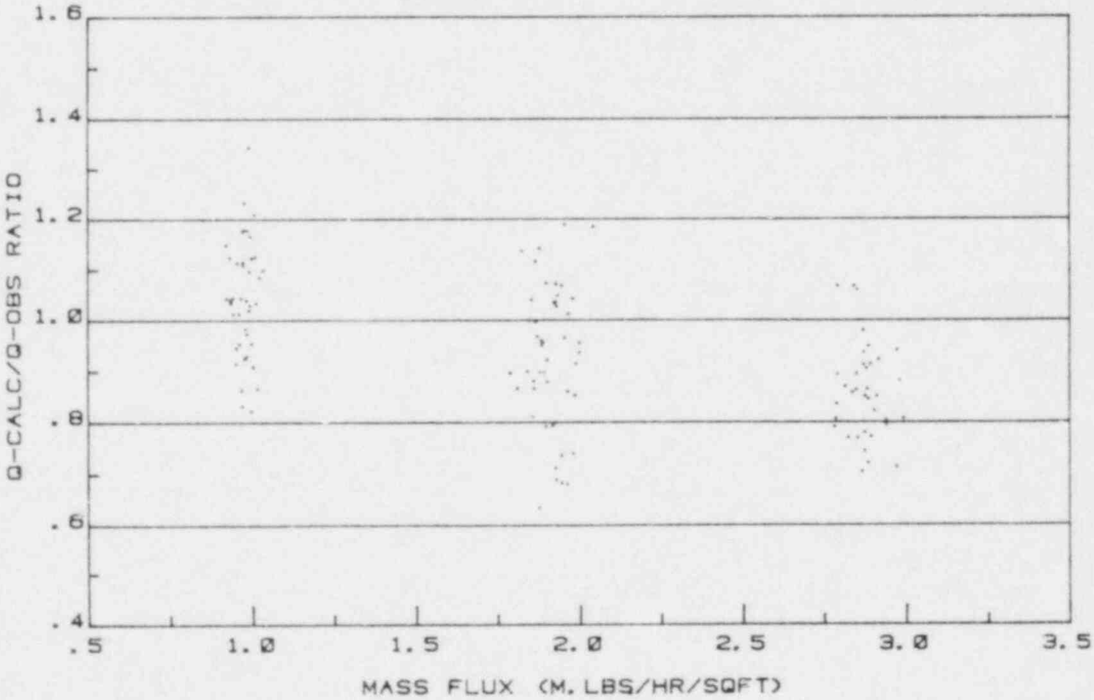

FIG. 5-43 PLOT OF Q-CALC/Q-OBS RATIO VERSUS PRESSURE
W-3 CORRELATION - FIRST CHF

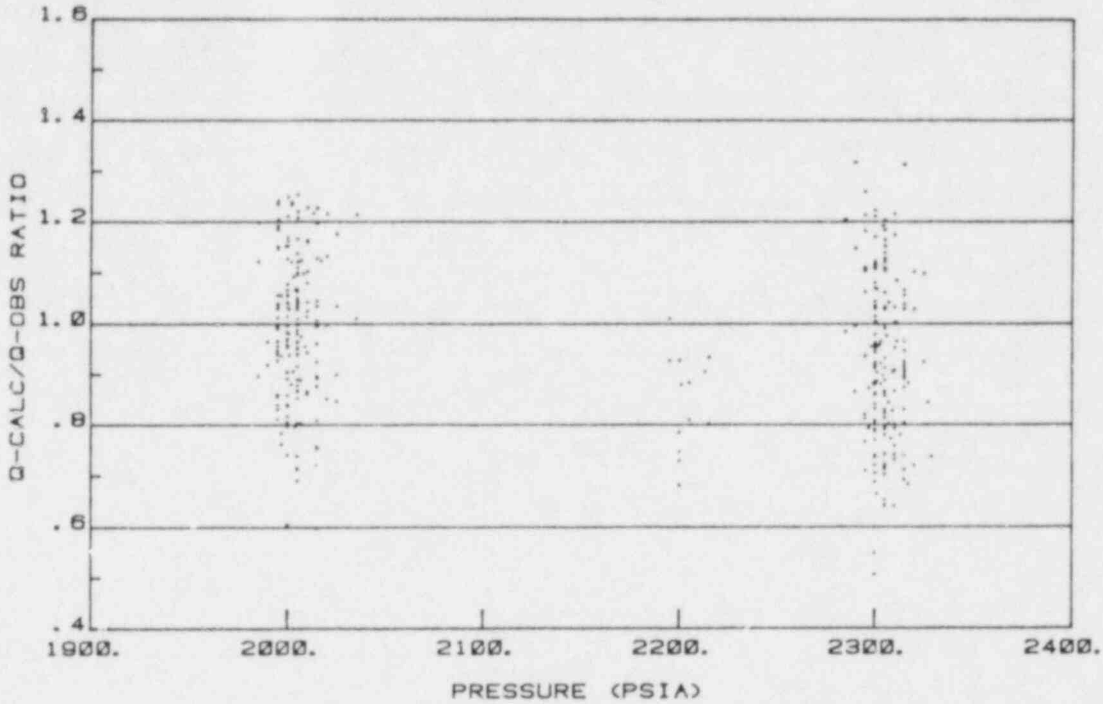

FIG. 5-44 PLOT OF Q-CALC/Q-OBS RATIO VERSUS PRESSURE
W-3 CORRELATION - HIGHER ORDER CHF

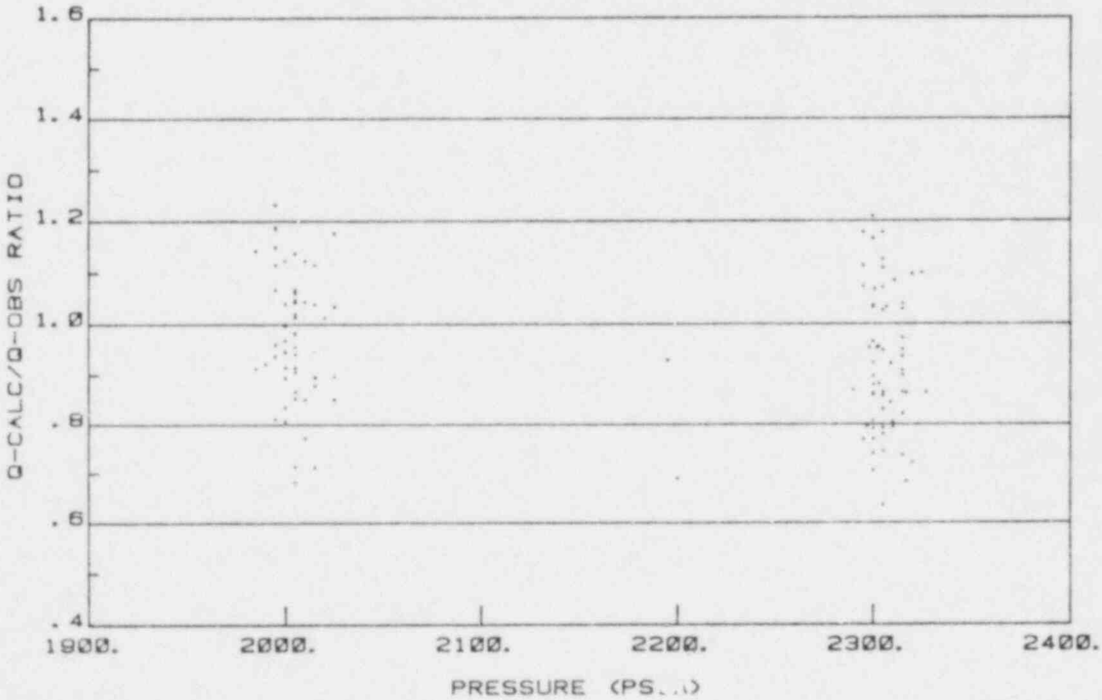

Rosal et al. (24) determined the measured local heat flux at the axial location giving minimum CHF ratio as calculated by the subchannel code for the measured total bundle power at the test inlet conditions. The predicted CHF is the heat flux at the same axial location as above and calculated from the minimum total bundle power for any point in the bundle to reach a CHFR of one for the given inlet conditions. The measured heat flux and predicted CHF as calculated above are then compared.

In the third method, adopted by Combustion Engineering (25), the location giving minimum CHF ratio on the heater rod indicating CHF is established with the aid of the subchannel code for the measured bundle power and the experimental inlet conditions. The measured and predicted values of CHF at this location of minimum CHFR for the heater rod indicating CHF are compared.

In the first two approaches, neither the location of the experimental CHF indication nor the experimental bundle power are used directly in establising thermal margin. In the third approach, the experimental location of the CHF indication is not used directly but the experimental normal power is used. Therefore, these approaches are inappropiate for the analysis of multiple CHF data.

In the present analysis, the measured local heat flux at the experimental location of the first and higher rank CHF indications was compared with the predicted CHF calculated using local conditions from the subchannel analysis for the measured bundle power and test inlet conditions.

The data used in this phase of the work consisted of 978 CHF points from 5 Combustion Engineering and 13 Westinghouse test sections having non-uniform axial heat flux distribution. For reasons stated earlier, the CHF events occurring in the peripheral subchannels were not included in the study, thus reducing the number of CHF points analyzed to 809. The pressure, mass flux, and local quality ranges covered by these data are

1500 to 2450 psia, 0.9 to 3.50 M.lbs/hr-ft^2, and -10 to +30% respectively. The results of the statistical analysis performed on these data with the CE-1 correlation, the B&W-2 correlation, and the Columbia correlation are presented in Tables 5-15, 5-16, and 5-17 respectively. The W-3 CHF correlation was not used in this analysis because it requires the application of F-factor which compares the heat flux at the location of minimum CHFR with the experimental heat flux at that location. Apparently such a comparison is not adequate for the analysis of multiple CHF events.

A comparison of these results with those of the BWR uniform axial heat flux data and the PWR uniform axial heat flux data reveal that the results of these three independet data sets are completely consistent. The three major findings of this study are:

1. The parametric studies show that the residual distributions with respect to local quality, mass flux, pressure, inlet quality, and local experimental CHF of the higher rank CHF events do not exhibit any unusual trends. On the contrary, the general characteristics of the higher rank CHF events are nearly identical to those of the first CHF.

2. All of the four CHF correlations examined (CE-1, B&W-2, W-3, and Columbia) predicted the higher rank CHF events with the same degree of accuracy as the first CHF.

3. The Columbia CHF correlation is in better agreement with the experimental results than the other three CHF correlations assessed (CE-1, B&W-2, and W-3) in predicting both the first CHF and the higher rank CHF occurrences.

It is worth noting that the first two conclusions are in agreement with the conclusions drawn from the analysis of the multiple CHF data based on the bundle average conditions using the Bowring correlation (1).

TABLE 5-15

ANALYSIS OF NON-UNIFORM AXIAL HEAT FLUX PWR DATA

NUMBER OF TEST SECTIONS	= 18
NUMBER OF DATA POINTS	= 809
PRESSURE RANGE (PSIA)	= 1500 TO 2450
MASS FLUX RANGE (M.LBS HR-SQFT)	= 0.90 TO 3.50
LOCAL QUALITY RANGE (%)	= -10. TO 30.

COLUMBIA CHF CORRELATION

CHF RANK	NO. OF POINTS	AVE. RATIO	RMS ERROR	STD. DEVIATION
FIRST CHF	809	1.011	0.081	0.082
SECOND CHF	386	1.004	0.087	0.087
THIRD CHF	192	0.996	0.076	0.076
FOURTH CHF	94	0.981	0.074	0.072
HIGHER ORDER CHF (SECOND & HIGHER)	672	0.999	0.082	0.082
ALL CHF	1481	1.005	0.081	0.081

TABLE 5-16

ANALYSIS OF NON-UNIFORM AXIAL HEAT FLUX PWR DATA

NUMBER OF TEST SECTIONS	= 18
NUMBER OF DATA POINTS	= 809
PRESSURE RANGE (PSIA)	= 1500 TO 2450
MASS FLUX RANGE (M.LBS HR-SQFT)	= 0.90 TO 3.50
LOCAL QUALITY RANGE (%)	= -10. TO 30.

C-E CHF CORRELATION

CHF RANK	NO. OF POINTS	AVE. RATIO	RMS ERROR	STD. DEVIATION
FIRST CHF	809	0.990	0.088	0.088
SECOND CHF	386	0.980	0.094	0.092
THIRD CHF	192	0.978	0.093	0.090
FOURTH CHF	94	0.956	0.085	0.072
HIGHER ORDER CHF (SECOND & HIGHER)	672	0.976	0.092	0.089
ALL CHF	1481	0.984	0.090	0.089

TABLE 5-17

ANALYSIS OF NON-UNIFORM AXIAL HEAT FLUX PWR DATA

NUMBER OF TEST SECTIONS	=	18
NUMBER OF DATA POINTS	=	809
PRESSURE RANGE (PSIA)	=	1500 TO 2450
MASS FLUX RANGE (M.LBS HR-SQFT)	=	0.90 TO 3.50
LOCAL QUALITY RANGE (%)	=	-10. TO 30.

B&W-2 CHF CORRELATION

CHF RANK	NO. OF POINTS	AVE. RATIO	RMS ERROR	STD. DEVIATION
FIRST CHF	809	1.021	0.091	0.088
SECOND CHF	386	1.006	0.092	0.092
THIRD CHF	192	0.999	0.094	0.094
FOURTH CHF	94	0.970	0.088	0.082
HIGHER ORDER CHF (SECOND & HIGHER)	672	0.999	0.092	0.092
ALL CHF	1481	1.011	0.091	0.091

Chapter 6

SUMMARY, CONCLUSIONS, AND RECOMMENDATIONS

Three data sets of rod bundle heat transfer tests performed at the Heat Transfer Research Facility of Columbia University are examined for multiple CHF events. They are:

1. 612 CHF points from 18 General Electric test sections simulating BWR cores with uniform axial heat flux distribution.
2. 819 CHF points from 15 Combustion Engineering test sections simulating PWR cores with uniform axial heat flux distribution.
3. 809 CHF points from 5 Combustion Engineering and 13 Westinghouse Electric test sections simulating PWR cores with non-uniform axial heat flux distribution.

The present study involved ascertaining the adequacy of the local conditions CHF correlations being presently used in nuclear reactor licensing in predicting CHF events of higher rank. The local conditions at the first and higher rank CHF locations for the CHF data in the above three sets were obtained using the COBRA IIIC subchannel code. The local conditions were substituted in various CHF correlations and their accuracy in predicting higher rank CHF events was assessed.

The BWR data were analyzed with the Columbia subchannel CHF correlation. Four CHF correlations, the CE-1, B&W-2, W-3, and the Columbia were employed in the analysis of the PWR uniform axial heat flux data. The PWR non-uniform axial heat flux data were studied using three correlations; CE-1, B&W-2, and Columbia correlation.

A combination of statistical analyses and parametric studies, based on the local conditions derived from the COBRA IIIC subchannel code, were employed to compare the characteristics of the higher rank CHF occurrences with the first CHF for the above mentioned three data sets independently. The results of all the three studies were very similar and led to the following three important conclusions:

1. The statistical results show that the presently available CHF correlations based on local conditions are adequate in the prediction of the CHf events of higher rank. These correlations predict the CHF events of higher rank with the same degree of accuracy as the first CHF.

2. The parametric studies indicate that the characteristic behavior of the CHF events of higher rank than first are nearly the same as those of the first CHF.

3. The Columbia CHF correlation is in better agreement with the experimental results than the other correlations assessed in predicting both the first CHF and the higher rank CHF events.

These conclusions are valid for rod bundle CHF tests under normal steady state conditions. The present study did not encompass the evaluation of the adequacy of the presently available local conditions CHF correlations in the prediction of multiple CHF events occurring due to rod bundle fuel abnormalities, such as bowed rods and heat flux spikes in non-uniform axial heat flux distribution tests. It is recommended that studies be conducted to ascertain the predictability of multiple CHF events observed during these abnormal rod bundle heat transfer tests, using the CHF correlations based on local conditions.

Chapter 7

REFERENCES

1. Nahavandi, A.N., Fighetti, C.F., Reddy, D.G., and Poon, T.C.L., "Multiple DNB Events", NUREG/CR-1953, BNL-NUREG-51345, January 1981.

2. Hovemeyer, W.E., Sreepada, S.R., and Casterline, J.E., "Uprated DC Power System and Thermal-Hydrualic Facilities at Columbia University", EPRI Report NP-773 (1978).

3. Fighetti, C.F. and Reddy, D.G., "Parametric Study of CHF Data. Volume-I Compilation of CHF Data Obtained at Columbia University", Final Report; EPRI Project RP-813-1 (1981).

4. Fighetti, C.F. and Reddy, D.G., "Parametric Study of CHF Data. Volume III CHF Data", Final Report; EPRI Project RP-813-1 (1981).

5. Rowe, D.S., "COBRA - A Digital Computer Program for Thermal Hydrualic Subchannel Analysis of Rod Bundle Nuclear Fuel Elements", BNWL-371, 1967, BNWL-1229, 1970, BNWL-B-82, 1972, BNWL-1695, 1973.

6. Bowring, R.W., "HAMBO - A Computer Program for the Subchannel Analysis of the Hydrualic and Burnout Characteristics of Rod Clusters, Part I: General Description", AEEW-R524, 1967,; "Part II: The Equations", AEEW-R582, 1968.

7. Chelmer, H., et al., "Subchannel Thermal Analysis of Rod Bundle Cores", Nuclear Engineering and Design, 21,3 (1972).

8. "TORC - A Computer Code for Determining the Thermal Margin of a Reactor Core", CENPD-161, July, 1975.

9. Lahey, R.T., and Schraub, F.A., "Mixing, Flow Regimes and Void Fraction for Two-Phase Flow in Rod Bundles", in Two-Phase Flow and Heat Transfer in Rod Bundles, Winter Annual Meeting of ASME, Los Angeles, Nov. 1969.

10. Fajeau, M., "Programme FLICA: Etude Thermodynamique d'un Reacteur ou d'unc Boucle d'Essai", CEA -R 3716, Centre d'Etudes Nucleaires, Saclay, France, 1969.

11. Castellana, F.S. and Bonilla, C.F., "Two-Phase Pressure Drop and Heat Transfer in Rod Bundles", in Two-Phase Flow and Heat Transfer in Rod Bundles, Winter Annual Meeting of ASME, Los Angeles, Nov. 1969.

12. St. Pierre, Carl C., "SASS Code-I Subchannel Analysis for the Steady State", APPE-41, Sept. 1966.

13. Collier, J.G., Convective Boiling and Condensation, McGraw-Hill Book Company (UK), 1972, pp 28, 38 to 47, 180 to 185.

14. Hsu, Y.Y. and Graham R.W., Transport Processes in Boiling and Two-Phase Systems, Hemisphere Publishing Corporation (US), 1976, pp 223 - 227.

15. Reddy, D.G. et al., "Two-Phase Friction Multiplier Correlation for PWR and BWR Fuel Assemblis", Topical Report, EPRI Project RP-813-1, 1981.

16. Reddy, D.G., "A Generalized Subchannel CHF Correlation for PWR and BWR Fuel Assemblies", D.Eng.Sc. Thesis, 1981.

17. Sher, N.C. and Green, S.J., "Boiling Pressure Drop in Thin Rectangular Channels", Chemical Engineering Symposium Series, No. 23 55: 75-84, 1959.

18. Bowring, R.W., "A New Mixed Flow Cluster Dryout Correlation for Pressures in the Range 0.6 - 15.5 MN/m^2 (90 - 2250 Psia) - for Use in a Transient Blowdown Code", Institute of Mechanical Engineers, 1977, pp. 175 - 179.

19. Reddy, D.G. and Fighetti, C.F., "Parametric Study of CHF Data. Volume-II A Generalized Subchannel CHF Correlation for PWR and BWR Fuel Assemblies", Final Report; EPRI Project RP-813-1 (1981).

20. Bowring, R.W., "WSC-2 - A Subchannel Dryout Correlation for Water-Cooled Clusters Over the Pressure Range 3.4 - 15.9 MPa (500 - 2300 Psia)", Technical Report AEEW-R983, 1979.

21. Lawrence, F.D., Woodman, B.W., Fighetti, C.F., and Hovemeyer, W.E., "Critical Heat Flux in PWR Fuel Assemblies", ASME 77-HT-92, Presented at the AIChE-ASME Heat Transfer Conference, Salt Lake City, Utah, Aug. 1976.

22. Gellerstedt, J.S. et al., "Correlation of Critical Heat Flux in a Bundle Cooled by Pressurized Water", in Two-Phase Flow and Heat Transfer in Rod Bundles, Winter Annual Meeting of ASME, Los Angeles, Nov. 1969.

23. Tong, L.S., "An Evaluation of the Departure from Nucleate

Boiling in Bundles of Reactor Fuel Rods", Nuclear Science Engineering, Vol. 33, 1968, pp. 7.

24. Rosal, E.R. et al., "High Pressure Rod Bundle DNB Data With Axially Non-Uniform Heat Flux", Nuclear Engineering and Design Vol. 31, 1974, pp. 1-20.

25. "C-E Critical Heat Flux, Critical Heat Flux Correlation for CE Fuel Assemblies With Standard Spacer Grids, Part 2: Non-Uniform Axial Power Distribution", CE - Report Number: CENPD-207, 1976.

A P P E N D I X - A

SUMMARY OF TEST SECTION GEOMETRY PARAMETERS

TEST SECTION NUMBER 13

TOTAL NUMBER OF RODS : 25
NUMBER OF HEATED RODS: 25
ROD PITCH (INCH) : .580
ROD DIAMETER (INCH) : .440
G.T. DIAMETER (INCH) : .000
HEATED LENGTH (INCH) : 84.000
ROD TO WALL GAP(INCH): .160
FLOW AREA (SQ.INCH) : 5.685
CORNER RADIUS (INCH) : .000

AXIAL HEAT FLUX DISTRIBUTION : UNIFORM

THERMOCOUPLE LOCATIONS :
(DISTANCE FROM INLET (INCH))

83.500 83.500 83.500 83.500

NUMBER OF GRIDS: 5 LOSS COEFF. GRID TYPE 1 : .815
TYPES OF GRIDS : 1

GRID TYPES AND GRID LOCATION:
(DISTANCE FROM INLET (INCH))

1 5.50 1 21.50 1 37.50 1 53.50 1 69.50

ROD PATTERN

1	2	3	4	5
16	17	18	19	6
15	24	25	20	7
14	23	22	21	8
13	12	11	10	9

RADIAL POWER DISTRIBUTION:

.966	.963	.973	.968	.968
.966	1.134	1.134	1.130	.969
.970	1.130	.959	.967	.966
.960	1.132	.968	.968	.975
.973	.972	.957	.963	.971

TEST SECTION NUMBER 14

TOTAL NUMBER OF RODS : 25
NUMBER OF HEATED RODS: 25
ROD PITCH (INCH) : .580
ROD DIAMETER (INCH) : .440
G.T. DIAMETER (INCH) : .000
HEATED LENGTH (INCH) : 84.000
ROD TO WALL GAP(INCH): .160
FLOW AREA (SQ.INCH) : 5.685
CORNER RADIUS (INCH) : .000

AXIAL HEAT FLUX DISTRIBUTION : UNIFORM

THERMOCOUPLE LOCATIONS :
(DISTANCE FROM INLET (INCH))

83.500

NUMBER OF GRIDS: 5 LOSS COEFF. GRID TYPE 1 : .815
TYPES OF GRIDS : 1

GRID TYPES AND GRID LOCATION:
(DISTANCE FROM INLET (INCH))

1 5.50 1 21.50 1 37.50 1 47.50 1 66.50

ROD PATTERN

1	2	3	4	5
16	17	18	19	6
15	24	25	20	7
14	23	22	21	8
13	12	11	10	9

RADIAL POWER DISTRIBUTION:

.966	.963	.973	.968	.968
.966	1.134	1.134	1.130	.969
.970	1.130	.959	.967	.966
.960	1.132	.968	.968	.975
.973	.972	.957	.963	.971

TEST SECTION NUMBER 16

TOTAL NUMBER OF RODS : 22
NUMBER OF HEATED RODS: 21
ROD PITCH (INCH) : .580
ROD DIAMETER (INCH) : .440
G.T. DIAMETER (INCH) : 1.135
HEATED LENGTH (INCH) : 84.000
ROD TO WALL GAP(INCH): .160
FLOW AREA (SQ.INCH) : 5.282
CORNER RADIUS (INCH) : .000

AXIAL HEAT FLUX DISTRIBUTION : UNIFORM

THERMOCOUPLE LOCATIONS :
(DISTANCE FROM INLET (INCH))

83.500

NUMBER OF GRIDS: 5 LOSS COEFF. GRID TYPE 1 : .884
TYPES OF GRIDS : 1

GRID TYPES AND GRID LOCATION:
(DISTANCE FROM INLET (INCH))

1 5.50 1 21.50 1 37.50 1 53.50 1 69.50

ROD PATTERN

1	2	3	4	5
16	17	18	19	6
15	21	0	0	7
14	20	0	0	8
13	12	11	10	9

RADIAL POWER DISTRIBUTION:

.963	.960	.961	.950	.964
.962	1.117	1.118	1.124	.966
.969	1.122	.000	.000	.967
.969	1.119	.000	.000	.962
.959	.963	.961	.964	.962

TEST SECTION NUMBER 17

TOTAL NUMBER OF RODS : 22
NUMBER OF HEATED RODS: 21
ROD PITCH (INCH) : .580
ROD DIAMETER (INCH) : .440
G.T. DIAMETER (INCH) : 1.135
HEATED LENGTH (INCH) : 84.000
ROD TO WALL GAP(INCH): .160
FLOW AREA (SQ.INCH) : 5.282
CORNER RADIUS (INCH) : .000

AXIAL HEAT FLUX DISTRIBUTION : UNIFORM

THERMOCOUPLE LOCATIONS :
(DISTANCE FROM INLET (INCH))

83.500

NUMBER OF GRIDS: 4 LOSS COEFF. GRID TYPE 1 : .815
TYPES OF GRIDS : 1

GRID TYPES AND GRID LOCATION:
(DISTANCE FROM INLET (INCH))

1 9.50 1 28.50 1 47.50 1 66.50

ROD PATTERN

1	2	3	4	5
16	17	18	19	6
15	21	0	0	7
14	20	0	0	8
13	12	11	10	9

RADIAL POWER DISTRIBUTION:

.963	.960	.961	.949	.963
.962	1.118	1.117	1.120	.966
.968	1.133	.000	.000	.967
.968	1.116	.000	.000	.962
.958	.963	.961	.963	.962

TEST SECTION NUMBER 18

TOTAL NUMBER OF RODS : 22
NUMBER OF HEATED RODS: 21
ROD PITCH (INCH) : .580
ROD DIAMETER (INCH) : .440
G.T. DIAMETER (INCH) : 1.135
HEATED LENGTH (INCH) : 48.000
ROD TO WALL GAP(INCH): .160
FLOW AREA (SQ.INCH) : 5.282
CORNER RADIUS (INCH) : .000

AXIAL HEAT FLUX DISTRIBUTION : UNIFORM

THERMOCOUPLE LOCATIONS :
(DISTANCE FROM INLET (INCH))

47.500

NUMBER OF GRIDS: 3 LOSS COEFF. GRID TYPE 1 : .815
TYPES OF GRIDS : 1

GRID TYPES AND GRID LOCATION:
(DISTANCE FROM INLET (INCH))

1 1.50 1 17.50 1 33.50

ROD PATTERN

1	2	3	4	5
16	17	18	19	6
15	21	0	0	7
14	20	0	0	8
13	12	11	10	9

RADIAL POWER DISTRIBUTION:

.968	.968	.972	.977	.977
.971	1.095	1.085	1.092	.974
.970	1.089	.000	.000	.971
.974	1.093	.000	.000	.968
.968	.973	.969	.971	.974

TEST SECTION NUMBER 19

TOTAL NUMBER OF RODS : 22
NUMBER OF HEATED RODS: 21
ROD PITCH (INCH) : .580
ROD DIAMETER (INCH) : .440
G.T. DIAMETER (INCH) : 1.135
HEATED LENGTH (INCH) : 84.000
ROD TO WALL GAP(INCH): .160
FLOW AREA (SQ.INCH) : 5.282
CORNER RADIUS (INCH) : .000

AXIAL HEAT FLUX DISTRIBUTION : UNIFORM

THERMOCOUPLE LOCATIONS :
(DISTANCE FROM INLET (INCH))

83.500

NUMBER OF GRIDS: 4 LOSS COEFF. GRID TYPE 1 : .815
TYPES OF GRIDS : 1

GRID TYPES AND GRID LOCATION:
(DISTANCE FROM INLET (INCH))

1 9.50 1 28.50 1 47.50 1 66.50

ROD PATTERN

1	2	3	4	5
16	17	18	19	6
15	21	0	0	7
14	20	0	0	8
13	12	11	10	9

RADIAL POWER DISTRIBUTION:

.968	.961	.960	.968	.958
.962	1.118	1.119	1.115	.961
.960	1.116	.000	.000	.962
.949	1.132	.000	.000	.969
.963	.959	.967	.966	.968

TEST SECTION NUMBER 20

TOTAL NUMBER OF RODS : 22
NUMBER OF HEATED RODS: 21
ROD PITCH (INCH) : .580
ROD DIAMETER (INCH) : .440
G.T. DIAMETER (INCH) : 1.135
HEATED LENGTH (INCH) : 84.000
ROD TO WALL GAP(INCH): .160
FLOW AREA (SQ.INCH) : 5.282
CORNER RADIUS (INCH) : .000

AXIAL HEAT FLUX DISTRIBUTION : UNIFORM

THERMOCOUPLE LOCATIONS :
(DISTANCE FROM INLET (INCH))

83.500

NUMBER OF GRIDS: 5 LOSS COEFF. GRID TYPE 1 : .815
TYPES OF GRIDS : 1

GRID TYPES AND GRID LOCATION:
(DISTANCE FROM INLET (INCH))

1 5.50 1 21.50 1 37.50 1 53.50 1 69.50

ROD PATTERN

1	2	3	4	5
16	17	18	19	6
15	21	0	0	7
14	20	0	0	8
13	12	11	10	9

RADIAL POWER DISTRIBUTION:

.968	.961	.960	.968	.958
.962	1.118	1.119	1.115	.961
.960	1.116	.000	.000	.963
.949	1.132	.000	.000	.969
.963	.959	.967	.966	.968

TEST SECTION NUMBER 22

TOTAL NUMBER OF RODS : 22
NUMBER OF HEATED RODS: 21
ROD PITCH (INCH) : .580
ROD DIAMETER (INCH) : .440
G.T. DIAMETER (INCH) : 1.135
HEATED LENGTH (INCH) : 84.000
ROD TO WALL GAP(INCH): .160
FLOW AREA (SQ.INCH) : 5.282
CORNER RADIUS (INCH) : .000

AXIAL HEAT FLUX DISTRIBUTION : UNIFORM

THERMOCOUPLE LOCATIONS :
(DISTANCE FROM INLET (INCH))

83.500

NUMBER OF GRIDS: 5 LOSS COEFF. GRID TYPE 1 : 1.085
TYPES OF GRIDS : 1

GRID TYPES AND GRID LOCATION:
(DISTANCE FROM INLET (INCH))

1 5.50 1 21.50 1 37.50 1 53.50 1 69.50

ROD PATTERN

1	2	3	4	5
16	17	18	19	6
15	21	0	0	7
14	20	0	0	8
13	12	11	10	9

RADIAL POWER DISTRIBUTION:

.998	.995	1.005	1.001	1.000
.998	1.012	1.010	.995	1.001
1.002	.995	.000	.000	.998
.993	.991	.000	.000	1.008
1.005	1.005	.990	.995	1.003

TEST SECTION NUMBER 23

TOTAL NUMBER OF RODS : 22
NUMBER OF HEATED RODS: 21
ROD PITCH (INCH) : .580
ROD DIAMETER (INCH) : .440
G.T. DIAMETER (INCH) : 1.135
HEATED LENGTH (INCH) : 84.000
ROD TO WALL GAP(INCH): .160
FLOW AREA (SQ.INCH) : 5.282
CORNER RADIUS (INCH) : .000

AXIAL HEAT FLUX DISTRIBUTION : UNIFORM

THERMOCOUPLE LOCATIONS :
(DISTANCE FROM INLET (INCH))

83.500

NUMBER OF GRIDS: 10 LOSS COEFF. GRID TYPE 1 : 1.029
TYPES OF GRIDS : 1

GRID TYPES AND GRID LOCATION:
(DISTANCE FROM INLET (INCH))

1	5.50	1	13.50	1	21.50	1	29.50	1	37.50	1	45.50
1	53.50	1	61.50	1	69.50	1	77.50				

ROD PATTERN

1	2	3	4	5
16	17	18	19	6
15	21	0	0	7
14	20	0	0	8
13	12	11	10	9

RADIAL POWER DISTRIBUTION:

.998	.995	1.005	1.001	1.001
.998	1.012	1.010	.995	1.003
1.002	.995	.000	.000	1.001
.993	.991	.000	.000	1.008
1.005	1.005	.990	.995	.998

TEST SECTION NUMBER 24

TOTAL NUMBER OF RODS : 22
NUMBER OF HEATED RODS: 21
ROD PITCH (INCH) : .580
ROD DIAMETER (INCH) : .440
G.T. DIAMETER (INCH) : 1.115
HEATED LENGTH (INCH) : 84.000
ROD TO WALL GAP(INCH): .160
FLOW AREA (SQ.INCH) : 5.116
CORNER RADIUS (INCH) : .000
BLOCKAGE LENGTH(INCH): 1.000

AXIAL HEAT FLUX DISTRIBUTION : UNIFORM

THERMOCOUPLE LOCATIONS :
(DISTANCE FROM INLET (INCH))

83.500 83.500 83.500 83.500

NUMBER OF GRIDS: 4 LOSS COEFF. GRID TYPE 1 : .815
TYPES OF GRIDS : 1

GRID TYPES AND GRID LOCATION:
(DISTANCE FROM INLET (INCH))

1 11.00 1 29.25 1 47.50 1 67.75

ROD PATTERN

1	2	3	4	5
14	15	16	17	6
13	20	21	18	7
12	19	0	0	8
11	10	0	0	9

RADIAL POWER DISTRIBUTION:

.982	.976	.975	.982	.972
.975	.976	.981	.980	.976
.977	1.136	1.153	1.134	.963
.973	.977	.000	.000	.984
.967	.981	.000	.000	.981

TEST SECTION NUMBER 25

TOTAL NUMBER OF RODS : 22
NUMBER OF HEATED RODS: 21
ROD PITCH (INCH) : .580
ROD DIAMETER (INCH) : .440
G.T. DIAMETER (INCH) : 1.115
HEATED LENGTH (INCH) : 84.000
ROD TO WALL GAP(INCH): .160
FLOW AREA (SQ.INCH) : 5.116
CORNER RADIUS (INCH) : .000
BLOCKAGE LENGTH(INCH): 1.000

AXIAL HEAT FLUX DISTRIBUTION : UNIFORM

THERMOCOUPLE LOCATIONS :
(DISTANCE FROM INLET (INCH))

83.500

NUMBER OF GRIDS: 4 LOSS COEFF. GRID TYPE 1 : 1.086
TYPES OF GRIDS : 1

GRID TYPES AND GRID LOCATION:
(DISTANCE FROM INLET (INCH))

1 11.00 1 29.25 1 47.50 1 67.75

ROD PATTERN

1	2	3	4	5
14	15	16	17	6
13	20	21	18	7
12	19	0	0	8
11	10	0	0	9

RADIAL POWER DI. .RIBUTION:

.981	.975	.974	.981	.971
.974	.989	.980	.979	.975
.976	1.135	1.152	1.135	.962
.973	.976	.000	.000	.983
.966	.981	.000	.000	.980

TEST SECTION NUMBER 26

TOTAL NUMBER OF RODS	:	22
NUMBER OF HEATED RODS	:	21
ROD PITCH (INCH)	:	.580
ROD DIAMETER (INCH)	:	.440
G.T. DIAMETER (INCH)	:	1.115
HEATED LENGTH (INCH)	:	84.000
ROD TO WALL GAP(INCH)	:	.160
FLOW AREA (SQ.INCH)	:	5.116
CORNER RADIUS (INCH)	:	.000
BLOCKAGE LENGTH(INCH)	:	1.000

AXIAL HEAT FLUX DISTRIBUTION : UNIFORM

THERMOCOUPLE LOCATIONS :
(DISTANCE FROM INLET (INCH))

83.500

NUMBER OF GRIDS: 5　　　LOSS COEFF. GRID TYPE 1 : .815
TYPES OF GRIDS : 1

GRID TYPES AND GRID LOCATION:
(DISTANCE FROM INLET (INCH))

1 8.81　1 27.06　1 45.31　1 63.56　1 81.81

ROD PATTERN

1	2	3	4	5
14	15	16	17	6
13	20	21	18	7
12	19	0	0	8
11	10	0	0	9

RADIAL POWER DISTRIBUTION:

.970	.965	.969	.961	.967
.967	.978	.973	1.001	.961
1.001	1.166	1.164	1.161	.968
.970	.996	.000	.000	.965
.956	.965	.000	.000	.976

TEST SECTION NUMBER 27

TOTAL NUMBER OF RODS	:	22
NUMBER OF HEATED RODS	:	21
ROD PITCH (INCH)	:	.580
ROD DIAMETER (INCH)	:	.440
G.T. DIAMETER (INCH)	:	1.115
HEATED LENGTH (INCH)	:	84.000
ROD TO WALL GAP(INCH)	:	.160
FLOW AREA (SQ.INCH)	:	5.116
CORNER RADIUS (INCH)	:	.000
BLOCKAGE LENGTH(INCH)	:	1.000

AXIAL HEAT FLUX DISTRIBUTION : UNIFORM

THERMOCOUPLE LOCATIONS :
(DISTANCE FROM INLET (INCH))

83.500 83.500 83.500 83.500

NUMBER OF GRIDS: 4 LOSS COEFF. GRID TYPE 1 : 1.053
TYPES OF GRIDS : 1

GRID TYPES AND GRID LOCATION:
(DISTANCE FROM INLET (INCH))

1 11.75 1 30.00 1 48.25 1 66.50

ROD PATTERN

1	2	3	4	5
14	15	16	17	6
13	20	21	18	7
12	19	0	0	8
11	10	0	0	9

RADIAL POWER DISTRIBUTION:

.981	.975	.974	.981	.971
.974	.989	.980	.979	.975
.976	1.135	1.152	1.135	.962
.973	.976	.000	.000	.983
.966	.981	.000	.000	.980

TEST SECTION NUMBER 28

TOTAL NUMBER OF RODS	:	22
NUMBER OF HEATED RODS	:	21
ROD PITCH (INCH)	:	.580
ROD DIAMETER (INCH)	:	.440
G.T. DIAMETER (INCH)	:	1.115
HEATED LENGTH (INCH)	:	84.000
ROD TO WALL GAP(INCH)	:	.160
FLOW AREA (SQ.INCH)	:	5.116
CORNER RADIUS (INCH)	:	.000
BLOCKAGE LENGTH(INCH)	:	1.000

AXIAL HEAT FLUX DISTRIBUTION : UNIFORM

THERMOCOUPLE LOCATIONS :
(DISTANCE FROM INLET (INCH))

83.500

NUMBER OF GRIDS: 4 LOSS COEFF. GRID TYPE 1 : .815
TYPES OF GRIDS : 1

GRID TYPES AND GRID LOCATION:
(DISTANCE FROM INLET (INCH))

1 11.75 1 30.00 1 48.25 1 66.50

ROD PATTERN

1	2	3	4	5
14	15	16	17	6
13	20	21	18	7
12	19	0	0	8
11	10	0	0	9

RADIAL POWER DISTRIBUTION:

1.023	.990	1.006	.993	1.004
1.002	1.004	1.000	.978	.998
1.005	.984	.999	1.006	.998
1.006	1.016	.000	.000	.995
.995	.993	.000	.000	1.006

TEST SECTION NUMBER 29

TOTAL NUMBER OF RODS : 22
NUMBER OF HEATED RODS: 21
ROD PITCH (INCH) : .580
ROD DIAMETER (INCH) : .440
G.T. DIAMETER (INCH) : 1.115
HEATED LENGTH (INCH) : 84.000
ROD TO WALL GAP(INCH): .160
FLOW AREA (SQ.INCH) : 5.116
CORNER RADIUS (INCH) : .000
BLOCKAGE LENGTH(INCH): 1.000

AXIAL HEAT FLUX DISTRIBUTION : UNIFORM

THERMOCOUPLE LOCATIONS :
(DISTANCE FROM INLET (INCH))

83.500

NUMBER OF GRIDS: 10 LOSS COEFF. GRID TYPE 1 : .815
TYPES OF GRIDS : 1

GRID TYPES AND GRID LOCATION:
(DISTANCE FROM INLET (INCH))

1	4.75	1	12.75	1	20.75	1	28.75	1	36.75	1	44.75
1	52.75	1	60.75	1	68.75	1	76.75				

ROD PATTERN

1	2	3	4	5
14	15	16	17	6
13	20	21	18	7
12	19	0	0	8
11	10	0	0	9

RADIAL POWER DISTRIBUTION:

.976	.991	1.008	.994	1.005
1.003	1.005	1.002	.979	1.000
1.006	.985	1.020	1.007	1.000
1.008	1.017	.000	.000	.996
.996	.994	.000	.000	1.007

TEST SECTION NUMBER 59

TOTAL NUMBER OF RODS : 22
NUMBER OF HEATED RODS: 21
ROD PITCH (INCH) : .506
ROD DIAMETER (INCH) : .382
G.T. DIAMETER (INCH) : .980
HEATED LENGTH (INCH) : 150.000
ROD TO WALL GAP(INCH): .123
FLOW AREA (SQ.INCH) : 3.698
CORNER RADIUS (INCH) : .200
BLOCKAGE LENGTH(INCH): .890

AXIAL HEAT FLUX DISTRIBUTION : NON-UNIFORM
NUMBER OF AXIAL HEAT FLUX DISTRIBUTION POINTS: 19

NORMALIZED DISTRIBUTION (X,Y) :

.000	.400	.054	.400	.125	.655	.180	.842	.240	1.029
.287	1.169	.341	1.285	.419	1.414	.449	1.442	.479	1.466
.509	1.472	.539	1.461	.569	1.438	.599	1.403	.659	1.286
.749	1.052	.838	.771	.943	.400	1.000	.400		

THERMOCOUPLE LOCATIONS :
(DISTANCE FROM INLET (INCH))

143.360 129.160 114.960 100.760 86.560 72.360

NUMBER OF GRIDS: 11 LOSS COEFF. GRID TYPE 1 : 1.083
TYPES OF GRIDS : 1

GRID TYPES AND GRID LOCATION:
(DISTANCE FROM INLET (INCH))

1	2.61	1	16.81	1	31.01	1	45.21	1	59.41	1	73.61
1	87.81	1	102.01	1	116.21	1	130.41	1	144.61		

ROD PATTERN

1	2	3	4	5
14	15	16	17	6
13	20	21	18	7
12	19	0	0	8
11	10	0	0	9

RADIAL POWER DISTRIBUTION:

.965	.968	.975	.968	.971
.968	.969	.968	.969	.964
.965	1.199	1.193	1.193	.969
.964	.969	.000	.000	.968
.963	.973	.000	.000	.973

TEST SECTION NUMBER 60

TOTAL NUMBER OF RODS : 22
NUMBER OF HEATED RODS: 21
ROD PITCH (INCH) : .580
ROD DIAMETER (INCH) : .440
G.T. DIAMETER (INCH) : 1.115
HEATED LENGTH (INCH) : 150.000
ROD TO WALL GAP(INCH): .135
FLOW AREA (SQ.INCH) : 4.835
CORNER RADIUS (INCH) : .000
BLOCKAGE LENGTH(INCH): 1.000

AXIAL HEAT FLUX DISTRIBUTION : NON-UNIFORM
NUMBER OF AXIAL HEAT FLUX DISTRIBUTION POINTS: 18

NORMALIZED DISTRIBUTION (X,Y) :

.000	.326	.070	.833	.128	1.170	.186	1.440	.221	1.552
.256	1.620	.302	1.665	.332	1.683	.360	1.665	.384	1.638
.419	1.575	.477	1.418	.651	.810	.740	.540	.800	.428
.850	.349	.900	.315	1.000	.300				

THERMOCOUPLE LOCATIONS :
(DISTANCE FROM INLET (INCH))

140.050 122.670 105.250 87.850 70.450 53.050

NUMBER OF GRIDS: 9 LOSS COEFF. GRID TYPE 1 : 1.430
TYPES OF GRIDS : 1

GRID TYPES AND GRID LOCATION:
(DISTANCE FROM INLET (INCH))

1	2.05	1	16.45	1	33.85	1	51.25	1	68.65	1	86.05
1	103.45	1	120.85	1	138.25						

ROD PATTERN

1	2	3	4	5
14	15	16	17	6
13	20	21	18	7
12	19	0	0	8
11	10	0	0	9

RADIAL POWER DISTRIBUTION:

.966	.971	.966	.971	.966
.975	.966	.976	.966	.958
.969	1.201	1.198	1.201	.971
.971	.966	.000	.000	.964
.962	.956	.000	.000	.966

TEST SECTION NUMBER 66

TOTAL NUMBER OF RODS : 22
NUMBER OF HEATED RODS: 21
ROD PITCH (INCH) : .506
ROD DIAMETER (INCH) : .382
G.T. DIAMETER (INCH) : .980
HEATED LENGTH (INCH) : 150.000
ROD TO WALL GAP(INCH): .123
FLOW AREA (SQ.INCH) : 3.698
CORNER RADIUS (INCH) : .200
BLOCKAGE LENGTH(INCH): .890

AXIAL HEAT FLUX DISTRIBUTION : NON-UNIFORM
NUMBER OF AXIAL HEAT FLUX DISTRIBUTION POINTS: 20

NORMALIZED DISTRIBUTION (X,Y) :

.000	.561	.114	.701	.137	.713	.180	.725	.257	.760
.311	.795	.449	.912	.569	1.064	.665	1.216	.748	1.379
.778	1.426	.808	1.473	.838	1.480	.856	1.473	.880	1.442
.898	1.403	.922	1.316	.946	1.169	.988	.818	1.000	.748

THERMOCOUPLE LOCATIONS :
(DISTANCE FROM INLET (INCH))

149.500 143.360 137.450 129.160

NUMBER OF GRIDS: 11 LOSS COEFF. GRID TYPE 1 : 1.083
TYPES OF GRIDS : 1

GRID TYPES AND GRID LOCATION:
(DISTANCE FROM INLET (INCH))

1	2.61	1	16.81	1	31.01	1	45.21	1	59.41	1	73.61
1	87.81	1	102.01	1	116.21	1	130.41	1	144.61		

ROD PATTERN

1	2	3	4	5
14	15	16	17	6
13	20	21	18	7
12	19	0	0	8
11	10	0	0	9

RADIAL POWER DISTRIBUTION:

.987	.986	.988	.987	.988
.990	.989	.992	.988	.986
.988	1.073	1.069	1.072	.988
.990	.986	.000	.000	.991
.987	.989	.000	.000	.986

TEST SECTION NUMBER 68

TOTAL NUMBER OF RODS : 22
NUMBER OF HEATED RODS: 21
ROD PITCH (INCH) : .506
ROD DIAMETER (INCH) : .382
G.T. DIAMETER (INCH) : .980
HEATED LENGTH (INCH) : 150.000
ROD TO WALL GAP(INCH): .123
FLOW AREA (SQ.INCH) : 3.698
CORNER RADIUS (INCH) : .200
BLOCKAGE LENGTH(INCH): .890

AXIAL HEAT FLUX DISTRIBUTION : NON-UNIFORM
NUMBER OF AXIAL HEAT FLUX DISTRIBUTION POINTS: 19

NORMALIZED DISTRIBUTION (X,Y) :

.000	.400	.054	.400	.125	.655	.180	.842	.240	1.029
.287	1.169	.341	1.285	.419	1.414	.449	1.442	.479	1.466
.509	1.472	.539	1.461	.569	1.438	.599	1.403	.659	1.286
.749	1.052	.838	.771	.943	.400	1.000	.400		

THERMOCOUPLE LOCATIONS :
(DISTANCE FROM INLET (INCH))

143.360 129.160 114.960 100.760 86.560 72.360

NUMBER OF GRIDS: 11 LOSS COEFF. GRID TYPE 1 : 1.430
TYPES OF GRIDS : 1

GRID TYPES AND GRID LOCATION:
(DISTANCE FROM INLET (INCH))

1	2.61	1	16.81	1	31.01	1	45.21	1	59.41	1	73.61
1	87.81	1	102.01	1	116.21	1	130.41	1	144.61		

ROD PATTERN

1	2	3	4	5
14	15	16	17	6
13	20	21	18	7
12	19	0	0	8
11	10	0	0	9

RADIAL POWER DISTRIBUTION:

.965	.968	.975	.968	.971
.968	.969	.968	.969	.964
.965	1.199	1.193	1.193	.969
.964	.969	.000	.000	.968
.963	.973	.000	.000	.973

TEST SECTION NUMBER 71

```
TOTAL NUMBER OF RODS :  22
NUMBER OF HEATED RODS:  21
ROD PITCH (INCH)     :     .506
ROD DIAMETER (INCH)  :     .382
G.T. DIAMETER (INCH) :     .980
HEATED LENGTH (INCH) : 150.000
ROD TO WALL GAP(INCH):     .123
FLOW AREA (SQ.INCH)  :    3.698
CORNER RADIUS (INCH) :     .200
BLOCKAGE LENGTH(INCH):     .980
```

AXIAL HEAT FLUX DISTRIBUTION : NON-UNIFORM
NUMBER OF AXIAL HEAT FLUX DISTRIBUTION POINTS: 20

NORMALIZED DISTRIBUTION (X,Y) :

.000	.561	.114	.701	.137	.713	.180	.725	.257	.760
.311	.795	.449	.912	.569	1.064	.665	1.216	.748	1.379
.778	1.426	.808	1.473	.838	1.480	.856	1.473	.880	1.442
.898	1.403	.922	1.316	.946	1.169	.988	.818	1.000	.748

THERMOCOUPLE LOCATIONS :
(DISTANCE FROM INLET (INCH))

149.500 143.360 137.450 129.160

NUMBER OF GRIDS: 11 LOSS COEFF. GRID TYPE 1 : 1.430
TYPES OF GRIDS : 1

GRID TYPES AND GRID LOCATION:
(DISTANCE FROM INLET (INCH))

1	2.6.	1	16.81	1	31.01	1	45.00	21	1.00	59	1.00
1	87.81	1	102.01	1	116.21	1	130.41	1	144.61		

ROD PATTERN

1	2	3	4	5
14	15	16	17	6
13	20	21	18	7
12	19	0	0	8
11	10	0	0	9

RADIAL POWER DISTRIBUTION:

.989	.985	.990	.989	.989
.989	.990	.980	.989	.986
.994	1.073	1.069	1.073	.990
.987	.987	.000	.000	.992
.987	.989	.000	.000	.981

TEST SECTION NUMBER 108

TOTAL NUMBER OF RODS : 16
NUMBER OF HEATED RODS: 16
ROD PITCH (INCH) : .555
ROD DIAMETER (INCH) : .422
G.T. DIAMETER (INCH) : .000
HEATED LENGTH (INCH) : 96.000
ROD TO WALL GAP(INCH): .153
FLOW AREA (SQ.INCH) : 3.489
CORNER RADIUS (INCH) : .000

AXIAL HEAT FLUX DISTRIBUTION : NON-UNIFORM
NUMBER OF AXIAL HEAT FLUX DISTRIBUTION POINTS: 28

NORMALIZED DISTRIBUTION (X,Y) :

.000	.358	.052	.359	.104	.400	.156	.458	.208	.567
.260	.683	.313	.833	.365	.992	.417	1.133	.469	1.258
.495	1.305	.521	1.350	.547	1.410	.573	1.467	.599	1.522
.625	1.592	.651	1.640	.677	1.658	.703	1.640	.729	1.583
.755	1.510	.781	1.433	.833	1.233	.885	.993	.911	.815
.938	.633	.963	.520	1.000	.367				

THERMOCOUPLE LOCATIONS :
(DISTANCE FROM INLET (INCH))

90.000 87.000 84.000 80.000 76.000 70.000

NUMBER OF GRIDS: 9 LOSS COEFF. GRID TYPE 1 : 1.200
TYPES OF GRIDS : 2 LOSS COEFF. GRID TYPE 2 : .570

GRID TYPES AND GRID LOCATION:
(DISTANCE FROM INLET (INCH))

1	10.75	2	20.75	1	30.75	12	40.75	1	50.75	2	60.75
1	70.75	2	80.75	1	90.75						

ROD PATTERN

1	2	3	4
12	13	14	5
11	16	15	6
10	9	8	7

RADIAL POWER DISTRIBUTION:

.952	.952	.952	.952
.952	1.145	1.145	.952
.952	1.145	1.145	.952
.952	.952	.952	.952

TEST SECTION NUMBER 109

TOTAL NUMBER OF RODS	:	9
NUMBER OF HEATED RODS	:	9
ROD PITCH (INCH)	:	.658
ROD DIAMETER (INCH)	:	.500
G.T. DIAMETER (INCH)	:	.000
HEATED LENGTH (INCH)	:	168.000
ROD TO WALL GAP(INCH)	:	.184
FLOW AREA (SQ.INCH)	:	3.003
CORNER RADIUS (INCH)	:	.000

AXIAL HEAT FLUX DISTRIBUTION : NON-UNIFORM
NUMBER OF AXIAL HEAT FLUX DISTRIBUTION POINTS: 27

NORMALIZED DISTRIBUTION (X,Y) :

.000	.480	.059	.480	.119	.520	.179	.595	.238	.695
.298	.825	.357	.960	.386	1.030	.412	1.100	.446	1.175
.476	1.240	.506	1.300	.536	1.360	.565	1.415	.595	1.475
.625	1.520	.655	1.560	.685	1.580	.714	1.565	.744	1.515
.774	1.450	.804	1.355	.833	1.240	.863	1.105	.893	.940
.963	.600	1.000	.480						

THERMOCOUPLE LOCATIONS :
(DISTANCE FROM INLET (INCH))

162.000 158.000 152.000 142.000 138.000 132.000 122.000

NUMBER OF GRIDS: 17 LOSS COEFF. GRID TYPE 1 : 1.200
TYPES OF GRIDS : 2 LOSS COEFF. GRID TYPE 2 : .570

GRID TYPES AND GRID LOCATION:
(DISTANCE FROM INLET (INCH))

1	2.75	2	12.75	1	22.75	2	32.75	1	42.75	2	52.75
1	62.75	2	72.75	1	82.75	2	92.75	1	102.75	2	112.75
1	122.75	2	132.75	1	142.75	2	152.75	1	162.75		

ROD PATTERN

1	2	3
8	9	4
7	6	5

RADIAL POWER DISTRIBUTION:

1.000	1.000	1.000
1.000	1.000	1.000
1.000	1.000	1.000

TEST SECTION NUMBER 110

TOTAL NUMBER OF RODS : 16
NUMBER OF HEATED RODS: 16
ROD PITCH (INCH) : .555
ROD DIAMETER (INCH) : .422
G.T. DIAMETER (INCH) : .000
HEATED LENGTH (INCH) : 96.000
ROD TO WALL GAP(INCH): .153
FLOW AREA (SQ.INCH) : 3.489
CORNER RADIUS (INCH) : .000

AXIAL HEAT FLUX DISTRIBUTION : NON-UNIFORM
NUMBER OF AXIAL HEAT FLUX DISTRIBUTION POINTS: 28

NORMALIZED DISTRIBUTION (X,Y) :

.000	.358	.052	.359	.104	.400	.156	.458	.208	.567
.260	.683	.313	.833	.365	.992	.417	1.133	.469	1.258
.495	1.305	.521	1.350	.547	1.410	.573	1.467	.599	1.522
.625	1.592	.651	1.640	.677	1.658	.703	1.640	.729	1.583
.755	1.510	.781	1.433	.833	1.233	.885	.993	.911	.815
.938	.633	.963	.520	1.000	.367				

THERMOCOUPLE LOCATIONS :
(DISTANCE FROM INLET (INCH))

90.000 87.000 84.000 80.000 76.000 70.000

NUMBER OF GRIDS: 9 LOSS COEFF. GRID TYPE 1 : .640
TYPES OF GRIDS : 2 LOSS COEFF. GRID TYPE 2 : .570

GRID TYPES AND GRID LOCATION:
(DISTANCE FROM INLET (INCH))

1	10.75	2	20.75	1	30.75	2	40.75	1	50.75	2	60.75
1	70.75	2	80.75	1	90.75						

ROD PATTERN

1	2	3	4
12	13	14	5
11	16	15	6
10	9	8	7

RADIAL POWER DISTRIBUTION:

.951	.951	.951	.951
.951	1.146	1.146	.951
.951	1.146	1.146	.951
.951	.951	.951	.951

TEST SECTION NUMBER 111

TOTAL NUMBER OF RODS	:	16
NUMBER OF HEATED RODS	:	16
ROD PITCH (INCH)	:	.555
ROD DIAMETER (INCH)	:	.422
G.T. DIAMETER (INCH)	:	.000
HEATED LENGTH (INCH)	:	96.000
ROD TO WALL GAP(INCH)	:	.153
FLOW AREA (SQ.INCH)	:	3.489
CORNER RADIUS (INCH)	:	.000

AXIAL HEAT FLUX DISTRIBUTION : NON-UNIFORM

NUMBER OF AXIAL HEAT FLUX DISTRIBUTION POINTS: 28

NORMALIZED DISTRIBUTION (X,Y) :

.000	.358	.052	.359	.104	.400	.156	.458	.208	.567
.260	.683	.313	.833	.365	.992	.417	1.133	.469	1.258
.495	1.305	.521	1.350	.547	1.410	.573	1.467	.599	1.522
.625	1.592	.651	1.640	.677	1.658	.703	1.640	.729	1.583
.755	1.510	.781	1.433	.833	1.233	.885	.993	.911	.815
.938	.633	.963	.520	1.000	.367				

THERMOCOUPLE LOCATIONS :
(DISTANCE FROM INLET (INCH))

90.000 87.000 84.000 80.000 76.000 70.000

NUMBER OF GRIDS: 9 LOSS COEFF. GRID TYPE 1 : .640

TYPES OF GRIDS : 1

GRID TYPES AND GRID LOCATION:
(DISTANCE FROM INLET (INCH))

1	10.75	1	20.75	1	30.75	1	40.75	1	50.75	1	60.75
1	70.75	1	80.75	1	90.75						

ROD PATTERN

1	2	3	4
12	13	14	5
11	16	15	6
10	9	8	7

RADIAL POWER DISTRIBUTION:

.951	.951	.951	.951
.951	1.146	1.146	.951
.951	1.146	1.146	.951
.951	.951	.951	.951

TEST SECTION NUMBER 131

TOTAL NUMBER OF RODS : 16
NUMBER OF HEATED RODS: 16
ROD PITCH (INCH) : .555
ROD DIAMETER (INCH) : .422
G.T. DIAMETER (INCH) : .000
HEATED LENGTH (INCH) : 168.000
ROD TO WALL GAP(INCH): .102
FLOW AREA (SQ.INCH) : 3.052
CORNER RADIUS (INCH) : .000

AXIAL HEAT FLUX DISTRIBUTION : NON-UNIFORM
NUMBER OF AXIAL HEAT FLUX DISTRIBUTION POINTS: 22

NORMALIZED DISTRIBUTION (X,Y) :

.000	.540	.073	.577	.139	.638	.213	.724	.257	.798
.316	.896	.363	.994	.411	1.092	.440	1.153	.477	1.221
.528	1.300	.572	1.350	.602	1.374	.638	1.393	.660	1.386
.697	1.374	.734	1.337	.763	1.288	.800	1.215	.837	1.129
.881	1.006	1.000	.589						

THERMOCOUPLE LOCATIONS :
(DISTANCE FROM INLET (INCH))

152.000 148.000 142.000 136.000 129.000 122.000

NUMBER OF GRIDS: 13 LOSS COEFF. GRID TYPE 1 : 1.400
TYPES OF GRIDS : 2 LOSS COEFF. GRID TYPE 2 : .570

GRID TYPES AND GRID LOCATION:
(DISTANCE FROM INLET (INCH))

2	6.00	1	19.00	2	32.00	1	45.00	2	53.00	1	71.00
2	84.00	1	97.00	2	110.00	1	123.00	2	136.00	1	149.00
2	162.00										

ROD PATTERN

1	2	3	4
12	13	14	5
11	16	15	6
10	9	8	7

RADIAL POWER DISTRIBUTION:

.959	.959	.958	.962
.960	1.121	1.122	.960
.960	1.121	1.121	.961
.960	.960	.959	.958

TEST SECTION NUMBER 132

TOTAL NUMBER OF RODS	:	16
NUMBER OF HEATED RODS	:	16
ROD PITCH (INCH)	:	.555
ROD DIAMETER (INCH)	:	.422
G.T. DIAMETER (INCH)	:	.000
HEATED LENGTH (INCH)	:	168.000
ROD TO WALL GAP(INCH)	:	.102
FLOW AREA (SQ.INCH)	:	3.052
CORNER RADIUS (INCH)	:	.000

AXIAL HEAT FLUX DISTRIBUTION : NON-UNIFORM
NUMBER OF AXIAL HEAT FLUX DISTRIBUTION POINTS: 22

NORMALIZED DISTRIBUTION (X,Y) :

.000	.540	.073	.577	.139	.638	.213	.724	.257	.798
.316	.896	.363	.994	.411	1.092	.440	1.153	.477	1.221
.528	1.300	.572	1.350	.602	1.374	.638	1.393	.660	1.386
.697	1.374	.734	1.337	.763	1.288	.800	1.215	.837	1.129
.881	1.006	1.000	.589						

THERMOCOUPLE LOCATIONS :
(DISTANCE FROM INLET (INCH))

152.000 148.000 142.000 136.000 129.000 122.000

NUMBER OF GRIDS: 17
TYPES OF GRIDS : 2

LOSS COEFF. GRID TYPE 1 : 1.400
LOSS COEFF. GRID TYPE 2 : .570

GRID TYPES AND GRID LOCATION:
(DISTANCE FROM INLET (INCH))

2	3.00	1	13.00	2	23.00	1	33.00	2	43.00	1	53.00
2	63.00	1	73.00	2	83.00	1	93.00	2	103.00	1	113.00
2	123.00	1	133.00	2	143.00	1	153.00	2	163.00		

ROD PATTERN

1	2	3	4
12	13	14	5
11	16	15	6
10	9	8	7

RADIAL POWER DISTRIBUTION:

.959	.959	.958	.962
.960	1.121	1.122	.960
.960	1.121	1.121	.961
.960	.960	.959	.958

TEST SECTION NUMBER 133

TOTAL NUMBER OF RODS : 16
NUMBER OF HEATED RODS: 16
ROD PITCH (INCH) : .555
ROD DIAMETER (INCH) : .422
G.T. DIAMETER (INCH) : .000
HEATED LENGTH (INCH) : 168.000
ROD TO WALL GAP(INCH): .106
FLOW AREA (SQ.INCH) : 3.052
CORNER RADIUS (INCH) : .000

AXIAL HEAT FLUX DISTRIBUTION : NON-UNIFORM
NUMBER OF AXIAL HEAT FLUX DISTRIBUTION POINTS: 22

NORMALIZED DISTRIBUTION (X,Y) :

.000	.540	.073	.577	.139	.638	.213	.724	.257	.798
.316	.896	.363	.994	.411	1.092	.440	1.153	.477	1.221
.528	1.300	.572	1.350	.602	1.374	.638	1.393	.660	1.386
.697	1.374	.734	1.337	.763	1.288	.800	1.215	.837	1.129
.881	1.006	1.000	.589						

THERMOCOUPLE LOCATIONS :
(DISTANCE FROM INLET (INCH))

152.000 148.000 142.000 136.000 129.000 122.000

NUMBER OF GRIDS: 13 LOSS COEFF. GRID TYPE 1 : 1.400
TYPES OF GRIDS : 1

GRID TYPES AND GRID LOCATION:
(DISTANCE FROM INLET (INCH))

1	6.00	1	19.00	1	32.00	1	45.00	1	58.00	1	71.00
1	84.00	1	97.00	1	110.00	1	123.00	1	137.00	1	149.00
1	162.00										

ROD PATTERN

1	2	3	4
12	13	14	5
11	16	15	6
10	9	8	7

RADIAL POWER DISTRIBUTION:

.959	.959	.958	.961
.960	1.120	1.121	.960
.960	1.121	1.124	.961
.960	.960	.959	.958

TEST SECTION NUMBER 134

TOTAL NUMBER OF RODS : 16
NUMBER OF HEATED RODS: 16
ROD PITCH (INCH) : .555
ROD DIAMETER (INCH) : .422
G.T. DIAMETER (INCH) : .000
HEATED LENGTH (INCH) : 168.000
ROD TO WALL GAP(INCH): .106
FLOW AREA (SQ.INCH) : 3.052
CORNER RADIUS (INCH) : .000

AXIAL HEAT FLUX DISTRIBUTION : NON-UNIFORM
NUMBER OF AXIAL HEAT FLUX DISTRIBUTION POINTS: 22

NORMALIZED DISTRIBUTION (X,Y) :

.000	.540	.073	.577	.139	.638	.213	.724	.257	.798
.316	.896	.363	.994	.411	1.092	.440	1.153	.477	1.221
.528	1.300	.572	1.350	.602	1.374	.638	1.393	.660	1.386
.697	1.374	.734	1.337	.763	1.288	.800	1.215	.837	1.129
.881	1.006	1.000	.589						

THERMOCOUPLE LOCATIONS :
(DISTANCE FROM INLET (INCH))

152.000 148.000 142.000 136.000 129.000 122.000

NUMBER OF GRIDS: 10 LOSS COEFF. GRID TYPE 1 : 1.400
TYPES OF GRIDS : 2 LOSS COEFF. GRID TYPE 2 : .570

GRID TYPES AND GRID LOCATION:
(DISTANCE FROM INLET (INCH))

2	11.00	1	27.00	2	43.00	1	59.00	2	75.00	1	91.00
2	107.00	1	123.00	2	139.00	1	155.00				

ROD PATTERN

1	2	3	4
12	13	14	5
11	16	15	6
10	9	8	7

RADIAL POWER DISTRIBUTION:

.959	.960	.958	.960
.960	1.121	1.121	.960
.960	1.123	1.123	.960
.959	.958	.959	.960

TEST SECTION NUMBER 141

TOTAL NUMBER OF RODS	:	16
NUMBER OF HEATED RODS	:	16
ROD PITCH (INCH)	:	.555
ROD DIAMETER (INCH)	:	.422
G.T. DIAMETER (INCH)	:	.000
HEATED LENGTH (INCH)	:	96.000
ROD TO WALL GAP(INCH)	:	.153
FLOW AREA (SQ.INCH)	:	3.489
CORNER RADIUS (INCH)	:	.000

AXIAL HEAT FLUX DISTRIBUTION : NON-UNIFORM
NUMBER OF AXIAL HEAT FLUX DISTRIBUTION POINTS: 24

NORMALIZED DISTRIBUTION (X,Y) :

.000	.310	.052	.450	.104	.610	.156	.780	.208	.920
.260	1.080	.313	1.200	.365	1.320	.417	1.400	.469	1.460
.510	1.480	.521	1.480	.573	1.450	.604	1.410	.625	1.380
.667	1.300	.729	1.160	.771	1.060	.813	.950	.833	.875
.844	.840	.875	.740	.938	.530	1.000	.310		

THERMOCOUPLE LOCATIONS :
(DISTANCE FROM INLET (INCH))

84.000 81.000 78.000 74.000 64.000 58.000

NUMBER OF GRIDS: 9 LOSS COEFF. GRID TYPE 1 : 1.820
TYPES OF GRIDS : 2 LOSS COEFF. GRID TYPE 2 : .570

GRID TYPES AND GRID LOCATION:
(DISTANCE FROM INLET (INCH))

2	4.75	1	14.75	2	24.75	1	34.75	2	44.75	1	54.75
2	64.75	1	74.75	2	84.75						

ROD PATTERN

1	2	3	4
12	13	14	5
11	16	15	6
10	9	8	7

RADIAL POWER DISTRIBUTION:

.958	.958	.958	.958
.958	1.127	1.127	.958
.958	1.127	1.127	.958
.958	.958	.958	.958

TEST SECTION NUMBER 146

TOTAL NUMBER OF RODS : 16
NUMBER OF HEATED RODS: 16
ROD PITCH (INCH) : .555
ROD DIAMETER (INCH) : .422
G.T. DIAMETER (INCH) : .000
HEATED LENGTH (INCH) : 168.000
ROD TO WALL GAP(INCH): .106
FLOW AREA (SQ.INCH) : 3.052
CORNER RADIUS (INCH) : .000

AXIAL HEAT FLUX DISTRIBUTION : NON-UNIFORM
NUMBER OF AXIAL HEAT FLUX DISTRIBUTION POINTS: 22

NORMALIZED DISTRIBUTION (X,Y) :

.000	.540	.073	.577	.139	.638	.213	.724	.257	.798
.316	.896	.363	.994	.411	1.092	.440	1.153	.477	1.221
.528	1.300	.572	1.350	.602	1.374	.638	1.393	.660	1.386
.697	1.374	.734	1.337	.763	1.288	.800	1.215	.837	1.129
.881	1.006	1.000	.589						

THERMOCOUPLE LOCATIONS :
(DISTANCE FROM INLET (INCH))

152.000 148.000 144.000 136.000 129.000 122.000

NUMBER OF GRIDS: 13 LOSS COEFF. GRID TYPE 1 : 1.900
TYPES OF GRIDS : 2 LOSS COEFF. GRID TYPE 2 : .570

GRID TYPES AND GRID LOCATION:
(DISTANCE FROM INLET (INCH))

2	6.00	1	19.00	2	32.00	1	45.00	2	58.00	1	71.00
2	84.00	1	97.00	2	110.00	1	123.00	2	136.00	1	149.00
2	162.00										

ROD PATTERN

1	2	3	4
12	13	14	5
11	16	15	6
10	9	8	7

RADIAL POWER DISTRIBUTION:

.958	.958	.958	.958
.958	1.127	1.127	.958
.958	1.127	1.127	.958
.958	.958	.958	.958

TEST SECTION NUMBER 147

TOTAL NUMBER OF RODS : 16
NUMBER OF HEATED RODS: 16
ROD PITCH (INCH) : .555
ROD DIAMETER (INCH) : .422
G.T. DIAMETER (INCH) : .000
HEATED LENGTH (INCH) : 168.000
ROD TO WALL GAP(INCH): .106
FLOW AREA (SQ.INCH) : 3.052
CORNER RADIUS (INCH) : .000

AXIAL HEAT FLUX DISTRIBUTION : NON-UNIFORM
NUMBER OF AXIAL HEAT FLUX DISTRIBUTION POINTS: 22

NORMALIZED DISTRIBUTION (X,Y) :

.000	.540	.073	.577	.139	.638	.213	.724	.257	.798
.316	.896	.363	.994	.411	1.092	.440	1.153	.477	1.221
.528	1.300	.572	1.350	.602	1.374	.638	1.393	.660	1.386
.697	1.374	.734	1.337	.763	1.288	.800	1.215	.837	1.129
.881	1.006	1.000	.589						

THERMOCOUPLE LOCATIONS :
(DISTANCE FROM INLET (INCH))

152.000 148.000 142.000 136.000 129.000 122.000

NUMBER OF GRIDS: 13 LOSS COEFF. GRID TYPE 1 : 1.710
TYPES OF GRIDS : 2 LOSS COEFF. GRID TYPE 2 : .570

GRID TYPES AND GRID LOCATION:
(DISTANCE FROM INLET (INCH))

2	6.00	1	19.00	2	32.00	1	45.00	2	58.00	1	71.00
2	84.00	1	97.00	2	110.00	1	123.00	2	136.00	1	149.00
2	162.00										

ROD PATTERN

1	2	3	4
12	13	14	5
11	16	15	6
10	9	8	7

RADIAL POWER DISTRIBUTION:

.959	.960	.958	.960
.960	1.121	1.121	.960
.960	1.123	1.123	.960
.959	.958	.959	.960

TEST SECTION NUMBER 162

TOTAL NUMBER OF RODS : 25
NUMBER OF HEATED RODS: 24
ROD PITCH (INCH) : .496
ROD DIAMETER (INCH) : .374
G.T. DIAMETER (INCH) : .485
HEATED LENGTH (INCH) : 168.000
ROD TO WALL GAP(INCH): .100
FLOW AREA (SQ.INCH) : 3.721
CORNER RADIUS (INCH) : .000

AXIAL HEAT FLUX DISTRIBUTION : NON-UNIFORM
NUMBER OF AXIAL HEAT FLUX DISTRIBUTION POINTS: 27

NORMALIZED DISTRIBUTION (X,Y) :

.000	.390	.032	.416	.064	.475	.097	.543	.129	.619
.193	.819	.258	1.048	.322	1.250	.354	1.353	.387	1.440
.419	1.505	.432	1.527	.451	1.544	.483	1.548	.515	1.544
.541	1.535	.562	1.505	.580	1.483	.612	1.418	.662	1.287
.771	.939	.831	.743	.870	.612	.908	.525	.941	.460
.967	.427	1.000	.416						

THERMOCOUPLE LOCATIONS :
(DISTANCE FROM INLET (INCH))

134.000 123.500 112.000 101.500 90.000

NUMBER OF GRIDS: 15 LOSS COEFF. GRID TYPE 1 : 1.250
TYPES OF GRIDS : 2 LOSS COEFF. GRID TYPE 2 : .570

GRID TYPES AND GRID LOCATION:
(DISTANCE FROM INLET (INCH))

1	3.00	2	14.00	1	25.00	2	36.00	1	47.00	2	58.00
1	69.00	2	80.00	1	91.00	2	102.00	1	113.00	2	124.00
1	135.00	2	146.00	1	157.00						

ROD PATTERN

1	2	3	4	5
16	17	18	19	6
15	24	25	20	7
14	23	22	21	8
13	12	11	10	9

RADIAL POWER DISTRIBUTION:

.951	.950	.951	.951	.951
.950	1.099	1.099	1.099	.951
.950	1.099	.000	1.099	.951
.950	1.099	1.099	1.099	.951
.951	.950	.951	.950	.951

TEST SECTION NUMBER 164

TOTAL NUMBER OF RODS : 25
NUMBER OF HEATED RODS: 25
ROD PITCH (INCH) : .496
ROD DIAMETER (INCH) : .374
G.T. DIAMETER (INCH) : .000
HEATED LENGTH (INCH) : 168.000
ROD TO WALL GAP(INCH): .100
FLOW AREA (SQ.INCH) : 3.796
CORNER RADIUS (INCH) : .000

AXIAL HEAT FLUX DISTRIBUTION : NON-UNIFORM
NUMBER OF AXIAL HEAT FLUX DISTRIBUTION POINTS: 27

NORMALIZED DISTRIBUTION (X,Y) :

.000	.390	.032	.416	.064	.475	.097	.543	.129	.619
.193	.819	.258	1.048	.322	1.250	.354	1.353	.387	1.440
.419	1.505	.432	1.527	.451	1.544	.483	1.548	.515	1.544
.541	1.535	.562	1.505	.580	1.483	.612	1.418	.662	1.287
.771	.939	.831	.743	.870	.612	.908	.525	.941	.460
.967	.427	1.000	.416						

THERMOCOUPLE LOCATIONS :
(DISTANCE FROM INLET (INCH))

134.000 123.500 112.000 101.500 90.000

NUMBER OF GRIDS: 15 LOSS COEFF. GRID TYPE 1 : 1.250
TYPES OF GRIDS : 2 LOSS COEFF. GRID TYPE 2 : .570

GRID TYPES AND GRID LOCATION:
(DISTANCE FROM INLET (INCH))

1	3.00	2	14.00	1	25.00	2	36.00	1	47.00	2	58.00
1	69.00	2	80.00	1	91.00	2	102.00	1	113.00	2	124.00
1	135.00	2	146.00	1	157.00						

ROD PATTERN

1	2	3	4	5
16	17	18	19	6
15	24	25	20	7
14	23	22	21	8
13	12	11	10	9

RADIAL POWER DISTRIBUTION:

.946	.948	.947	.947	.946
.948	1.095	1.095	1.095	.946
.946	1.095	1.095	1.095	.949
.946	1.095	1.095	1.095	.946
.946	.947	.946	.946	.946

TEST SECTION NUMBER 301

TOTAL NUMBER OF RODS : 16
NUMBER OF HEATED RODS: 16
ROD PITCH (INCH) : .738
ROD DIAMETER (INCH) : .563
G.T. DIAMETER (INCH) : .000
HEATED LENGTH (INCH) : 72.000
ROD TO WALL GAP(INCH): .133
FLOW AREA (SQ.INCH) : 5.128
CORNER RADIUS (INCH) : .410

AXIAL HEAT FLUX DISTRIBUTION : UNIFORM

THERMOCOUPLE LOCATIONS :
(DISTANCE FROM INLET (INCH))

71.500

NUMBER OF GRIDS: 7 LOSS COEFF. GRID TYPE 1 : .800
TYPES OF GRIDS : 1

GRID TYPES AND GRID LOCATION:
(DISTANCE FROM INLET (INCH))

1 5.50 1 15.00 1 24.50 1 34.00 1 43.50 1 53.00
1 62.50

ROD PATTERN

1	2	3	4
12	13	14	5
11	16	15	6
10	9	8	7

RADIAL POWER DISTRIBUTION:

1.010	.995	.998	.995
1.002	.998	1.018	.997
1.008	1.000	.995	.990
1.002	.997	1.000	1.000

TEST SECTION NUMBER 302

TOTAL NUMBER OF RODS : 16
NUMBER OF HEATED RODS: 16
ROD PITCH (INCH) : .738
ROD DIAMETER (INCH) : .563
G.T. DIAMETER (INCH) : .000
HEATED LENGTH (INCH) : 72.000
ROD TO WALL GAP(INCH): .133
FLOW AREA (SQ.INCH) : 5.128
CORNER RADIUS (INCH) : .410

AXIAL HEAT FLUX DISTRIBUTION : UNIFORM

THERMOCOUPLE LOCATIONS :
(DISTANCE FROM INLET (INCH))

71.500

NUMBER OF GRIDS: 4 LOSS COEFF. GRID TYPE 1 : 1.470
TYPES OF GRIDS : 1

GRID TYPES AND GRID LOCATION:
(DISTANCE FROM INLET (INCH))

1 8.00 1 17.50 1 37.00 1 56.50

ROD PATTERN

1	2	3	4
12	13	14	5
11	16	15	6
10	9	8	7

RADIAL POWER DISTRIBUTION:

1.002	.988	1.004	1.004
.988	1.004	.988	1.013
1.006	.993	1.003	.996
1.015	.988	1.003	1.006

TEST SECTION NUMBER 303

TOTAL NUMBER OF RODS	:	16
NUMBER OF HEATED RODS	:	16
ROD PITCH (INCH)	:	.738
ROD DIAMETER (INCH)	:	.563
G.T. DIAMETER (INCH)	:	.000
HEATED LENGTH (INCH)	:	72.000
ROD TO WALL GAP(INCH)	:	.133
FLOW AREA (SQ.INCH)	:	5.128
CORNER RADIUS (INCH)	:	.410

AXIAL HEAT FLUX DISTRIBUTION : UNIFORM

THERMOCOUPLE LOCATIONS :
(DISTANCE FROM INLET (INCH))

71.500

NUMBER OF GRIDS: 3 LOSS COEFF. GRID TYPE 1 : 1.470
TYPES OF GRIDS : 1

GRID TYPES AND GRID LOCATION:
(DISTANCE FROM INLET (INCH))

1 14.50 1 34.00 1 53.50

ROD PATTERN

1	2	3	4
12	13	14	5
11	16	15	6
10	9	8	7

RADIAL POWER DISTRIBUTION:

1.002	.989	1.004	1.004
.989	1.004	.989	1.005
1.006	.994	1.003	.996
1.016	.989	1.003	1.006

TEST SECTION NUMBER 305

TOTAL NUMBER OF RODS : 16
NUMBER OF HEATED RODS: 16
ROD PITCH (INCH) : .738
ROD DIAMETER (INCH) : .563
G.T. DIAMETER (INCH) : .000
HEATED LENGTH (INCH) : 72.000
ROD TO WALL GAP(INCH): .133
FLOW AREA (SQ.INCH) : 5.128
CORNER RADIUS (INCH) : .410

AXIAL HEAT FLUX DISTRIBUTION : UNIFORM

THERMOCOUPLE LOCATIONS :
(DISTANCE FROM INLET (INCH))

71.500

NUMBER OF GRIDS: 3 LOSS COEFF. GRID TYPE 1 : 1.470
TYPES OF GRIDS : 1

GRID TYPES AND GRID LOCATION:
(DISTANCE FROM INLET (INCH))

1 14.50 1 34.00 1 53.50

ROD PATTERN

1	2	3	4
12	13	14	5
11	16	15	6
10	9	8	7

RADIAL POWER DISTRIBUTION:

.755	.991	.991	.755
.991	1.263	1.263	.991
.991	1.263	1.263	.991
.755	.991	.991	.755

TEST SECTION NUMBER 306

```
TOTAL NUMBER OF RODS :   16
NUMBER OF HEATED RODS:   16
ROD PITCH (INCH)      :    .738
ROD DIAMETER (INCH)   :    .563
G.T. DIAMETER (INCH) :    .000
HEATED LENGTH (INCH) :  72.000
ROD TO WALL GAP(INCH):    .137
FLOW AREA (SQ.INCH)   :   5.208
CORNER RADIUS (INCH) :    .400
```

AXIAL HEAT FLUX DISTRIBUTION : UNIFORM

THERMOCOUPLE LOCATIONS :
(DISTANCE FROM INLET (INCH))

71.500

NUMBER OF GRIDS: 3   LOSS COEFF. GRID TYPE 1 : 1.470
TYPES OF GRIDS :   1

GRID TYPES AND GRID LOCATION:
(DISTANCE FROM INLET (INCH))

1 14.87   1 34.37   1 53.87

ROD PATTERN

1	2	3	4
12	13	14	5
11	16	15	6
10	9	8	7

RADIAL POWER DISTRIBUTION:

1.000	1.000	1.000	1.000
1.000	1.000	1.000	1.000
1.000	1.000	1.000	1.000
1.000	1.000	1.000	1.000

TEST SECTION NUMBER 307

TOTAL NUMBER OF RODS : 16
NUMBER OF HEATED RODS: 16
ROD PITCH (INCH) : .738
ROD DIAMETER (INCH) : .563
G.T. DIAMETER (INCH) : .000
HEATED LENGTH (INCH) : 48.000
ROD TO WALL GAP(INCH): .137
FLOW AREA (SQ.INCH) : 5.208
CORNER RADIUS (INCH) : .400

AXIAL HEAT FLUX DISTRIBUTION : UNIFORM

THERMOCOUPLE LOCATIONS :
(DISTANCE FROM INLET (INCH))

47.500

NUMBER OF GRIDS: 2
TYPES OF GRIDS : 1

LOSS COEFF. GRID TYPE 1 : 1.470

GRID TYPES AND GRID LOCATION:
(DISTANCE FROM INLET (INCH))

1 10.37 1 29.87

ROD PATTERN

1	2	3	4
12	13	14	5
11	16	15	6
10	9	8	7

RADIAL POWER DISTRIBUTION:

1.000	1.000	1.000	1.000
1.000	1.000	1.000	1.000
1.000	1.000	1.000	1.000
1.000	1.000	1.000	1.000

TEST SECTION NUMBER 307.1

TOTAL NUMBER OF RODS	:	16
NUMBER OF HEATED RODS	:	16
ROD PITCH (INCH)	:	.738
ROD DIAMETER (INCH)	:	.563
G.T. DIAMETER (INCH)	:	.000
HEATED LENGTH (INCH)	:	48.000
ROD TO WALL GAP(INCH)	:	.137
FLOW AREA (SQ.INCH)	:	5.208
CORNER RADIUS (INCH)	:	.400

AXIAL HEAT FLUX DISTRIBUTION : UNIFORM

THERMOCOUPLE LOCATIONS :
(DISTANCE FROM INLET (INCH))

47.500

NUMBER OF GRIDS: 2 LOSS COEFF. GRID TYPE 1 : 1.470
TYPES OF GRIDS : 1

GRID TYPES AND GRID LOCATION:
(DISTANCE FROM INLET (INCH))

1 10.37 1 29.87

ROD PATTERN

1	2	3	4
12	13	14	5
11	16	15	6
10	9	8	7

RADIAL POWER DISTRIBUTION:

1.000	1.000	1.000	1.000
1.000	1.000	1.000	1.000
1.000	1.000	1.000	1.000
1.000	1.000	1.000	1.000

TEST SECTION NUMBER 308

TOTAL NUMBER OF RODS	:	16
NUMBER OF HEATED RODS	:	16
ROD PITCH (INCH)	:	.738
ROD DIAMETER (INCH)	:	.563
G.T. DIAMETER (INCH)	:	.000
HEATED LENGTH (INCH)	:	72.000
ROD TO WALL GAP(INCH)	:	.137
FLOW AREA (SQ.INCH)	:	5.208
CORNER RADIUS (INCH)	:	.400

AXIAL HEAT FLUX DISTRIBUTION : UNIFORM

THERMOCOUPLE LOCATIONS :
(DISTANCE FROM INLET (INCH))

71.500

NUMBER OF GRIDS: 3 LOSS COEFF. GRID TYPE 1 : 1.470
TYPES OF GRIDS : 1

GRID TYPES AND GRID LOCATION:
(DISTANCE FROM INLET (INCH))

1 14.87 1 34.37 1 53.87

ROD PATTERN

1	2	3	4
12	13	14	5
11	16	15	6
10	9	8	7

RADIAL POWER DISTRIBUTION:

1.210	1.110	1.110	.940
1.110	.940	.940	.940
1.110	.940	.940	.930
.940	.940	.940	.940

TEST SECTION NUMBER 309

TOTAL NUMBER OF RODS	:	16
NUMBER OF HEATED RODS	:	16
ROD PITCH (INCH)	:	.738
ROD DIAMETER (INCH)	:	.563
G.T. DIAMETER (INCH)	:	.000
HEATED LENGTH (INCH)	:	72.000
ROD TO WALL GAP(INCH)	:	.137
FLOW AREA (SQ.INCH)	:	5.208
CORNER RADIUS (INCH)	:	.400

AXIAL HEAT FLUX DISTRIBUTION : UNIFORM

THERMOCOUPLE LOCATIONS :
(DISTANCE FROM INLET (INCH))

71.500

NUMBER OF GRIDS: 3 LOSS COEFF. GRID TYPE 1 : 1.470
TYPES OF GRIDS : 1

GRID TYPES AND GRID LOCATION:
(DISTANCE FROM INLET (INCH))

1 14.87 1 34.37 1 53.87

ROD PATTERN

1	2	3	4
12	13	14	5
11	16	15	6
10	9	8	7

RADIAL POWER DISTRIBUTION:

.940	.940	1.100	.940
.940	1.210	.940	1.100
1.110	.950	.950	.940
.940	1.100	.940	.940

TEST SECTION NUMBER 310

TOTAL NUMBER OF RODS : 16
NUMBER OF HEATED RODS: 16
ROD PITCH (INCH) : .738
ROD DIAMETER (INCH) : .563
G.T. DIAMETER (INCH) : .000
HEATED LENGTH (INCH) : 72.000
ROD TO WALL GAP(INCH): .137
FLOW AREA (SQ.INCH) : 5.208
CORNER RADIUS (INCH) : .400

AXIAL HEAT FLUX DISTRIBUTION : UNIFORM

THERMOCOUPLE LOCATIONS :
(DISTANCE FROM INLET (INCH))

71.500

NUMBER OF GRIDS: 3 LOSS COEFF. GRID TYPE 1 : 1.470
TYPES OF GRIDS : 1

GRID TYPES AND GRID LOCATION:
(DISTANCE FROM INLET (INCH))

1 14.87 1 34.37 1 53.87

ROD PATTERN

1	2	3	4
12	13	14	5
11	16	15	6
10	9	8	7

RADIAL POWER DISTRIBUTION:

1.610	1.610	1.130	.950
1.610	1.220	.950	.660
1.110	.950	.660	.650
.950	.660	.650	.650

TEST SECTION NUMBER 311

TOTAL NUMBER OF RODS	:	16
NUMBER OF HEATED RODS	:	16
ROD PITCH (INCH)	:	.738
ROD DIAMETER (INCH)	:	.563
G.T. DIAMETER (INCH)	:	.000
HEATED LENGTH (INCH)	:	72.000
ROD TO WALL GAP(INCH)	:	.137
FLOW AREA (SQ.INCH)	:	5.232
CORNER RADIUS (INCH)	:	.400

AXIAL HEAT FLUX DISTRIBUTION : UNIFORM

THERMOCOUPLE LOCATIONS :
(DISTANCE FROM INLET (INCH))

71.500

NUMBER OF GRIDS: 3
TYPES OF GRIDS : 1

LOSS COEFF. GRID TYPE 1 : 1.470

GRID TYPES AND GRID LOCATION:
(DISTANCE FROM INLET (INCH))

1 14.87 1 34.37 1 53.87

ROD PATTERN

1	2	3	4
12	13	14	5
11	16	15	6
10	9	8	7

RADIAL POWER DISTRIBUTION:

1.000	1.000	1.000	1.000
1.000	1.000	1.0C0	1.000
1.000	1.000	1.000	1.000
1.000	1.000	1.000	1.000

TEST SECTION NUMBER 312

TOTAL NUMBER OF RODS : 16
NUMBER OF HEATED RODS: 16
ROD PITCH (INCH) : .738
ROD DIAMETER (INCH) : .563
G.T. DIAMETER (INCH) : .000
HEATED LENGTH (INCH) : 72.000
ROD TO WALL GAP(INCH): .137
FLOW AREA (SQ.INCH) : 5.232
CORNER RADIUS (INCH) : .400

AXIAL HEAT FLUX DISTRIBUTION : UNIFORM

THERMOCOUPLE LOCATIONS :
(DISTANCE FROM INLET (INCH))

71.500

NUMBER OF GRIDS: 3 LOSS COEFF. GRID TYPE 1 : 1.470
TYPES OF GRIDS : 1

GRID TYPES AND GRID LOCATION:
(DISTANCE FROM INLET (INCH))

1 14.87 1 34.37 1 53.87

ROD PATTERN

1	2	3	4
12	13	14	5
11	16	15	6
10	9	8	7

RADIAL POWER DISTRIBUTION:

1.271	1.271	1.041	.897
1.271	1.041	.897	.897
1.041	.897	.897	.897
.897	.897	.897	.897

TEST SECTION NUMBER 313

TOTAL NUMBER OF RODS	:	16
NUMBER OF HEATED RODS	:	16
ROD PITCH (INCH)	:	.738
ROD DIAMETER (INCH)	:	.563
G.T. DIAMETER (INCH)	:	.000
HEATED LENGTH (INCH)	:	72.000
ROD TO WALL GAP(INCH)	:	.137
FLOW AREA (SQ.INCH)	:	5.232
CORNER RADIUS (INCH)	:	.400

AXIAL HEAT FLUX DISTRIBUTION : UNIFORM

THERMOCOUPLE LOCATIONS :
(DISTANCE FROM INLET (INCH))

71.500

NUMBER OF GRIDS: 7 LOSS COEFF. GRID TYPE 1 : .800
TYPES OF GRIDS : 1

GRID TYPES AND GRID LOCATION:
(DISTANCE FROM INLET (INCH))

1 5.50 1 15.00 1 24.50 1 34.00 1 43.50 1 53.00
1 62.50

ROD PATTERN

1	2	3	4
12	13	14	5
11	16	15	6
10	9	8	7

RADIAL POWER DISTRIBUTION:

.988	.993	1.002	1.015
.990	.997	1.019	1.002
1.002	1.009	.998	.996
.988	1.005	1.006	.989

TEST SECTION NUMBER 314

TOTAL NUMBER OF RODS : 16
NUMBER OF HEATED RODS: 16
ROD PITCH (INCH) : .738
ROD DIAMETER (INCH) : .563
G.T. DIAMETER (INCH) : .000
HEATED LENGTH (INCH) : 72.000
ROD TO WALL GAP(INCH): .137
FLOW AREA (SQ.INCH) : 5.232
CORNER RADIUS (INCH) : .400

AXIAL HEAT FLUX DISTRIBUTION : UNIFORM

THERMOCOUPLE LOCATIONS :
(DISTANCE FROM INLET (INCH))

71.500

NUMBER OF GRIDS: 3 LOSS COEFF. GRID TYPE 1 : 1.470
TYPES OF GRIDS : 1

GRID TYPES AND GRID LOCATION:
(DISTANCE FROM INLET (INCH))

1 14.87 1 34.37 1 53.87

ROD PATTERN

1	2	3	4
12	13	14	5
11	16	15	6
10	9	8	7

RADIAL POWER DISTRIBUTION:

1.285	1.285	1.085	.889
1.285	1.085	.889	.889
1.085	.889	.889	.889
.889	.889	.889	.889

TEST SECTION NUMBER 315

TOTAL NUMBER OF RODS : 16
NUMBER OF HEATED RODS: 16
ROD PITCH (INCH) : .738
ROD DIAMETER (INCH) : .563
G.T. DIAMETER (INCH) : .000
HEATED LENGTH (INCH) : 72.000
ROD TO WALL GAP(INCH): .137
FLOW AREA (SQ.INCH) : 5.232
CORNER RADIUS (INCH) : .400

AXIAL HEAT FLUX DISTRIBUTION : UNIFORM

THERMOCOUPLE LOCATIONS :
(DISTANCE FROM INLET (INCH))

71.500

NUMBER OF GRIDS: 3 LOSS COEFF. GRID TYPE 1 : 1.470
TYPES OF GRIDS : 1

GRID TYPES AND GRID LOCATION:
(DISTANCE FROM INLET (INCH))

1 14.87 1 34.37 1 53.87

ROD PATTERN

1	2	3	4
12	13	14	5
11	16	15	6
10	9	8	7

RADIAL POWER DISTRIBUTION:

.992	.990	.989	1.018
.992	1.005	.993	.999
1.001	1.014	1.001	.999
.990	1.004	1.003	1.008

TEST SECTION NUMBER 316

```
TOTAL NUMBER OF RODS :   16
NUMBER OF HEATED RODS:   16
ROD PITCH (INCH)      :    .738
ROD DIAMETER (INCH)   :    .563
G.T. DIAMETER (INCH)  :    .000
HEATED LENGTH (INCH)  :  72.000
ROD TO WALL GAP(INCH):     .137
FLOW AREA (SQ.INCH)   :   5.232
CORNER RADIUS (INCH)  :    .400
```

AXIAL HEAT FLUX DISTRIBUTION : UNIFORM

THERMOCOUPLE LOCATIONS :
(DISTANCE FROM INLET (INCH))

71.500

NUMBER OF GRIDS: 3 LOSS COEFF. GRID TYPE 1 : 1.470
TYPES OF GRIDS : 1

GRID TYPES AND GRID LOCATION:
(DISTANCE FROM INLET (INCH))

1 14.87 1 34.37 1 53.87

ROD PATTERN

1	2	3	4
12	13	14	5
11	16	15	6
10	9	8	7

RADIAL POWER DISTRIBUTION:

.992	.990	.989	1.018
.992	1.005	.993	.999
1.001	1.014	1.001	.999
.990	1.004	1.003	1.008

TEST SECTION NUMBER 316.1

```
TOTAL NUMBER OF RODS :  16
NUMBER OF HEATED RODS:  16
ROD PITCH (INCH)     :     .738
ROD DIAMETER (INCH)  :     .563
G.T. DIAMETER (INCH) :     .000
HEATED LENGTH (INCH) :   72.000
ROD TO WALL GAP(INCH):     .137
FLOW AREA (SQ.INCH)  :    5.232
CORNER RADIUS (INCH) :     .400
```

AXIAL HEAT FLUX DISTRIBUTION : UNIFORM

THERMOCOUPLE LOCATIONS :
(DISTANCE FROM INLET (INCH))

71.500

NUMBER OF GRIDS: 3 LOSS COEFF. GRID TYPE 1 : 1.470
TYPES OF GRIDS : 1

GRID TYPES AND GRID LOCATION:
(DISTANCE FROM INLET (INCH))

1 14.87 1 34.37 1 53.87

ROD PATTERN

1	2	3	4
12	13	14	5
11	16	15	6
10	9	8	7

RADIAL POWER DISTRIBUTION:

.992	.990	.989	1.018
.992	1.005	.993	.999
1.001	1.014	1.001	.999
.990	1.004	1.003	1.008

TEST SECTION NUMBER 318

TOTAL NUMBER OF RODS : 16
NUMBER OF HEATED RODS: 16
ROD PITCH (INCH) : .738
ROD DIAMETER (INCH) : .563
G.T. DIAMETER (INCH) : .000
HEATED LENGTH (INCH) : 72.000
ROD TO WALL GAP(INCH): .137
FLOW AREA (SQ.INCH) : 5.232
CORNER RADIUS (INCH) : .400

AXIAL HEAT FLUX DISTRIBUTION : UNIFORM

THERMOCOUPLE LOCATIONS :
(DISTANCE FROM INLET (INCH))

71.500

NUMBER OF GRIDS: 3 LOSS COEFF. GRID TYPE 1 : 1.470
TYPES OF GRIDS : 1

GRID TYPES AND GRID LOCATION:
(DISTANCE FROM INLET (INCH))

1 14.87 1 34.37 1 53.87

ROD PATTERN

1	2	3	4
12	13	14	5
11	16	15	6
10	9	8	7

RADIAL POWER DISTRIBUTION:

.922	.928	.932	.940
.929	1.232	1.204	.920
.922	1.221	1.230	.929
.928	.931	.915	.917

APPENDIX - B

TYPICAL TEST CONDITIONS FOR CHF TESTS FROM THREE DATA SETS

TEST SECTION NUMBER 13

SRL	RUN	PRESS	TEMP	G(AVE)	Q(AVE)	CHF RODS			
1	13	2300.	618.0	2.030	.374	24.0	19.0		
2	14	2005.	603.0	2.007	.357	24.0			
3	15	1800.	602.0	2.007	.331	18.0	19.0	24.0	
4	16	2300.	592.0	2.021	.429	24.0			
5	17	2000.	574.0	1.995	.428	24.0			
6	18	1810.	573.0	2.014	.394	24.0			
7	[illegible]	2300.	575.0	2.064	.479	24.0	23.0		
8	[illegible]	2005.	560.0	2.008	.460	24.0			
9	[illegible]	1805.	561.0	1.975	.411	24.0			
10	22	2290.	562.0	1.988	.491	24.0			
11	[illegible]	2000.	531.0	1.942	.512	24.0			
12	24	1813.	531.0	1.961	.489	24.0			
13	25	2329.	625.0	2.949	.471	24.0			
14	26	2315.	614.0	3.010	.507	24.0	23.0		
15	27	2010.	613.0	2.988	.435	19.0	24.0		
16	28	1805.	605.0	2.916	.392	24.0			
17	29	2327.	605.0	3.004	.543	24.0	23.0		
18	30	2005.	603.0	2.997	.462	24.0	19.0		
19	31	2317.	601.0	3.005	.542	23.0	24.0		
20	32	1985.	589.0	3.019	.518	24.0	19.0	23.0	
21	33	1805.	590.0	3.008	.449	24.0			
22	34	1815.	580.0	2.982	.478	24.0			
23	35	2005.	579.0	3.014	.538	24.0			
24	36	1815.	565.0	3.002	.526	24.0			
25	37	2315.	570.0	1.033	.303	24.0			
26	38	2010.	572.0	1.001	.294	24.0	19.0	18.0	17.0
27	39	1815.	569.0	1.002	.295	19.0			
28	40	2305.	538.0	1.022	.334	24.0			
29	41	1934.	540.0	1.007	.333	24.0			
30	42	1795.	539.0	.998	.329	19.0			
31	43	2295.	536.0	2.001	.538	24.0			
32	44	2010.	510.0	1.981	.553	24.0			
33	45	1790.	505.0	1.979	.533	24.0			
34	46	2305.	502.0	1.014	.371	24.0			
35	47	2020.	504.0	1.001	.367	24.0			

TEST SECTION NUMBER 13 (CONTINUED)

SRL	RUN	PRESS	TEMP	G(AVE)	Q(AVE)	CHF RODS		
36	48	1790.	500.0	1.003	.386	17.0	18.0	19.0
37	49	2285.	472.0	.993	.401	24.0		
38	50	1985.	472.0	.990	.390	24.0		
39	51	1810.	472.0	.980	.379	17.0	24.0	
40	52	1405.	577.0	1.998	.363	19.0	24.0	
41	53	1395.	568.0	1.976	.383	19.0	24.0	
42	54	1405.	533.0	1.993	.421	19.0		
43	55	1410.	512.0	1.988	.466	19.0		
44	56	905.	515.0	1.961	.482	24.0	19.0	
45	57	915.	502.0	1.999	.508	19.0	24.0	
46	58	895.	489.0	1.969	.524	24.0		
47	67	1440.	564.0	2.864	.438	19.0		
48	68	1410.	552.0	3.017	.469	19.0		
49	69	1400.	545.0	3.008	.479	19.0		
50	70	1395.	560.0	1.031	.321	24.0	19.0	
51	71	1410.	521.0	.992	.351	24.0		
52	72	900.	514.0	.969	.404	24.0	19.0	
53	73	1405.	477.0	.997	.406	24.0		
54	74	900.	477.0	.993	.437	24.0		
55	75	905.	441.0	.983	.476	24.0		
56	76	610.	463.5	.952	.424	24.0	19.0	
57	77	625.	439.0	.991	.456	24.0		
58	78	605.	430.0	.963	.459	24.0		
59	79	1795.	500.0	.986	.366	19.0		
60	80	2290.	530.0	.492	.239	17.0	24.0	18.0
61	81	1995.	532.0	.489	.247	19.0	17.0	24.0
62	82	1790.	531.0	.480	.248	24.0	19.0	17.0
63	83	2310.	488.0	.514	.270	24.0	17.0	19.0
64	84	1965.	490.0	.503	.275	19.0		
65	85	1790.	490.0	.502	.274	19.0	17.0	24.0
66	86	2290.	432.0	.504	.303	24.0		
67	87	2005.	430.0	.495	.312	17.0	24.0	
68	88	1800.	432.0	.494	.312	19.0	24.0	17.0
69	89	1415.	552.0	.487	.266	19.0	24.0	
70	90	1400.	525.0	.489	.284	19.0	24.0	

TEST SECTION NUMBER 13 (CONTINUED)

SRL	RUN	PRESS	TEMP	G(AVE)	Q(AVE)	CHF RODS
71	91	1405.	481.0	.497	.311	19.0 24.0
72	92	905.	507.0	.505	.314	17.0 18.0 19.0 24.0
73	93	900.	477.0	.513	.339	17.0 18.0 19.0 24.0
74	94	900.	450.0	.492	.347	18.0 24.0
75	95	605.	459.0	.487	.322	17.0 18.0 19.0 24.0
76	96	600.	431.0	.499	.338	17.0 18.0 24.0
77	97	605.	408.0	.490	.354	17.0 18.0 24.0
78	98	2325.	425.0	.314	.250	18.0 24.0
79	99	2000.	425.0	.302	.265	24.0 19.0 17.0 18.0
80	100	1805.	424.0	.311	.268	24.0 19.0 17.0
81	101	2325.	390.0	.319	.265	18.0 24.0
82	102	2020.	387.0	.319	.274	24.0 17.0 18.0 19.0
83	103	1800.	394.0	.299	.273	19.0 24.0 17.0
84	104	2325.	342.0	.291	.283	18.0 24.0 17.0 19.0 23.0
85	105	2000.	347.0	.290	.287	17.0 24.0 18.0
86	106	1800.	345.0	.290	.294	19.0 17.0 24.0 18.0
87	107	1395.	402.0	.315	.291	19.0 24.0 17.0
88	108	900.	397.0	.297	.286	18.0 24.0 17.0
89	109	595.	403.0	.322	.269	18.0 24.0 17.0
90	110	1400.	378.0	.302	.302	24.0 19.0 17.0 18.0 23.0
91	111	900.	372.0	.293	.288	18.0 24.0
92	112	600.	374.0	.292	.272	18.0 24.0 17.0 19.0
93	113	1415.	355.0	.297	.307	19.0 24.0 17.0 18.0
94	114	910.	349.0	.297	.309	18.0 24.0 17.0 19.0
95	115	585.	347.0	.288	.278	18.0 24.0
96	116	435.	426.0	.957	.391	24.0 18.0 17.0
97	117	410.	402.0	1.010	.444	24.0
98	118	415.	388.0	.976	.466	18.0 24.0
99	120	400.	411.0	.488	.310	17.0 18.0 24.0
100	121	405.	396.0	.503	.323	18.0 24.0 17.0
101	122	410.	358.0	.498	.346	18.0 24.0
102	123	221.	350.0	.491	.282	24.0 18.0 17.0
103	124	207.	323.0	.498	.294	17.0 18.0 24.0
104	125	215.	299.0	.515	.316	18.0 17.0 24.0
105	126	395.	394.0	.315	.250	17.0 18.0 19.0 24.0

TEST SECTION NUMBER 13 (CONTINUED)

SRL	RUN	PRESS	TEMP	G(AVE)	Q(AVE)	CHF RODS
106	127	395.	371.0	.283	.253	18.0 17.0 24.0
107	128	400.	329.0	.291	.271	18.0 17.0 19.0
108	129	205.	350.0	.250	.199	17.0 18.0 19.0 20.0
109	130	200.	298.0	.286	.224	17.0 18.0 19.0 23.0 24.0
110	131	210.	275.0	.299	.252	17.0 18.0 19.0 24.0
111	132	205.	265.0	.106	.202	17.0 18.0 19.0 24.0

TEST SECTION NUMBER 59

SRL	RUN	PRESS	TEMP	G(AVE)	Q(AVE)	CHF RODS
1	15	2390.	624.5	1.991	.281	21.3
2	16	2195.	610.0	2.079	.296	21.3 21.2 18.2
3	17	1995.	605.5	2.072	.271	21.3
4	18	2400.	593.0	2.009	.332	21.3
5	19	2195.	587.5	2.006	.319	21.3
6	20	2005.	580.0	2.023	.310	21.3 20.2 21.2 18.2
7	21	2395.	564.5	1.996	.378	21.3
8	22	2195.	562.0	2.021	.358	21.3
9	23	1995.	551.5	2.008	.348	21.2
10	24	2395.	526.5	2.009	.434	21.3
11	25	2215.	529.5	1.986	.410	21.3 20.2
12	26	2005.	521.0	1.993	.390	21.2 20.2
13	27	2400.	605.5	2.449	.378	21.3
14	28	2405.	626.5	2.968	.395	21.3 21.4 18.4
15	29	2200.	620.0	3.042	.377	21.3
16	30	2015.	603.0	2.998	.370	21.3
17	31	2415.	594.5	2.973	.476	21.3 18.4 21.4 18.3 18.2
18	32	2205.	594.5	3.041	.434	21.3
19	33	2200.	599.0	2.497	.358	21.3
20	34	2015.	590.5	2.550	.353	21.3
21	35	2000.	570.0	3.032	.436	21.3
22	36	2410.	558.5	2.995	.544	21.3 15.2
23	37	2200.	545.5	2.999	.542	21.3
24	38	2000.	538.0	2.974	.507	21.3
25	39	2415.	539.0	2.494	.512	21.3
26	40	1995.	533.0	2.490	.483	21.3
27	41	2000.	527.5	2.484	.460	21.3 18.2
28	42	2415.	528.5	2.999	.617	21.4 18.4 20.6 21.3 18.2 18.3
29	50	2400.	566.5	1.967	.380	21.3 18.3
30	51	2195.	566.5	2.023	.368	21.3 21.2 18.3
31	52	2395.	584.0	1.513	.284	21.2 21.3 20.2 18.3
32	53	2200.	572.0	1.535	.284	21.2 20.2
33	54	2000.	561.0	1.556	.281	21.2 20.2
34	55	2400.	585.0	1.050	.210	21.2 20.2
35	56	2200.	579.5	1.027	.204	21.2 20.2 20.3 18.2

TEST SECTION NUMBER 59 (CONTINUED)

SRL	RUN	PRESS	TEMP	G(AVE)	Q(AVE)	CHF RODS
36	57	2000.	571.0	1.019	.209	21.2 20.2 20.3
37	58	2410.	544.0	1.012	.243	21.2 20.2
38	59	2200.	522.5	1.009	.242	21.2 20.2
39	60	2000.	523.0	1.008	.241	21.2
40	61	2405.	486.5	1.018	.291	21.2 20.2
41	62	2195.	469.5	1.011	.284	21.2
42	63	2005.	465.0	1.008	.280	21.2
43	64	2405.	518.5	1.534	.371	21.3 21.2 20.2
44	65	2205.	501.0	1.523	.366	21.2 20.2
45	66	2005.	488.5	1.531	.350	21.2
46	67	2415.	505.5	1.978	.469	21.3
47	68	2215.	501.5	1.962	.450	21.3 21.2
48	69	2005.	487.5	1.992	.445	21.2
49	70	2405.	461.0	1.962	.532	21.3 20.2
50	71	2215.	459.5	1.981	.517	21.3
51	72	2005.	457.0	1.982	.491	21.2 18.2
52	73	2405.	534.5	2.825	.583	21.3
53	74	2210.	520.5	2.851	.576	21.3 18.3 18.2
54	75	2000.	510.0	2.870	.560	21.3 18.2 21.2
55	76	2405.	424.5	.991	.337	21.2 20.2 21.3 18.2
56	77	2190.	421.5	1.007	.320	21.2
57	78	2415.	414.5	1.007	.347	21.2 20.2 21.3 18.2
58	79	2015.	404.5	1.017	.332	21.2
59	80	1755.	395.0	1.016	.336	21.2
60	81	1755.	386.5	1.015	.345	21.2 20.2
61	82	1750.	450.5	1.002	.297	21.2
62	83	1755.	431.5	2.001	.492	21.2
63	84	1755.	470.5	1.968	.425	21.2
64	85	1755.	496.5	1.999	.400	21.2
65	86	1495.	494.5	1.989	.402	20.3 21.3
66	87	1745.	504.0	2.403	.446	21.2
67	88	2205.	510.5	2.879	.601	21.3
68	89	2010.	500.5	3.008	.606	21.3 18.2
69	90	1755.	482.0	2.964	.579	21.3 21.2 18.2 18.3
70	91	1505.	471.5	3.038	.562	18.3 20.3 21.3

TEST SECTION NUMBER 59 (CONTINUED)

SRL	RUN	PRESS	TEMP	G(AVE)	Q(AVE)	CHF RODS			
71	92	1755.	528.0	2.017	.364	20.3	20.2	21.2	
72	93	1505.	520.5	2.014	.371	20.3			
73	94	1755.	526.5	3.055	.493	21.3	18.3	21.2	
74	95	1500.	518.5	3.024	.465	20.3	18.4		
75	96	1755.	558.5	1.960	.319	20.3	21.3		
76	97	1760.	550.5	2.968	.437	21.3	20.3	18.3	
77	98	1500.	560.0	2.824	.382	18.4	20.4		
78	99	1755.	576.0	1.983	.295	21.3	20.3		
79	100	1745.	578.0	2.633	.340	20.3			
80	101	1750.	588.0	3.000	.359	20.3	20.4	18.4	21.3
81	102	2205.	626.5	3.981	.458	18.[illegible]	20.4		
82	103	2005.	605.0	3.984	.457	18.4			
83	104	2205.	576.5	4.008	.608	21.3			
84	105	2000.	575.0	4.007	.555	21.3			
85	106	1750.	542.5	1.517	.288	20.3	21.3		
86	107	1750.	482.0	1.504	.344	21.2			
87	108	1755.	488.0	1.018	.275	21.2			
88	109	1505.	452.0	1.992	.452	20.3	21.3	21.2	
89	110	1755.	333.0	1.035	.390	20.3	21.2	20.2	

TEST SECTION NUMBER 304

SRL	RUN	PRESS	TEMP	G(AVE)	Q(AVE)	CHF RODS			
1	129	1000.	527.5	.507	.391	15.0	16.0	14.0	13.0
2	130	1000.	501.0	.514	.421	15.0	13.0	14.0	16.0
3	131	1000.	471.0	.510	.442	13.0	14.0	15.0	16.0
4	132	1000.	435.0	.512	.476	16.0			
5	133	1000.	399.5	.514	.510	16.0	15.0	14.0	13.0
6	134	1000.	361.0	.509	.536	15.0			
7	135	1000.	322.0	.507	.571	15.0			
8	136	1000.	525.0	.782	.475	13.0			
9	137	1000.	494.0	.776	.512	13.0	14.0	15.0	16.0
10	138	1000.	471.0	.762	.543	13.0	14.0	15.0	16.0
11	139	1000.	443.0	.760	.571	13.0	14.0	15.0	
12	140	1000.	409.0	.766	.614	15.0	14.0	13.0	
13	141	1000.	382.0	.756	.648	13.0	14.0	15.0	
14	142	1000.	349.0	.760	.685	13.0	14.0		
15	143	1000.	524.0	1.023	.572	13.0	15.0		
16	144	1000.	500.0	1.017	.599	13.0	15.0		
17	145	995.	473.0	1.019	.636	13.0			
18	146	1000.	450.0	1.023	.670	13.0			
19	147	1001.	421.0	1.011	.710	13.0			
20	148	1001.	389.0	1.030	.765	13.0			
21	149	1000.	526.0	1.281	.613	15.0	14.0	13.0	
22	150	1000.	501.0	1.263	.643	15.0	13.0		
23	151	1000.	474.5	1.276	.680	15.0	13.0		
24	152	1000.	452.0	1.273	.713	15.0	13.0		
25	153	1000.	423.5	1.287	.754	13.0			
26	154	1000.	400.0	1.279	.795	13.0			

NRC FORM 335 (11 81) U.S. NUCLEAR REGULATORY COMMISSION **BIBLIOGRAPHIC DATA SHEET**		1. REPORT NUMBER (Assigned by DDC) NUREG/CR-2855 BNL-NUREG-51570	
4. TITLE AND SUBTITLE (Add Volume No., if appropriate) Subchannel Analysis of Multiple CHF Events		2. (Leave blank)	
		3. RECIPIENT'S ACCESSION NO.	
7. AUTHOR(S) D. G. Reddy, C. F. Fighetti, Columbia University		5. DATE REPORT COMPLETED MONTH May	YEAR 1982
9. PERFORMING ORGANIZATION NAME AND MAILING ADDRESS (Include Zip Code) Heat Transfer Research Facility, Department of Chemical Engineering, Columbia University, New York, New York 10027 — Under subcontract to Brookhaven Nat'l Lab, Upton, NY 11973		DATE REPORT ISSUED MONTH August	YEAR 1982
		6. (Leave blank)	
		8. (Leave blank)	
12. SPONSORING ORGANIZATION NAME AND MAILING ADDRESS (Include Zip Code) U. S. Nuclear Regulatory Commission, Office of Nuclear Reactor Regulation, Division of Systems Integration, Washington, DC 20555		10. PROJECT/TASK/WORK UNIT NO.	
		11. FIN NO. A3353	
13. TYPE OF REPORT Technical	PERIOD COVERED (Inclusive dates)		
15. SUPPLEMENTARY NOTES		14. (Leave blank)	

16. ABSTRACT (200 words or less)

This report provides the results of an NRC sponsored study to determine the adequacy of critical heat flux (CHF) correlations presently used in the nuclear industry in predicting higher order CHF occurences. The BAW-2, CE-1, W-3, and Columbia CHF correlations were used to analyze test data obtained from experiments conducted at the Heat Transfer Research Facility of Columbia University. The conclusions drawn from this study are: (1) higher order CHF events have the same characteristics as the first CHF; and (2) the CHF correlations presently available are adequate in predicting higher order CHF events.

17. KEY WORDS AND DOCUMENT ANALYSIS	17a. DESCRIPTORS
17b. IDENTIFIERS/OPEN-ENDED TERMS	

18. AVAILABILITY STATEMENT	19. SECURITY CLASS (This report) unclassified	21. NO. OF PAGES
UNLIMITED	20. SECURITY CLASS (This page) unclassified	22. PRICE $

NRC FORM 335 (11 81)

UNITED STATES
NUCLEAR REGULATORY COMMISSION
WASHINGTON, D.C. 20555

OFFICIAL BUSINESS
PENALTY FOR PRIVATE USE, $300

FOURTH CLASS MAIL
POSTAGE & FEES PAID
USNRC
WASH D C
PERMIT No G 67

120555078877 1 ANR2
US NRC
ADM DIV OF TIDC
POLICY & PUBLICATIONS MGT BR
PDR NUREG COPY
LA 212
WASHINGTON DC 20555